CENTRO DE INVESTIGACIÓN Y DE ESTUDIOS AVANZADOS DEL INSTITUTO POLITÉCNICO NACIONAL

UNIDAD ZACATENCO

DEPARTAMENTO DE CONTROL AUTOMÁTICO

“Modelado, Simulación y Detección de Fallas en una Red de Tuberías”

TESIS

Que presenta

Sina Razvarz

Para obtener el grado de

DOCTOR EN CIENCIAS

EN LA ESPECIALIDAD DE

CONTROL AUTOMÁTICO

Director de la Tesis:

Dr. Cristóbal Vargas Jarillo

Ciudad de México Agosto, 2019

II

CENTRO DE INVESTIGACIÓN Y DE ESTUDIOS AVANZADOS DEL INSTITUTO POLITÉCNICO NACIONAL

UNIDAD ZACATENCO

DEPARTMENT OF AUTOMATIC CONTROL

"Modelling, Simulation and Fault Detection in a Pipeline Networks"

DISSERTATION

Presented by

Sina Razvarz

To Obtain the Degree of

DOCTOR OF SCIENCE

With the Specialty in

AUTOMATIC CONTROL

Advisor:

Dr. Cristóbal Vargas Jarillo

Mexico City **August, 2019**

This thesis is dedicated to my parents, parents in law, my brothers and specially my wife

For their endless love, support and encouragement

Contents

List of Figures

List of Tables

Nomenclature

ρ	Fluid density	kg/m^3
u	Flow velocity	m/s
∇	Divergence	-
p	Pressure	$kg/m.s^2$
t	Time	s
υ	Kinematic viscosity	m^2/s
Re	Reynolds number	-
(e)	Roughness coefficient of the pipe	
g	Body acceleration	m/s^2
F_f	External force	$kg.m/s^2$
L	Length of pipe	m
α	Coefficient of changing the pressure	-
F_b	Body force	$kg.m/s^2$
F_g	Sum of external forces-nonlinear component force	$kg.m/s^2$
D	Diameter of a pipeline	m
A	Cross section of a pipe	m^2
n	Angular velocity of motor	rad/s
τ	Motor torque	$kg.m^2/s^2$
τ_p	Frictional torque of the motor	$kg.m^2/s^2$
ω	Load constant	
T	Rotation inertia time constant	$kg.m^2$
$\ddot{X}_p$	Acceleration of pump	m/s^2
$\dot{X}_p$	Velocity of pump	m/s
X_p	Position of pump	m
f_p	External force generated by pump	$kg.m/s^2$
m_p	Volumetric mass of pump	kg
A_b	Blockage area	m^2
H_{1b}	Blockage pressure head	m

f_b	Friction factor for blockage	
f	Friction factor	
R	The covariance matrices of measure noises	
D	The covariance matrices of process noises	
$P^{\tilde{\imath}}$	The a priori covariance matrix	
J^i	The Jacobian matrix	
η	Discharge coefficient	
Δt	The time step	
i	The index of discrete time	
$\mathbb{C}$	Controllability	
O	Observability	
κ	Kalman filter	
$\psi(t)$	Controller input	
e(t)	Error	
k_p	Proportional gain	
k_d	Differential gain	
k_i	Integral gain	
Γ	Matrix of acceleration	
γ	Component of matrix	
$\bar{\gamma}$	Upper bound of γ	
Φ	Matrix of velocity	
ϕ	Component of matrix	
J_t	Inertia of torsional actuator	
r_t	Radius of the disc	m
m_t	Mass of torsional actuator	kg
u_θ	Control input of the motor	
$\ddot{\theta}_t$	Angular acceleration of the torsional actuator	
$\ddot{\theta}$	Angular acceleration of the motor	
c	Torsional viscous friction coefficient	
F_c	Coulomb friction	
x^d	Desired reference	

Λ	Positive definite matrix
Π	Sum matrix
ϑ	Integral element
Ξ	Boundary condition of ϕ
Ω	Lower bound of Lipschitz
$\widehat{\ }$	Equilibrium point parameter
$\sim$	Lipschitz condition function
λ_{min}	Minimum eigenvalues of the matrix
λ_{Max}	Maximum eigenvalues of the matrix
f	Lipschitz over elements

Acronyms

TRFL	Technical Rule For Pipelines
UK	United Kingdom
US	United States
API	Application Programming Interface
CFR	Code of Federal Regulations
CSO	Certification Standards Organization
NDT	Non-Destructive Testing
MPI	Magnetic Particle Inspection
ANN	Artificial Neural Networks
FFT	Fast Fourier Transform
GPS	Global Positioning System
OTDR	Optical Time Domain Reflectometry
NN	Neural Networks
PIG	Pipeline Intervention Gadget
NPW	Negative Pressure Wave
SCADA	Supervisory Control And Data Acquisition
RTTM	Real Time Transient Model
FDI	Fault Detection and Isolation
DDC	Direct Digital Control
PID	Proportional–Integral–Derivative
PD	Proportional–Derivative
PI	Proportional–Integral
PDE	Partial Differential Equation
psig	Pound-force per square inch

Chapter One: Introduction

1.1. Economic importance of pipelines

Everything from water to crude oil is being transported through millions of miles of pipelines all over the world. Transport and distribution networks are very elaborated and continuously growing. This network is prone to many risks. The pipelines are vulnerable to losing their functionality by internal and external corrosion, cracking, third party damage and manufacturing flaws [1]. However, pipelines are among the safest means for transportation. The major threat that occurs in pipelines is leakage.

Pipeline leaks can lead to excessive economical loss as well as posing environmental hazards. Mathematical modeling of the flow in a pipeline with a leak can be used to evaluate the loss caused by the leak and provide a guide for pipeline operation as well as an aid for leak detection.

Pipelines originated over 5,000 years ago by the Egyptians who used copper pipes to transport clean water to their cities. The first use of pipelines for transportation of hydrocarbons dates back to approximately 500 BC in China where bamboo pipes were used to transport natural gas for use as a fuel from drill holes near the grounds surface. The natural gas was then used as fuel to boil salt water, producing steam which was condensed into clean drinking water. [2]

It is said that as early as 400 BC wax-coated bamboo pipes were used to bring natural gas into cities, lighting up China’s capital, Beijing.

Pipeline system is one of the most commonly used methods of fluid transportation all over the world. In the United States (US), there are over 241,402 km length of pipelines used for crude oil conveyance, and about 490,850 km for the transmission of natural-gas from source to end locations [3]. There are about a total of 16,023 km production pipelines commissioned for the transportation of crude oil and natural gas in England [4]. Similarly, in Nigeria, there are roughly 124 km lengths of pipelines used for the transportation of condensate, 4,045 km for gas, 164 km for liquid petroleum gas, 4,441 km for crude oil, and about 3,940 km of pipes are used for refined petroleum product lines.

However, aside from the process industries, pipelines are also utilized for aviation fuel and

hydraulic piping as well as air pressure chambers in aircraft. Typically, these lines can be operated up to 5,000 psi [5], and up to 1,400 psig(Pound-force per square inch) for natural-gas pipelines [6]. Consequently, pipes of circular shapes are mainly used due to the structural strength and the uniform cross-sectional area the shape offers. Leak of any of these lines can lead to spillage of hydrocarbon fluid into the surrounding environment, and consequently result in fire or outright explosion of the pipeline system. The resultant effects may include: production loss, damage to the environment and potential loss of lives. On the other hand, blockage of pipelines can result in pressure build-up and eventual explosion of the pipeline system if it is not appropriately noticed and rectified.

Leakages and blockages in pipelines can be attributed to a whole number of factors, such as: faulty or substandard material used for pipe manufacturing; excessive operating temperature of the piping system, fluid contamination occasioned by deposition of debris, scales, carbon monoxide and bio-film build up. Others are intentional and unintentional third party damage, operations outside the design limit [7] and corrosion. Corrosion is one of the major causes of failure in onshore gas and hazardous liquids transmission pipelines in the US and has been responsible for about 18 percent of incidents both on-and off-shore pipelines within the period of 1988 to 2008 [8]. Therefore, pipeline systems must be designed with leakage and blockage detection systems so that pipeline systems can be safe as reasonably practicable in such a way that operators are proactive, rather than being reactive to occurrence of unexpected pipeline failure [9]. The effect of pipeline failure can only be minimized when early signs of leakage and blockage defects are detected in a timely manner.

Modern pipelines originated in the second half of the 19th century and since their adoption have grown drastically in size and number. While drilling for water, crude oil was accidentally discovered in underground reservoirs. This crude oil was not very popular until simple refineries came into existence.

The oil was transported to these refineries in wooden vats that were even transported across rivers via barges pulled by horses. One alternative method of transport was by way of railway tanker cars. However, this meant that the oil supply was controlled by the large railway owners.

So, to make transport independent and more reasonably priced, pipelines were adopted as a more economical means of transportation. The transported oil was boiled off in refineries to obtain the by-products or naphtha, petroleum, heavy crude oil, coal tar and benzene. The petroleum was used as a fuel for lighting and the benzene produced was initially considered an unwanted by product [2].

This situation changed drastically with the invention of the automobile which instantly increased the demand for consistent and reliable supplies of gasoline and resulted in the need for many more pipelines. Pipelines today transport a wide variety of materials including oil, crude oil, refined products, natural gases, condensate, process gases, as well as fresh and salt water. Today there are some 1.2 million miles of transport pipelines around the world, with some well over 1,000 miles in length. The total length of these pipelines lined up end to end would encircle the earth 50 times over.

The construction of these longer pipelines with larger diameters also increased the need for more intelligent leak detection systems to better detect and localize accidental releases.

Where it was once enough to have inspectors walking the length of pipelines and visually inspecting for evidence of leaks, today this is no longer possible. In many cases, due to the longer lengths and the rigorous runs of remotely located pipelines, physical access may be limited. Pipelines can run through snowy landscapes, across mountain ranges, along bodies of water, or be located underground or subsea, even at depths exceeding 1 mile [2].

1.2. Resumen

Desde el agua hasta el petróleo crudo, se transportan a través de millones de millas de tuberías en todo el mundo. Las redes de transporte y distribución son muy elaboradas y están en continuo crecimiento. Estas están propensas a muchos riesgos. Las tuberías son vulnerables a perder su funcionalidad por corrosión interna y externa, grietas, daños de terceros y fallas de fabricación. Sin embargo, se encuentran entre los medios más seguros para el transporte. La mayor amenaza que ocurre en las tuberías es la fuga.

Las fugas y el bloqueo de los sistemas de tuberías de petróleo, gas, agua y otras redes de tuberías pueden causar serios problemas ambientales. Existen métodos numéricos para detectar estos defectos en los sistemas de tuberías, como la radiografía, ultrasonidos, inspección de partículas magnéticas, presión transitoria y métodos de ondas acústicas.

En este trabajo se estudia el modelado transitorio en tiempo real (RTTM) basado en modelos de flujo de tubería, que se construyen utilizando ecuaciones de conservación de masa y momento. El objetivo de la tesis es emplear métodos RTTM para identificar fugas y bloqueos en los sistemas de tuberías. Además, la investigación tiene como objetivo utilizar los modelos de control en tuberías llenas de líquido con y sin defectos para desarrollar la conservación de la masa y la conservación del momento basado en el método de detección de defectos para las tuberías. Los datos para la capacitación de la red se generarán mediante un código informático desarrollado expresamente para simular el flujo en tuberías con, sin fugas y bloqueos.

1.3. Abstract

Name of University: CINVESTAV-IPN
Submitted by: Sina Razvarz
Degree title: Doctor of Philosophy
Thesis title: Modelling, Simulation and Fault Detection in a Fluid Pipeline Networks
Date: 27 August, 2019

Everything from water to crude oil are being transported through millions of miles of pipelines all over the world. Transport and distribution network are very elaborate and continuously growing. This network are prone to many risks. The pipelines are vulnerable to losing their functionality by internal and external corrosion, cracking, third party damage and manufacturing flaws. However, pipelines are among the safest means for transportation. The major threat that occurs in pipelines is leakage.
Leakage and blockage of oil and gas pipeline systems, water pipelines and other pipe networks can cause serious environmental problems. There are numerical methods for detecting these defects in pipeline systems such as radiographic, ultrasonic, magnetic particle inspection, pressure transient and acoustic wave methods.

In this study, real time transient modeling (RTTM) is studied based on pipe flow models, which are constructed using equations of conservation of mass, and conservation of momentum.
The aim of the thesis is to employ RTTM methods to identify leakage and blockage in pipe systems. Moreover, the research is also aimed at using the control models in fluid-filled pipes with and without defects to develop conservation of mass, conservation of momentum based on defect detection method for pipelines. The data for network training will generate by computer code expressly developed for simulating flow in pipelines with and without leaks and blockages.

1.4. Regulations

In many countries it has become necessary to observe official requirements in order to ensure safety of pipelines, particularly for hazardous materials. These requirements include:

- Germany-TRFL, the Technical Rule for Pipelines
- United States of America:
  - API 1130, which deals with computational pipeline monitoring for liquids
  - API 1149, which deals with variable uncertainties in pipelines and their effects on leak detection performance.
  - The former API 1155, which contains performance criteria for leak detection systems, which has since been replaced by API 1130.
  - American 49 CFR 195, which regulates the transport of hazardous liquids via pipeline.
- Canada-CSA Z662, regarding oil and gas pipelines regardless of the specific national regulations,

These rules are observed internationally and often form the basis for the selection of a suitable leak detection system. As we have just learned, leak detection systems are subject to official regulations. Leak detection systems must be sensitive, reliable, accurate, and robust. Sensitivity is a combined measurement, which takes into account the minimum detectable leak rate as well as the time it takes until a leak is detected. Here it is best to indicate the total leaked volume that escapes until the leak is detected.

Table. 1.1. Regulations

Title	Content of requirement
TRFL	Technical Rules For Pipelines
API 1130	Computational pipeline monitoring for liquids
API 1149	Pipeline variable uncertainties and their effects on leak detection
API 1155 (replaced by API 1130)	Performance criteria for leak detection system
49 CFR 195	Transport of hazardous liquids via pipeline
CSA Z662	Oil and gas pipelines

1.5. Aim and objectives of the research

The aims of the study are to develop a novel leakage and blockage detection method for fluid-filled pipeline systems. The specific objectives are as follows:

i) Modelling of a method for detection of blockage and location of that in pipeline

ii) Analysis of observability as well as controllability in the pipeline systems.

iii) Modelling of a method for leakage and location of that in pipeline

iv) Conduct extensive literature review on hazards associated with leakage and blockage in pipelines.

v) To use Matlab to simulate water-filled pipes with and without leakage and blockage

1.6. Research methodology

The research methodology focuses on five basic areas: literature review, modelling and analysis of pipeline, modelling and analysis of pipeline with leakage, modelling and analysis of pipeline with blockage, simulation testing, and data processing (using Matlab) and examples

1.7. Literature review

Relevant literature review was conducted within the context of hazards associated with pipeline explosions caused by leakage and blockage in pipelines. This was followed by causes of leakage and blockage defects in pipeline and afterwards, several leakage and blockage detection methods currently in use in the pipeline industries were reviewed. This was done by exploring the Cinvestav's library, academic websites and forums such as; Elsevier, Compendium, Academia, Research Gate, Wikipedia, ASME and IEEE as well as websites located via Google internet search engine.

1.8. Structure of the thesis

The thesis is structured into six chapters, references and appendices:

Chapter one highlights the introduction of the research background, with review on the economy of pipelines and the existing leakage and blockage detection methods. Also, it includes the research aim and objectives, as well as the layout of the thesis.

In chapter two, a detailed literature survey of pipelines defects, pipeline failures, causes of leakages and blockages in pipeline systems is presented.

Chapter three deals with the background theory of the fluid dynamic in pipelines and modelling of flow in pipelines.

Chapter four presents the modelling and monitoring of flow in a water-filled pipe with leakage, also it is simulate the leakage in a two sections pipeline.

Chapter five presents the results and steps taken in modelling a Blockage in pipeline.

In Chapter six control of flow in pipelines using the PD and PID controllers are presented. We have proposed to design PID and PD controllers which is used for controlling the flow rate.

Finally, in chapter seven summaries and conclusions of the research work are presented by highlighting the research achievements against set goals and objectives.

1.9 Acknowledgments

I would like to express my sincere gratitude to my advisor Prof. Cristóbal Vargas Jarillo, for the continuous support of my Ph.D study and research, for his patience, motivation, enthusiasm and immense knowledge. His guidance helped me throughout my research and writing of this thesis. I could not have imagined having a better advisor and mentor for my Ph.D study.

Besides my advisor, I would like to thank my thesis committee members: Prof. Wen Yu Liu Prof. Alejandro Justo Malo Tamayo, Prof. Martha Rzedowski Calderón and Prof. Tovar Rodriguez Julio Cesar. Also I would like to thank my friends in my institution.

Last but not the least, I would like to thank my family: my parents, my wife and brothers for supporting me spiritually throughout writing this thesis and my life in general.

1.10 Publications

Most contributions described in this thesis have appeared in various publications. Below are the list of publications:

1. **Razvarz, S.,** Vargas-jarillo, C., Jafari, R., Gegov, A. (2019): *Flow Control of Fluid in Pipelines Using PID Controller*. In: IEEE Access, doi: 10.1109/ACCESS.2019.2897992, (**IF: 3.557**).
2. Jafari, R., **Razvarz, S.,** Vargas-Jarillo, C., Yu, W. (2019): *Control of Flow Rate in Pipeline Using PID Controller*. In: 16th IEEE International Conference on Networking, Sensing and Control, (IEEE ICNSC 2019) May 9-11, 2019, Banff, Canada. 2019, Vol. 1, pp.293-298. DOI: 10.1109/ICNSC.2019.8743311.
3. **Razvarz, S.,** Vargas-Jarillo, C., Jafari, R. (2019)*"Pipeline Monitoring Architecture Based on Observability and Controllability Analysis,"* 2019 IEEE International Conference on Mechatronics (ICM), Ilmenau, Germany, 2019, Vol. 1, pp. 420-423.

   doi: 10.1109/ICMECH.2019.8722875.
4. Jafari, R., **Razvarz, S.,** Vargas-Jarillo, C., Gegov, A. (2019): *The Effect of Baffles on Heat Transfer*. In Proceedings of the 16th International Conference on Informatics in Control,

Automation and Robotics (ICINCO 2019), Prague, Czech Republic, Volume 2, pages 607-612. ISBN: 978-989-758-380-3 29-31.

5. **Razvarz, S.,** Vargas-Jarillo, C. (2019): *Blockage detection in Pipeline based on observer*. In : Journal of Electronics, **(IF:1.764)** (under review).
6. **Razvarz, S.,** Vargas-Jarillo, C. (2019): *Using of PD controller for controlling the flow rate in pipelines*, In: The 16th International Conference on Electrical Engineering, Computing Science and Automatic Control (CCE), Mexico City, Mexico, September 11-13, 2019 (under review).
7. **Razvarz, S.,** Vargas-Jarillo, C. (2019): *Modelling and Analysis of flow rate and pressure head in pipelines*, In: The 16th International Conference on Electrical Engineering, Computing Science and Automatic Control (CCE), Mexico City, Mexico, September 11-13, 2019 (under review).

Chapter Two: Pipeline Flaws

2.1. Introduction

In this chapter, a brief account of pipeline failures and the devastating effects to the environment and human lives are investigated in addition to the causes of leakage and blockage in pipeline systems. Following, detection technics based leakage and blockage detection methods are investigated. They include visual inspection method, fluid odorant technique, mass balance method, real time transient modelling, pressure deviation method, supervising controls and data acquisition system (SCADA) based leakage and blockage detection methods. Finally, this chapter presents the modelling and simulation of a simple pipeline water filled.

2.2. Pipeline flaw histories

The risks associated with pipeline explosion as a result of leakage and blockage in pipe cannot be over emphasized.

Account of pipeline failures can be traced back to the first of July 1959, when a petroleum pipeline operated by Pemex Ltd exploded in Vernet, Mexico, and killed many people. Specifically, the record showed that about eleven people lost their lives while over forty persons were injured [10].

In another development, eight out of twelve team members were killed on January 17, 1962 due to a gas pipeline explosion in Edson; a town of Alberta, Canada [11].

The second incident occurred in Sundre, Alberta; a natural gas pipeline operated by Albert gasGas Trunk line Co Ltd was enveloped with a large fire after an explosion. The fire ball was said to be so intense that hairs of people living over 183 meters away from the pipeline were scorched by fire. However, only two of the company workers were killed by the explosion [12]. In a related development, in 1978 after the event of 1959 that occurred in Mexico, another gas pipeline failure occurred in Colonia Benito Juarez, Mexico, which reportedly killed 52 people [13]. In September 19, 2012, twenty six people were confirmed dead while forty eight others sustained injury due to an explosion of a natural gas pipeline

near Mexico's border with the United States [14]. Furthermore, there were a total of 81 minor and major incidents of natural gas transmission line within one year alone in the US [15].

Similarly, in 2010, a natural gas pipeline exploded in San Bruno, California killing 8 people while 28 homes were destroyed. The destructive effect from the incident due to the sluggish response from the company personnel was also blamed on the lack of automatic shut-off valves [16].

The literature reviewed above as well as Refs. [17] [18] [19] [20] [21] [22] [23] [24] [25] [26] show that pipeline explosions have occurred across the developed and developing countries of the world. Many of these explosions happened in the United States, Canada and Russia, thus making these three countries to have the largest number of pipeline disasters in the world. The US has the highest number of pipeline explosions, while Russia has the highest number fatalities resulting from pipeline failures.

Nevertheless, pipelines are generally regarded as a safe way for hydrocarbon fluid transportation; a far cheaper and better alternative to trucks and tankers. Thus, the risks inherent in the transportation of these pressurised fluids through pipelines can be said to be analogous to the risks associated with travelling by air plane. When a pipeline fails, the consequences can be catastrophic. Therefore, the causes of pipeline leakage and blockage must be evaluated in detail to enable the development of novel leakage and blockage detection methods that can be incorporated into a robust pipeline design that will be safe and reasonably practicable to operate.

2.3. Methods for flaw detection in pipelines techniques

In this section, we first look at available flaw detection methods, which could be classified based on their technical approach. There are a number of non-destructive testing methods currently used for the detection of leakage and blockage defects in pipeline systems and without interfering with the functioning of the lines, but they have their various limitations and shortcomings. Basically, some of the current non-destructive testing (NDT) methods used for defect detection in pipe a include [27] ultrasonic, radiographic, magnetic particle inspection (MPI), dye penetrant, eddy current and electro-magnetic methods, pressure

transients, and acoustic wave techniques. The first five methods are local-based techniques, which require that the sensors or dye be scanned over every part of the surface of the piping system when performing pipe inspection. This is thus a daunting task that can cost significant amounts of time and resources. Furthermore, some of those methods often miss defects when deployed for use [28], and may lack the capacity to effectively estimate the location and size of the defect.

Moreover, in terms of their relative capital costs, for instance, a portable computer-based ultrasonic system is considered to be the most expensive, followed by radiography equipment and then the other mentioned local techniques. It is interesting to note that aside from the equipment cost, other expenses that operators must contend with when using the radiographic method includes consumable and man power costs [8].

However, the pressure transients [29] [30] [31] [32] [33] [34] [35] [36] [37] [38] [39]and acoustic wave techniques [40] [41] [42] [43] [44] [45] [46] [47]are cheaper and are global methods, which can monitor the effect of a defect in a pipeline system by monitoring the pipe response.

There are two general ways for leak detection: hardware based methods and software based methods.

Hardware based methods consist of six parts as a follow:

1-Acoustic

2-Optical

3-Vapor sampling

4-Cable sensor

5-Soil monitoring

6- Pipeline Intervention Gadget (PIG)

and Software-based Methods consist are six main parts as a follow

1-Mass/Volume balance

2-Negative pressure wave

3-Real time transient modeling

4-Pressure point analysis

5-Digital signal processing

6-Statistical

2.4. Hardware based leak detection

Hardware based methods for leak detection and localization, detect the presence of leaks from outside the pipeline by visual observation or by using appropriate equipment. These kind of techniques are featured by a very good sensitivity to leaks and are high precise for finding the leak location. However, they are expensive and installation of their equipment is a very complex task. As a result, their uses are restricted to places with high potential of risk like near rivers or nature protection areas or in conditions which under pipe the is transferring a hazardous material [48].

2.4.1 Acoustic leak detection

The acoustic pressure wave method analyses the rarefaction waves produced when a leak occurs. The principle of this method is based on the fact that when a leak happens, it produces an acoustic noise around the place of leakage. When a pipeline wall breakdown occurs, fluid or gas escapes in the form of a high velocity jet producing a low frequency acoustic signal which is detected and investigated. If this signal features differ from the base line, an alarm will be activated [49]. This produces negative pressure waves, which propagate in both directions within the pipeline and can be detected and analyzed. The operating principles of the method are based on the very important characteristic of pressure waves to travel over long distances at the speed of sound guided by the pipeline walls. The received signal is stronger near the leak site thus enabling leak localization. In the acoustic methods, the most common approach for detecting and localizing of leakage involves cross-correlation. The amplitude of a pressure wave increases with the leak size. A complex mathematical algorithm analyzes data from pressure sensors and is able in a matter of seconds to point to

the location of the leakage with accuracy less than 50 m.

However, the method is unable to detect an ongoing leak after the initial event. After the pipeline wall breaksdown (or rupture), the initial pressure waves subside and no subsequent pressure waves are generated. Therefore, if the system fails to detect the leak (for instance, because the pressure waves were masked by transient pressure waves caused by an operational event such as a change in pumping pressure or valve switching), the system will not detect the ongoing leak.

Location of the leak can be identified based on sound propagation velocity, time lag and distance between sensing points. It can be found by using the following equation

$$d_1 = \frac{d - c\, t_{peak}}{2} \qquad (1)$$

Where d_1 is the distance from the sensor 1 to the leak, d is a distance between the two sensors, c is a sound wave propagation velocity and indicates time difference between the arrivals of identical frequencies to each sensor. The performance of the leak detection depends on the distance between the sensors d. The shorter the distance between the sensors leads to higher accuracy. Obviously all variables of this equation can be found easily from the experiment[6].

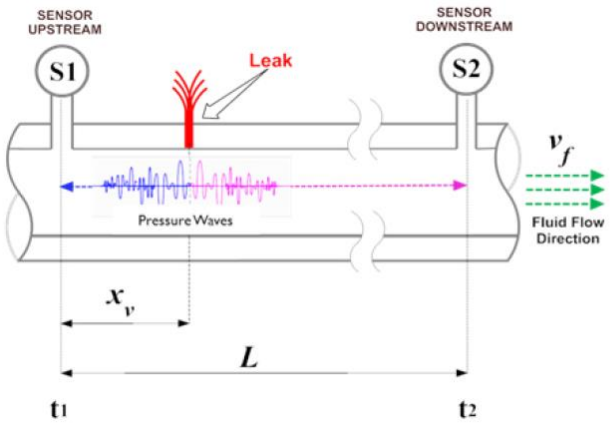

Figure 1.1 Acoustic leak detection[6]

Acoustic sensors and computational systems based on artificial neural networks (ANN) are used for leak detection. The detection procedure was based on the fact that leakage could change the amplitude or speed of signal propagation [50]. Blesito [50] and Garcia [51] have used neural network for leak detection and have received flexible and promising results. Shibata [52] used ANN for leak detection. She assembled the sound noise data through some microphones inserted at certain distances from the crash. Then a fast Fourier transform (FFT) was applied to the data and at last, it fed forward to a neural network for final decision-making. Zhao [53] applied neural networks for pattern recognition in oil pipelines. The experimental data from acoustic sensors preprocessed and got through a filter bank to extract frequencies of 1 kHz, 5 kHz and 9 kHz. The dynamic of these noises were used as input to neural networks. Neural training was carried out with database from an experimental pipeline in both states of healthy and with leak occurrence (transient and steady). The result was satisfactory for short pipelines up to 100 meters but since many microphones should be used along the pipeline which makes this method a very costly one, it is not an efficient approach for long pipelines.

Avelino [54] proposed a real time leak detection system using sonic technology. He exploited wavelet transform for feature extraction and a neural network technique for decision making on leak occurrence in an oil pipeline. The system is composed of two 32-bit DSP's, four piezo resistive sensors, two global positioning system (GPS). The piezo resistive sensors were placed at both ends of the pipeline. These sensors are very sensitive to small changes and their mechanism is based on change of electrical resistance of the material due to variation of mechanical stress. Using two pressure sensors at each station provided the capability to identify the signal direction during a pressure fall caused by the leak. After preprocessing of the extracted signals from sensors, Wavelet decomposition was applied. Finally, the outputs of wavelet decomposition were fed into the NN as its input. Leaks were identified by pressure fall. Therefore, situations where the pressure was rising or stable were discarded. The challenge of this work was finding an optimum sampling rate. After trying some sampling rate such as 100 Hz, 200 Hz and 500 Hz and 1 kHz, they come up with the sampling rate of 1 kHz. The advantage of this work was its ability of

differentiating between leak occurrences and switching on/off pumps. However, it is not an efficient method for long pipeline and location of the leak could not be identified by this method.

In what regards the advantages of using this technique, it could be said that unceasing monitoring of the system is possible. Furthermore, acoustic signals are applicable in leak localization and also estimation of leak's size [48]. However, sometimes high background or flow noise like noise produced by vehicles or valve or pump may cover the actual leak signal. An important factor of limited application of this technique for leak detection is associated with its financial drawback matters; installing plentiful sensors which are needed for long pipelines inspection based on this technique is significantly expensive.

2.4.2. Fiber optic sensors

The fiber optic sensing leak detection method relies on the installation of a fiber optic cable all along the pipeline. Its principle is as a leak occurs in pipeline the substance inside the pipeline gets in touch with fiber cable. Therefore, the temperature of the cable changes due to this contact. By measuring, the temperature changes in fiber cable leak could be detected.

This technique is based on the Raman Effect or Optical Time Domain Reflectometry (OTDR). The laser light is scattered as the laser pulse spreads through the fiber because of molecular vibrations. Therefore, the backscattered light carries the information of local temperature along the pipeline. Indeed, Raman backscattered light has two frequency-shifted components: the Stokes and the Anti-Stokes components. The amplitude of the Anti-Stokes component varies dramatically with regard of temperature variations. However, the amplitude of the Stokes component is not affected by temperature.

Therefore some filtering is needed to isolate Anti-stoke components from stokes components [55]. The problem associated with this technique is low magnitude of backscattered light. To overcome his issue high numerical aperture multimode fibers are used. However, another difficulty arises by using multimode fibers which is related to their severe attenuation features. Therefore, the distance range Raman-based systems will be confined to approximately 10 km [56].

Brillion scattering also happens due to interaction between propagation optical signals and thermally acoustic waves. This interaction leads to rise in frequency-shifted components. Consequently, the Brillouin shift carries information of temperature and strain. On the other side, the Raman-based technique changes the intensity of the backscattered light. Brillouin based techniques are more accurate and more stable on the long term, since intensity-based systems suffer from a high sensitivity to drifts.

In the northeast of Berlin, a 55 km pipeline was equipped with a fiber optics leakage detection system during the construction phase of the pipeline in 2002 by the company GESO. The reports until 2004 showed the leakage detection system has been in operation for and one leakage was detected [56]. One main benefit to using fiber optic is its insensitivity to electromagnetic interference. However, some disadvantages such as high costs and the stability over time limited wide range application of this method for pipeline monitoring. Moreover, this method could not be applied to existing buried pipelines. Consequently, it may need some excavation to reach the place where the optical cable should be installed for sensing purposes.

2.4.3. Vapor or liquid sensing tubes.

The vapor or liquid sensing tube based leak detection method involves the installation of a tube along the entire length of the pipeline. If a leak happens, the content of pipe gets in touch of tube. The tube is full of air in atmospheric pressure. Once the leak occurs, the leaking substance penetrates into the tube. First, to assess the concentration distribution in the sensor tube, a column of air with constant speed is forced into the tube. There are gas sensors at the end of sensor tube. Every increase in gas concentration leads to a peak in gas concentration, which its size is an indication of the size of the leak.

The detected line is equipped with an electrolytic cell. This cell diffuses an exact volume of test gas into the tube constantly. This gas along with air passes through the whole length of the sensor tube. When the test gas travels through the detector unit, it produces an end peak. Therefore, the end peak is a sign of the whole length of the sensor tube. Leak localization is carried on by calculating the ratio of end peak arrival to leak peak arrival [57].

As shortcoming of this method, it could be mentioned that its speed of leak detection is very low. In addition, it is not very practical for applying in long pipelines, as the cost of its equipment is very high. The other drawback of vapor sensing tubes is the difficulty of their application in pipelines above ground or in deep sites.

2.4.4 Liquid sensing cables

Liquid sensing cables are placed near to a pipeline and their main function is representation of changes in transmitted energy pulses that has happened due to impedance differentials. Safe energy pulses are continually sent through the cable. As these energy pulses travel down the cable, reflections are returned to the monitoring unit and a "map" of the reflected energy from the cable is stored in memory. The presence of liquids on the sensor cable, in sufficient quantities to "wet" the cable, will alter its electrical properties. This alteration will cause a change of the reflection at that location. The alteration is then used to determine the location of a potential leak. For localization time delay between input pulse and reflected pulse are used. This method works well for multiple leak detection and localization for short pipelines.

2.4.5. Soil monitoring

Soil monitoring technique exploits an inexpensive and non-hazardous gaseous tracer to be guided into pipeline. This tracer is featured as a very volatile gas which escapes from the pipeline at the exact location of leak. By analyzing the soil above the pipeline the presence of leakage and its location could be estimated [58]. Producing low false alarms along with detectability of very small leaks could be mentioned as advantages of this method. But on the other side the method is very expensive because the tracer should be injected into the pipe unceasingly in detection process. It also is not feasible in cases with uncovered pipelines.

2.4.6. Pipeline Intervention Gadget (PIG)

Pipeline pigs are utilized for a variety of tasks in pipeline integrity management. The maintenance tool, pipeline pigs are introduced into the line via a pig trap, which includes a launcher and receiver. Without interrupting flow, the pig is then forced through it by product

flow, or it can be towed by another device or cable. Usually cylindrical or spherical, pigs sweep the line by scraping the sides of the pipeline and pushing debris ahead. As the travel along the pipeline, there are a number of functions the pig can perform, from clearing the line to inspecting the interior. This includes cleaning the pipelines, separating product batches, as well as gauging pipeline condition.

The original pigs were made from straw wrapped in wire and used for cleaning. There are two main hypotheses for why the process is called "pipeline pigging," although neither have been proved. One theory is that "pig" stands for Pipeline Intervention Gadget (PIG).

PIGs can be introduced into pipelines directly through PIG traps [59], and while it passed, the leather squeaked against the sides of the pipe, sounding like a squealing pig.

It can help gain valuable information about corrosion, cracks, wall thickness as well as existing leaks in pipelines.

Engineers must consider a number of criteria when selecting the proper pig for a pipeline. First, it’s important to define what task the pig will be performing. Also, size and operating conditions are important to regard. Finally, pipeline layout is integral to consider when choosing a pig. Because every pipeline is different, there is not a set schedule for pigging a line, although the quantity of debris collected in a pipeline and the amount of wear and tear on it can increase the frequency of pigging.

The pig advances through the pipeline, propelled by the medium and gathers data along the way. A receiver is used to guide the pig out of the pipeline in order to subsequently analyze the collected data. Various techniques are used to collect pipeline information using smart pigs; two of the most common are the magnetic flux leakage method and the ultrasonic principle.

With the magnetic flux leakage method, a strong permanent magnet is used to magnetize the pipeline. Any changes to the wall of the pipe, such as corrosion, change the magnetic flux lines which are then recorded by sensing probes attached to the pig. Following pigging, the recorded signals are evaluated based on reference signals to detect any defects or Abnormalities in the pipe wall.

When it comes to the method based on the ultrasonic principle, the pig transmits ultrasonic pulses into the pipeline wall and receives their reflected signals. The signals are reflected by both the inner and outer pipe walls and based on the running speed of the pig; the thickness of the pipe wall can be derived.

By using smart pigs, existing leaks can be detected as well as any damage to the pipeline which could result in leaks. Prior to commissioning pipelines they are often pigged and the results used as the baseline for further inspections. This is called zero or baseline pigging.

It's important to ensure that the pipeline is piggable in the first place. This means that you must be certain that there are no obstacles in the pipeline such as restrictions or fittings making the passage too narrow and that there are pig launchers and receivers to capture the pig.

In addition, the speed of the pig must be kept between 3-15 feet per second to obtain accurate results.

2.5. Software based leak detection

The internal method is based on monitoring of internal pipeline parameters (pressure, flow and temperature). Generally, the effectiveness of the internal based methods depends on the uncertainties associated with the system's characteristics, operating conditions and collected data.

2.5.1. Mass-Volume balance

Mass balance (and volume balance) are, in effect the same method based on the principle of conservation of mass. The principle states that a fluid enters the pipe section either remains in the pipe section or leaves the pipe section. In standard pipeline networks, the flow entering and leaving the pipes can metered. A leak can be identified if the difference between upstream and downstream flow measurements changes by more than established threshold value [48].

This approach is already commercialized and has been used in the oil pipeline industry. This method is very sensitive to pipeline instrumentation accuracy. The main weakness of the

mass balance method is the assumption of steady state. As a result of this assumption, the detection period has to be increased in order to prevent false alarms.

Therefore, the response time to the leak will be delayed, which is undesirable. For instance, a 1% leak needs about 60 minutes to be detected [48]. Another significant disadvantage of mass balance method is location of the leak is unknown. Consequently, in real application other methods are required in conjunction with mass balance method after the leak has been detected to identify the location of the leak.

2.5.2. Real time transient modeling

This leak detection technique is based on pipe flow models, which are constructed using equations of conservation of mass, conservation of momentum and conservation of energy. The difference between the measured value and the estimated value of the flow is used to determine the presence of leaks. For building this model, flow, pressure and temperature measurements at both ends of the pipeline are necessary. Furthermore, to design a reliable system with minimum false alarm the noise level should be continuously inspected to modify the model [48].

Billman and Isermann [60] used this approach for leak detection and localization. Their leak detection method is based on mathematical dynamic models, nonlinear adaptive state observers and a correlation detection technique. The method was tested by Siebert [61] at a 68 km gasoline pipeline. The results revealed that detection of leakage with size of 0.2% of inlet flow was feasible in 90 second. In addition, leak location could be estimated with accuracy of 0.9%. Verde et. al [62] used a linearized pipe flow model on an N-node model for leak detection. The only measurements were pressure and flow rate at both ends of the pipe. Since the fluid model in the pipe is given by a set of partial differential equations, a finite dimension nonlinear model was acquired by having pressure measurements as input. The output of the model is the estimated flow rate at extremes. Verde [62] in another paper extended his method for finding two simultaneous leakages in pipeline. Continuing to work on model-based leak detection and estimation, Verde designed a framework for leak reconstruction in pipelines using second-order sliding mode [63]. Single leak and multiple

leaks are both studied in this paper. In the case of a single leak, the necessary and sufficient condition that allows estimating the position of the leak is determined and discussed. Under such a condition, an algorithm that determines the position and flow of the leak in finite-time is introduced. In the case of two leaks with known positions, a finite-time estimation of the leaks flow is obtained.

Aamo [64] designed and later revised [65] a detection system that uses an adaptive Luenberger-type observer based system on two coupled partial differential equations of the fluid flow. The main advantage of this method is that it has the ability to detect very small leaks (less than 1 percent of flow) and it could estimate the leak size accurately. In addition the delay of leak detection is negligible. However, on the other hand, this method is very expensive as it should deal with processing of huge data sets in real [48].

2.5.3. Negative pressure wave

When the pipeline leak occurs, the fluid pressure drops suddenly at the position of the leak and generates negative pressure wave, which propagates with a certain speed towards both upstream and downstream of the pipeline. Two pressure sensors are installed at the beginning station and the end station of the pipeline respectively. The negative pressure wave received by the two sensors can identify pipeline leak and furthermore locate the leak by calculating the time difference between the arrival times of the negative wave at each end [66].

Literature [66] in 2002 introduced using negative pressure wave method and wavelet algorithm to detect and locate leaks. Since April 2001 until now, this method has been used in "island-Yongan" and "island-Jixian" line of victory oil field. Support vector machine learning was used to analyze the readings from pressure sensors and to make decision on the presence of leak in the pipe. In this work negative pressure wave (NPW) detection was considered as a two-class pattern classification task. The two classes are " negative pressure wave present" and " negative pressure wave absent". With an SVM formulation, a nonlinear classifier is trained using supervised learning to automatically detect the presence of NPW in pressure curve. By this method, small or slow leak can be easily recognized out of noise.

A signal processing method that has been widely used along with negative pressure wave is

wavelet transform. Li et al [53] used the wavelet transform for leak detection. The monitoring system acquired internal parameters of the pipeline from the existing SCADA system. The reported time delay for leak detection by this method is 2 minutes and estimation error for leak localization is stated 2%. Marco Ferrante [67] developed a transient based leak detection procedure based on extracted pressure signals which are prone to abnormality due to any fault in pipe. By processing these pressure signals using wavelet transform their sensitive feature are extracted. The rapid variation in signals leads to rise of local maxima in wavelet transform modulus. The sequence of modulus local maxima was constructed. Based on the properties of the random noise level, chains connected to false alarm were filtered.

The amplitude of pressure signals is related to leak magnitude, while the arrival time of reflected signal is related to leak location. Henrique V. da Silva [68]proposed a leak detection methodology based on clustering and classification. They used a fuzzy system for classifying the running mode.

Four pressure transducers were connected to a computer and leak simulated at different locations along the pipeline. The position was calculated by estimating the arrival time of the negative wave at the transducers and the knowledge of the wave speed. The drawback of the method was its incapability of finding leak location. However, this method still has not exploited in long pipeline [48].

2.5.4. Pressure point analysis

This method detects the occurrence of leaks by comparing the current pressure signal with a running statistical trend taken over a period of time along the pipeline by pressure monitoring and flow monitoring devices. The principle of this method is based on the fact of pressure drop because of leak occurrence. Using an appropriate statistical analysis of most recent pressure measurements, a sudden change in statistic properties of pressure measurement such as their mean value is detected. If the mean of newer data is considerably smaller than the mean of older data, then a leak alarm is generated. This method may require sensitive high resolution but not necessarily very precise instrumentation. Therefore, the lower overall installation costs are not very high. Furthermore, this method is able to identify the

occurrence of leaks, but not necessarily the presence of them. Since this method use of pressure drop as a leak signature, it can yield false alarms, as the pressure drop is not unique to the leak event.

2.5.5. Statistical leak detection

A statistical leak detection system uses advance statistical technique to analyze the flow rate, pressure and temperature measurements of a pipeline. This method is appropriate for complex pipe system as it can be monitored continuously for continual changes in the line and flow/pressure instruments. In addition, this technique could be used for leak localization. Using statistical analysis is also very easy and applicable into different pipeline systems [48]. The main objective of this system is to minimize the rate of false alarm. It is also suitable for real time application and has been successfully tested in oil pipeline systems. The main disadvantage of statistical leak detection is that noise interferes in the statistical analyses, and some leaks were hidden in the noise, which prevented them from being detected.

2.5.6. Digital signal processing

Another method for leak detection is using digital signal processing techniques. The procedure of this method is that the response of the pipeline to a known input is measured over a period of time. Afterwards, this response is compared with the later measurements. Based on comparison of their signal's features like frequency response or wavelet transform coefficients a leak alarm could be generated. Similar to statistical methods this technique does not need a pipeline model.

The problem associated with using this method for leak detection is only leak occurrence could be detected not leak presence unless the size of present leak increases considerably.

The selection must always be made while taking into consideration the requirements placed on the application. That means it is necessary to make a decision for each application. Among other things, proper selection depends on the desired results, the cost of installation, operation, maintenance and servicing of the leak detection system and the installation conditions such as if, a pipeline has to be dug up or uncovered. Modern leak detection systems function in a wide variety of environments and allow for individual adaptation to

customer surroundings, guaranteeing optimal performance under all normal operating conditions.

2.6. Causes of leakage in pipelines

Typically, most leakages in pipelines are caused by improper welds of pipe joints, corrosion, millscale and accidental damage during pipeline construction. Defect caused during pipeline construction may include girth and seam weld defects, misalignment, and by stress concentration. Also, other forms of leakage defects in pipes include: indentation damage, corrosion at the girth weld, damage to the external coating and third party damage. These factors are discussed as follows.

2.6.1. Failure due to stress concentration

Cracks in pipes can be caused by stress concentration in a pipeline system. For example, in gas distribution pipeline, the polyethylene (PE) pipes are normally used are fused together end-to-end. However, when there is stress concentration in the fusion joints, cracks can be initiated. Initially, the cracks are small but later they propagate and become large when undetected [69]. This can result to leakage in the pipe when the crack eventually penetrates through the pipe wall.

2.6.2. Third party damage

Generally, this involves mechanical damage such as a gorging which results in reduction of the pipe wall thickness, or distortion of the pipe wall such as a dent. Others are theft, terrorist attack and sabotage

2.6.3. Corrosion

Most pipelines, including those used in oil refinery and chemical plant carry fluids that are highly corrosive and erosive. The corrosion section may propagate over time when left undetected. Similarly, aboveground and buried steel pipelines are susceptible to external corrosion [70].

Stress corrosion cracking is the cracking of a material produced by the combined action of corrosion and tensile stress.

2.7. Causes of blockage in pipelines

Blockage in pipelines is caused by factors such as traces of water in gas to form gas hydrates, wax formation, deposition of solid particles associated with crude oil and gas production

Others are pipeline plugs due to inappropriate pig processes, wax formation and other foreign matters associated with crude oil production. Also, the interior of ageing pipelines can become encrusted with scale. Some of these factors are discussed in details as follows.

2.7.1 Sand and debris accumulation

Most pipelines used for crude oil or natural gas transportation from production wells are prone to deposit of solid particles such as sands and debris, and if these particles are allowed to accumulate over time, they can lead to pipeline plugs. In a severe case, pipeline plugs can cause production interruption and pipe failure.

2.7.2 Roots

Roots grow toward breaks and cracks in the pipes in search of a source. If roots get inside the pipe, they form root balls that clog the line. Products are available that chemically treat roots which have found their way into pipes

2.7.3 Grease

Dispose of grease and fats with your trash-don’t put them down the drain! Grease collects and hardens inside the pipes and forms a plug.

Chapter Three: Modelling

3.1 Introduction

Billman and Isermann [60] designed an observer with friction adaptation. In the event of a leak, the outputs from the observer differs from the measurements, and this is exploited in a correlation technique that detects, quantifies and locates the leak. Verde [71] used a bank of observers, computed by the method for fault detection and isolation developed by Hou and Müller [72].

The bank of observers are computed using the recursive numerical procedure suggested by Hou and Müller [72]. However it was shown in Salvesen [73] that due to the simple structure of the discretized model, the observers may be written explicitly. This is important, because it removes the need for recomputing the bank of observers when the operating point of the pipeline is changed. Verde [62] also proposed a nonlinear version, using an extremely coarse discretization grid. The detection method of Verde [71] using a bank of observers, can potentially detect multiple leaks. However, multiple simultaneous leaks is an unlikely event, so the complex structure of a bank of N observers seems unnecessary.

Aamo et al. [64] instead employed ideas from adaptive control, treating the magnitude and location of a single point leak as constant unknown parameters in an adaptive Luenberger-type observer based on a set of two coupled one dimensional first order nonlinear hyperbolic partial differential equations. Heuristic update laws for adaptation of the friction coefficient, magnitude of the leak and the position of the leak was suggested.

We simplified a pipeline without considering convective changes and the variations of temperature and density. It is assumed that flow rate and pressure at the inlet and outlet of the pipeline are the only the available measurements. Assuming the fluid to be slightly compressible and the duct walls slightly deformable; the convective changes in velocity to be negligible; the cross section area of the pipe and the fluid density to be constant, then the dynamics of the pipeline fluid will be described by the momentum equation and continuity equation are partial differential equations.

3.2 Lagrangian and Eulerian specification of the flow

A classical theory is a physical theory that predicts how one or more physical fields interact

with matter through field equations.

3.2.1 Lagrangian field

In classical theory the Lagrangian specification of the field is a way of looking at fluid motion where the observer follows an individual fluid parcel as it moves through space and time. [74] [75]. This can be visualized as sitting in a boat and drifting down a river.

The Lagrangian specification, individual fluid parcels are followed through time. The fluid parcels are labelled by some (time-independent) vector field x_0. In the Lagrangian description, the flow is described by a function $X(x_0, t)$ giving the position of the parcel labeled x_0 at time t.

3.2.2 Eulerian field

The Eulerian specification of the flow field is a way of looking at fluid motion that focuses on specific locations in the space through which the fluid flows as time passes. [74] [75].This can be visualized by sitting on the bank of a river and watching the water pass the fixed location.

In the Eulerian specification of a field, it is represented as a function of position *x* and time *t*. the flow velocity is represented by a function $u(x, t)$.

3.2.2.1 The Euler equation.

The force acting on any fluid volume is equal to the pressure integral over the surface: $F = \int p\, ds$ $[N = N/m^2 * m^2 2]$ or $[kg.m/s^2 = kg/m.s^2 * m^2]$

The force acting on a unit volume is thus ∇p and it must be equal to the product of the mass ρ and the acceleration dv/dt [76].

$$f = \rho \frac{dv}{dt} \qquad (2)$$

The latter is not the rate of change of the fluid velocity at a fixed point in space but the rate of change of the velocity of a given fluid particle as it moves about in space.

One uses the chain rule of differentiation to express this derivative in terms of quantities

referring to points fixed in space. During the time dt the fluid particle changes its velocity by du, which is composed of two parts, temporal and spatial:

$$du = dt\frac{\partial u}{\partial t} + dr.\nabla u = dt\frac{\partial u}{\partial t} + dx\frac{\partial u}{\partial x} + dy\frac{\partial u}{\partial y} + dz\frac{\partial u}{\partial z} \quad (3)$$

Then

$$du = dt[\frac{\partial u}{\partial t} + \frac{dx}{dt}\frac{\partial u}{\partial x} + \frac{dy}{dt}\frac{\partial u}{\partial y} + \frac{dz}{dt}\frac{\partial u}{\partial z}] \quad (4)$$

It is the change in the fixed point plus the difference at two points dr apart,

where $dr = udt$ is the distance moved by the fluid particle during dt.

Dividing (3) by dt we obtain the substantial derivative as a local derivative plus a convective derivative:

$$\frac{du}{dt} = \frac{\partial u}{\partial t} + u.\nabla u \quad (5)$$

3.3. Dynamical flow modeling for flow in the pipe

3.3.1. Momentum equation

We write now the second law of Newton for a unit mass of a fluid, we come to the equation derived by Euler:

$$F = ma \quad (6)$$

we have $f = \nabla p$ where f is force density that is the gradient of pressure. It has the physical dimensions of force per unit volume. Force density is a vector field representing the flux density of the hydrostatic force within the bulk of a fluid. Force density is represented by the symbol, where P is the pressure

$$\nabla p = \rho\frac{du}{dt} = \rho\left(\frac{\partial u}{\partial t} + u.\nabla u\right) \quad (7)$$

$$\frac{\partial u}{\partial t} + u.\nabla u = \frac{\nabla p}{\rho} \quad (8)$$

Euler introduced, the acceleration of a fluid ,considered as due to the difference of the pressure exerted by the enclosing walls.

We can also add an external body force per unit mass

$$\frac{\partial u}{\partial t} + u.\nabla u = \frac{\nabla p}{\rho} + f_b \tag{9}$$

For pipeline we have

$$u.\nabla u = 0 \tag{10}$$

Because in dot product when two non-zero vector are orthogonal the angle between them are zero and according the definition of dot product that is [77]

$$a.b = a\ b\ cos\theta \tag{11}$$

The $u.\nabla u = 0$

and body force for pipe define as above [76]

$$s = \frac{f}{2D}u^2 \tag{12}$$

Where D the diameter (m) and f the friction coefficient.

then we have

$$\frac{\partial u}{\partial t} - \frac{1}{\rho}\frac{\partial p}{\partial z} - \frac{f}{2D}u^2 = 0 \tag{13}$$

Therefore

$$\frac{\partial u}{\partial t} - \frac{1}{\rho}\frac{g}{g}\frac{\partial p}{\partial z} - \frac{f}{2D}u^2 = 0 \tag{14}$$

So A the section area (m^2).

$$A\left[\frac{\partial u}{\partial t} - \frac{1}{\rho}\frac{g}{g}\frac{\partial p}{\partial z} - \frac{f}{2D}\frac{A^2}{A^2}u^2 = 0\right] \tag{15}$$

Thus

$$A\frac{\partial u}{\partial t} - A\frac{g}{\rho g}\frac{\partial p}{\partial z} - \frac{Af}{2D}\frac{A^2}{A^2}u^2 = 0 \quad (16)$$

Then

$$\frac{\partial Au}{\partial t} - Ag\frac{\partial}{\partial z}\frac{p}{\rho g} - \frac{Af}{2D}\frac{A^2}{A^2}u^2 = 0 \quad (17)$$

we kept fluid flow $Q = Au$ and pressure head (pressure head is the internal energy of a fluid due to the pressure exerted on its container obtain. It may also be called static pressure head) as $H = \frac{P}{\rho g}$ in equation (17) and

$$\frac{\partial Q}{\partial t} - Ag\frac{\partial}{\partial z}H - \frac{f}{2D}\frac{Q^2}{A} = 0 \quad (18)$$

where H is the pressure head (m), Q the flow (m^3/s), z the length coordinate (m), t the time coordinate (s), g the gravity (m/s^2), A the section area (m^2), D the diameter (m) and f the friction coefficient.

3.3.2 Continuity equation

To derive the continuity equation, we apply the law of conservation of mass to a control volume.

Let B be momentum of a fluid, and let β be the corresponding intensive property. An intensive property is defined as the amount of B per unit mass of a system, i.e., $\beta = \lim_{\Delta m \to 0} \frac{\Delta B}{\Delta B}$. The total amount of B in a control volume, B_{cv}, is then

$$B_{cv} = \int_{cv} \beta \rho d\forall \quad (19)$$

in which $m =$ mass, $\rho =$ mass density and $d\forall =$ differential volume of the fluid. We are interested in relating the time rate of change of property B of the system to that of the control volume and the inflow and outflow of B across the control surface. At time t, part of the system occupies the control volume while another part is about to move into the control volume. At time $t + \Delta t$, part of the system occupies the control volume while another part

has moved out. Property B of the system at times t and $t + \Delta t$ may be written as

$$B_{sys}(t) = B_{cv}(t) + \Delta B_{in}$$
$$B_{sys}(t + \Delta t) = B_{cv}(t + \Delta t) + \Delta B_{out} \quad (20)$$

where the subscripts sys and cv refer to the system and the control volume, and the subscripts in and out refer to the inflow and outflow from the control volume respectively, and ΔB_{in} and ΔB_{out} are inflow and outflow of property B into or out of the control volume during a time interval Δt.

The time rate of change of property B of the system is

$$\frac{dB_{sys}}{dt} = \lim_{\Delta t \to 0} \frac{B_{sys}(t + \Delta t) - B_{sys}(t)}{\Delta t} \quad (21)$$

By substituting the expressions for $B_{sys}(t)$ from (21) into (20) and rearranging the terms yield

$$\frac{dB_{sys}}{dt} = \lim_{\Delta t \to 0} \frac{B_{cv}(t + \Delta t) - B_{cv}(t)}{\Delta t} + \lim_{\Delta t \to 0} \frac{B_{out}(t)}{\Delta t} - \lim_{\Delta t \to 0} \frac{B_{in}(t)}{\Delta t} \quad (22)$$

Now, as Δt approaches zero in the limit, the first term on the right-hand side of (22) represents the time rate of change of property B in the control volume, i.e.,

$$\frac{dB_{cv}}{dt} = \lim_{\Delta t \to 0} \frac{B_{cv}(t + \Delta t) - B_{cv}(t)}{\Delta t} \quad (23)$$

By substituting (19) into (23)

$$\lim_{\Delta t \to 0} \frac{B_{cv}(t + \Delta t) - B_{cv}(t)}{\Delta t} = \frac{d}{dt} \int_{cv} \beta \rho d\forall \quad (24)$$

we can write

$$\lim_{\Delta t \to 0} \frac{\Delta v \; B_{out}(t)}{\Delta t} = (\beta \rho A V_s)_{out} \quad (25)$$

$$\lim_{\Delta t \to 0} \frac{\Delta v \; B_{in}(t)}{\Delta t} = (\beta \rho A V_s)_{in}$$

Where $A = \text{cross} - \text{sectional area of the conduit and } V_s = \text{flow velocity measured relative}$ to the control surface.

$$\frac{dB_{sys}}{dt} = \frac{d}{dt}\int_{cv} \beta \rho d\forall + (\beta \rho A V_s)_{out} - (\beta \rho A V_s)_{in} \qquad (26)$$

Note that the velocity, V is with respect to the control surface, since it accounts for the inflow or outflow from the control volume. For a fixed control volume, $V_s = \text{fluid flow velocity}$. However, if the control volume stretches or contracts with respect to time, then the control surface is not fixed and V_s in (26) is the relative flow velocity, i.e., $V_s = (V - W)$, where W is the velocity of the control surface at section 1 for inflow and at section 2 for outflow. Both V and W are measured with respect to the coordinate axes. Hence, a general form of (26) for an expanding or contracting control volume in a one-dimensional flow may be written as

$$\frac{dB_{sys}}{dt} = \frac{d}{dt}\int_{cv} \beta \rho d\forall + (\beta \rho A(V - W))_{out} - (\beta \rho A(V - W))_{in} \qquad (27)$$

To apply the Reynolds transport theorem for the conservation of mass, the intensive property of the fluid is mass/unit mass, i.e., $\beta = \lim_{\Delta m \to 0} \frac{\Delta m}{\Delta m} = 1$. In addition, since the mass of a system remains constant, $\frac{dM_{sys}}{dt} = 0$. Hence, applying (27) to the control volume shown in Fig. 2-2 and substituting $\beta = 0$, we obtain

$$\frac{d}{dt}\int_{cv} \beta \rho d\forall + \rho_2 A_2 (V_2 - W_2) - \rho_1 A_1 (V_1 - W_1) = 0 \qquad (28)$$

with using Leibnitz's rule to the first term on the left-hand side gives

$$\frac{d}{dt}\int_{f_1(t)}^{f_2(t)} \frac{\partial}{\partial t} F(x,t) + F(f_2(t),t)\frac{df_2}{dt} - F(f_1(t),t)\frac{df_1}{dt} \qquad (29)$$

we have

$$\int_{x_1}^{x_2} \frac{\partial}{\partial t}(\rho A)dx + \rho_2 A_2 \frac{dx_2}{dt} - \rho_1 A_1 \frac{dx_1}{dt} + \rho_2 A_2 (V_2 - W_2) - \rho_1 A_1 (V_1 - W_1) = 0 \quad (30)$$

Noting that $\frac{dx_2}{dt} = W_2$ and $\frac{dx_1}{dt} = W_1$, this equation simplifies to

$$\int_{x_1}^{x_2} \frac{\partial}{\partial t}(\rho A)dx + \rho_2 A_2 V_2 - \rho_1 A_1 V_1 = 0 \quad (31)$$

Where $\Delta x = x_2 - x_1$. Dividing throughout by Δx and letting Δx approach zero

$$\frac{\partial}{\partial t}(\rho A) + \frac{\partial}{\partial x}(\rho A V) = 0 \quad (32)$$

Expansion of the terms inside the parentheses gives

$$A\frac{\partial \rho}{\partial t} + \rho \frac{\partial A}{\partial t} + \rho A \frac{\partial V}{\partial x} + \rho V \frac{\partial A}{\partial x} + AV \frac{\partial \rho}{\partial x} = 0 \quad (33)$$

By rearranging terms, using expressions for the total derivatives, and dividing throughout by ρA, we obtain

$$\frac{1}{\rho}\frac{d\rho}{dt} + \frac{1}{A}\frac{dA}{dt} + \frac{\partial V}{\partial x} = 0 \quad (34)$$

Typically the variables of interest are the pressure intensity p and the flow velocity V. To write this equation in terms of these variables, we express the derivatives of ρ and A in terms of P and V as follows.

The bulk modulus of elasticity, of a fluid

$$K = \frac{dp}{d\rho/\rho} \quad (35)$$

This equation may be written as

$$\frac{d\rho}{dt} = \frac{\rho}{K}\frac{dP}{dt} \tag{36}$$

Now, for a circular conduit having radius R,

$$\frac{dA}{dt} = 2\pi R\frac{dR}{dt} \tag{37}$$

In terms of the strain, ϵ this equation may rewritten as

$$\frac{dA}{dt} = 2\pi R^2\frac{1}{R}\frac{dR}{dt} \tag{38}$$

or

$$\frac{1}{A}\frac{dA}{dt} = 2\frac{d\epsilon}{dt} \tag{39}$$

As indicated earlier, we assume that the conduit walls are linearly elastic, i.e., stress is proportional to strain. This is true for most common pipe wall materials, e.g., metal, wood, concrete, etc. Then

$$\epsilon = \frac{\sigma_2 - \mu\sigma_1}{E} \tag{40}$$

where $\sigma_2 =$ hoop stress, $\sigma_1 =$axial stress, and $\mu =$ Poisson ratio. To simplify the derivation, we assume the conduit has expansion joints throughout its length. Therefore, the axial stress, $\sigma_1 = 0$. Hence, (40) becomes

$$\epsilon = \frac{\sigma_2}{E} \tag{41}$$

Now, the hoop stress in a thin-walled conduit

$$\sigma_2 = \frac{pD}{2e} \tag{42}$$

where $p =$ inside pressure; $e =$thickness of the conduit walls and $D =$ conduit diameter. By taking the time derivative of (42), we obtain

$$\frac{d\sigma_2}{dt} = \frac{p}{2e}\frac{dD}{dt} + \frac{D}{2e}\frac{dp}{dt} \tag{43}$$

Based on (43), we may write (44) as

$$E\frac{d\epsilon}{dt} = \frac{p}{2e}\frac{dD}{dt} + \frac{D}{2e}\frac{dp}{dt} \tag{44}$$

which may be simplified as

$$\frac{d\epsilon}{dt} = \frac{\frac{D}{2e}\frac{dp}{dt}}{E - \frac{pD}{2e}} \tag{45}$$

It follows from Eqs. (41) and (45)that

$$\frac{1}{A}\frac{dA}{dt} = \frac{\frac{D}{2e}\frac{dp}{dt}}{E - \frac{pD}{2e}} \tag{46}$$

Substituting (36) and (46) into (34) and simplifying, the resulting equation becomes

$$\frac{\partial V}{\partial x} + \left(\frac{1}{K} + \frac{1}{\frac{eE}{D} + \frac{P}{2}}\right)\frac{dp}{dt} = 0 \tag{47}$$

Since $p/2 \ll eE/D$ in typical engineering applications, this equation may be written as

$$\frac{\partial V}{\partial x} + \left(\frac{1}{K} + \frac{1}{\frac{eE}{DK}}\right)\frac{dp}{dt} = 0 \tag{48}$$

Let us define

$$a^2 = \frac{\frac{K}{\rho}}{1 + \frac{DK}{eE}} \tag{49}$$

that a is the velocity of pressure wave in an elastic conduit filled with a slightly compressible fluid.

$$\frac{\partial p}{\partial t} + V\frac{\partial p}{\partial x} + \rho a^2 \frac{\partial V}{\partial x} = 0 \tag{50}$$

In most of the engineering applications, the convective acceleration terms, $V(\partial V/\partial x)$ and $V(\partial p/\partial x)$ are small as compared to the other terms. Similarly, the slope term is usually small and may be neglected. Therefore, dropping these terms from the governing equations, we obtain

$$\frac{\partial p}{\partial t} + \rho a^2 \frac{\partial V}{\partial x} = 0 \tag{51}$$

It is a common practice in hydraulic engineering to compute pressures in the pipeline in terms of the piezo metric head, H, above a specified datum and use the discharge, Q, as the second variable instead of the flow velocity V. Now, $Q = VA$ and the pressure intensity p may be written as

$$P = \rho g(H - z) \tag{52}$$

in which z = elevation of the pipe centerline above the specified datum.

We assumed in the derivation of the governing equations ((50) and (20)) that the fluid is slightly compressible, and the conduit walls are slightly deformable. Therefore, we may neglect the spatial variation of ρ and flow area A due to the variation of the inside pressure with x. However, the small variation of ρ and A is indirectly taken into account by considering the wave velocity a to have a finite value. Note that if the fluid is considered incompressible and the conduit walls are assumed rigid, then the wave velocity becomes infinite, and a pressure or velocity change is felt instantaneously throughout the system. For

a horizontal pipe, $\frac{dz}{dx} = 0$. Hence, with these assumptions,

It follows from (52) that $\partial p/\partial t = \rho g(\partial H/\partial t)$ and $\partial p/\partial x = \rho g(\partial H/\partial x)$. By substituting these relationships into Eqs. (51) and (52), we obtain

$$\frac{\partial H}{\partial t} + \frac{a^2}{gA}\frac{\partial Q}{\partial x} = 0 \tag{53}$$

Finally, the continuity equation, presented as follow:

$$\frac{\partial H}{\partial t} + \frac{a^2}{gA}\frac{\partial Q}{\partial x} = 0 \tag{54}$$

that a is the velocity of pressure wave (m/s) in an elastic conduit filled with a slightly compressible fluid.

The head pressure (H) and Flow rate (Q) are functions of position and time as $H(x,t)$ and$Q(x,t)$, and $x \in [0, L]$ that L is length of pipe. Initial conditions and boundary conditions that can control and measure are the pressure heads in the beginning and end of the pipeline. The conditions will be defined by:

$$\begin{cases} H(0,t) = H_{in}(t) \\ H(L,t) = H_{out}(t) \end{cases} \tag{55}$$

For the system with small change in flow rate Q, the momentum equation (18) from nonlinear system can be linearized to

$$\frac{\partial Q}{\partial t} + Ag\frac{\partial}{\partial x}H + \frac{fQ}{DA} = 0 \tag{56}$$

3.4. Modelling of flow in pipeline

The idea to detect and isolate leaks which will be used in this thesis is to directly get on-line estimation of magnitudes and locations of possible leaks via an observer. This means first

using some model which should be more tractable for observer design than the direct partial differential equations (54) and (56), and then choosing some appropriate input variations to ensure leak detectability (similarly to persistent excitation classically required in identification problems or in state affine observers).

A simple way to get some more appropriate model for observer design is to use some finite-dimensional approximation, for instance via finite differences for space discretization. This means dividing the pipeline into a given number of sections, while keeping time as a continuous variable. The flow dynamics are then described via the flow rates in each section and the pressures at each section end.

The pipeline model can described and defined by (54) and (56).

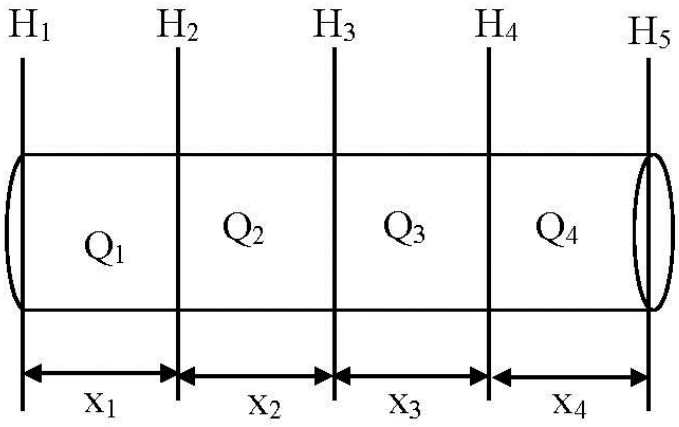

Figure 3.1 Finite difference for a pipeline with four section and actuations at the beginning and end of sections.

Solutions of these equations are complex. However, several methods are used to numerically integrate them, that some of main method used by Chaudry [78] and Wyllie [79] with using characteristics and finite difference method. In this work the finite difference method will use because this is a simple way to get more convenient model for observer and controllable

and structure of results proper for imagination of nonlinear observers. In finite difference for discretization space by dividing the pipeline into N number of sections, while keeping time as a continuous variable. The flow dynamics are then described via the flow rate in each section and the pressures at each section end. For example, with four section that showed in figure 3.1, the variables are H_1, H_2, H_3, H_4, H_5 for Head pressure and Q_1, Q_2, Q_3, Q_4 are flow rate.

Control Variable considered the pressure at beginning and end of pipe ($H_1\ and\ H_5$) and directly measured are flow rates ($Q_1\ and\ Q_4$).

3.5. Steady state model

3.5.1. Case 1

The idea in this section is design and fund a model for these (54) systems.

A General linearized model, which can be written as

$$\frac{dx}{dt} = Ax + Bu \tag{57}$$

$$y = Cx \tag{58}$$

Where $x(t)$ is the state vector containing the n unknown flow perturbation quantities at each point. The vectors $u(t)$ and $y(t)$ contain the system forcing inputs and outputs respectively.

In purposed model, inputs and output presented as $x = (Q_1\ Q_2\ Q_3\ Q_4\ \ H_2\ \ H_3\ \ H_4\ )^T$,$u \coloneqq [H_{in}, H_{out}\ ]^T = (H_1\ \ H_5\ )^T$ and $y = (Q_1\ \ Q_4\ )^T$.

For finding, $\dot{x}$ from equation (54) we have

$$\frac{\partial H(x,t)}{\partial t} + \frac{a^2}{gA}\frac{\partial Q(x,t)}{\partial x} = 0 \tag{59}$$

Thus

$$\frac{\partial H(x,t)}{\partial t} = -\frac{a^2}{gA}\frac{\partial Q(x,t)}{\partial x} \tag{60}$$

which can be written as a difference between the two points

$$\frac{\partial H(x,t)}{\partial t} = -\frac{a^2}{gA}\frac{\Delta Q(x,t)}{\Delta x} \tag{61}$$

This equation may be written as

$$\frac{\partial H(x,t)}{\partial t} = -\frac{a^2}{gA\Delta x}\Delta Q(x,t) \tag{62}$$

Then

$$\frac{\partial H(x_i,t)}{\partial t} = -\frac{a^2}{gA\Delta x}(Q(x_i,t) - Q(x_{i-1},t)) \tag{63}$$

For equation (56) we can write

$$\frac{\partial Q}{\partial t} + Ag\frac{\partial}{\partial x}H + \frac{fQ}{DA} = 0 \tag{64}$$

Then

$$\frac{\partial Q}{\partial t} = -Ag\frac{\partial H}{\partial x} - \frac{fQ}{DA} = 0 \tag{65}$$

Therefore,

$$\frac{\partial Q}{\partial t} = \frac{-Ag}{\partial x}\partial H - \frac{fQ}{DA} \tag{66}$$

Thus by using a difference between two points

$$\frac{\partial Q}{\partial t} = \frac{-Ag}{\Delta x}\Delta H - \frac{fQ}{DA} \tag{67}$$

Therefore,

$$\frac{\partial Q(x_i,t)}{\partial t} = \frac{-Ag}{\Delta x}(H(x_i,t) - H(x_{i-1},t)) - \frac{f}{DA}Q(x_i,t) \qquad (68)$$

Finally, from equations (63) and (68) for $\dot{x}$

$$\dot{H}_1 = \frac{-a^2}{gA\Delta x}(Q_1 - Q_0) \qquad \dot{Q}_1 = \frac{-Ag}{\Delta x}(H_2 - H_1) - \frac{f}{DA}Q_1$$

$$\dot{H}_2 = \frac{-a^2}{gA\Delta x}(Q_2 - Q_1) \qquad \dot{Q}_2 = \frac{-Ag}{\Delta x}(H_3 - H_2) - \frac{f}{DA}Q_2$$

$$\dot{H}_3 = \frac{-a^2}{gA\Delta x}(Q_3 - Q_2) \qquad \dot{Q}_3 = \frac{-Ag}{\Delta x}(H_4 - H_3) - \frac{f}{DA}Q_3 \qquad (69)$$

$$\dot{H}_4 = \frac{-a^2}{gA\Delta x}(Q_4 - Q_3) \qquad \dot{Q}_4 = \frac{-Ag}{\Delta x}(H_5 - H_4) - \frac{f}{DA}Q_4$$

$$\dot{H}_5 = \frac{-a^2}{gA\Delta x}(Q_5 - Q_4)$$

The model $x = (Q_1\ Q_2\ Q_3\ Q_4\ H_2\ H_3\ H_4)^T$, $u = (H_1\ H_5)^T$, $y = (Q_1\ Q_4)^T$ can modified as follows:

$$\dot{x}_1 = \frac{-Ag}{\Delta x}(x_5 - u_1) - \frac{f}{DA}x_1$$

$$\dot{x}_2 = \frac{-Ag}{\Delta x}(x_6 - x_5) - \frac{f}{DA}x_2 \qquad (70)$$

$$\dot{x}_3 = \frac{-Ag}{\Delta x}(x_7 - x_6) - \frac{f}{DA}x_3$$

$$\dot{x}_4 = \frac{-Ag}{\Delta x}(u_2 - x_7) - \frac{f}{DA}x_4$$

$$\dot{x}_5 = \frac{-a^2}{gA\Delta x}(x_2 - x_1)$$

$$\dot{x}_6 = \frac{-a^2}{gA\Delta x}(x_3 - x_2)$$

$$\dot{x}_7 = \frac{-a^2}{gA\Delta x}(x_4 - x_3)$$

The values of A, B, C can be written as the block matrices

$$A = \begin{bmatrix} A_1 & A_2 \\ A_3 & A_4 \end{bmatrix}, \tag{71}$$

$$B = \begin{bmatrix} B_1 \\ B_2 \end{bmatrix}, \tag{72}$$

$$C = [C_1 \quad C_2] \tag{73}$$

$$A_1 = \begin{bmatrix} N & 0 & 0 & 0 \\ 0 & N & 0 & 0 \\ 0 & 0 & N & 0 \\ 0 & 0 & 0 & N \end{bmatrix},$$

$$A_2 = \begin{bmatrix} M & 0 & 0 & 0 \\ -M & M & 0 & 0 \\ 0 & -M & M & 0 \\ 0 & 0 & -M & M \end{bmatrix}$$

$$A_3 = \begin{bmatrix} S & 0 & 0 & 0 \\ -S & S & 0 & 0 \\ 0 & -S & S & 0 \\ 0 & 0 & -S & S \end{bmatrix} \tag{74}$$

$$A_4 = \begin{bmatrix} 0 & 0 & 0 & 0 \\ 0 & 0 & 0 & 0 \\ 0 & 0 & 0 & 0 \\ 0 & 0 & 0 & 0 \end{bmatrix}$$

$$B_1 = \begin{bmatrix} M & 0 \\ -M & 0 \\ 0 & 0 \\ 0 & M \end{bmatrix}$$
$$B_2 = \begin{bmatrix} 0 & 0 \\ 0 & 0 \\ 0 & 0 \\ 0 & 0 \end{bmatrix} \quad (75)$$

$$C_1 = \begin{bmatrix} 1 & 0 & 0 & 0 \\ 0 & 0 & 0 & 1 \end{bmatrix}$$
$$C_2 = \begin{bmatrix} 0 & 0 & 0 & 0 \\ 0 & 0 & 0 & 0 \end{bmatrix} \quad (76)$$

Where N, M, S are defined as follows:

$$S = \frac{-a^2}{gA\Delta x}$$

$$N = \frac{-f}{DA}$$

$$M = \frac{-Ag}{\Delta x}$$

3.5.2. Case 2

The boundary conditions that can be controlled and measured are the initial pressure head in the beginning and the flow rate in the end of the pipeline. The input conditions are stated as

$$\begin{cases} Q(L,t) = Q_{out}(t) \\ H(0,t) = H_{in}(t) \end{cases} \quad (77)$$

and the output values are

$$\begin{cases} Q(0,t) = Q_{in}(t) \\ H(L,t) = H_{out}(t) \end{cases} \quad (78)$$

The vectors $u(t)$ and $y(t)$ contain the system forcing inputs and outputs respectively.

The suggested model, along with inputs and outputs are $x = (Q_1\ Q_2\ Q_3\ Q_4\ H_2\ H_3\ H_4\ H_5)^T$, $u \coloneqq [\ Q_{out}\ H_{in}]^T = (Q_5\ H_1\ )^T$ and $y = (Q_1\ H_5\ )^T$, respectively.

$$\begin{aligned}
\dot{Q}_1 &= \frac{-Ag}{\Delta x}(H_2 - H_1) - \frac{f}{DA}Q_1 \\
\dot{Q}_2 &= \frac{-Ag}{2\Delta x}(H_3 - H_1) - \frac{f}{DA}Q_2 \\
\dot{Q}_3 &= \frac{-Ag}{2\Delta x}(H_4 - H_2) - \frac{f}{DA}Q_3 \\
\dot{Q}_4 &= \frac{-Ag}{2\Delta x}(H_5 - H_3) - \frac{f}{DA}Q_4 \\
\dot{H}_2 &= \frac{-a^2}{2gA\Delta x}(Q_3 - Q_1) \\
\dot{H}_3 &= \frac{-a^2}{2gA\Delta x}(Q_4 - Q_2) \\
\dot{H}_4 &= \frac{-a^2}{2gA\Delta x}(Q_5 - Q_3) \\
\dot{H}_5 &= \frac{-a^2}{gA\Delta x}(Q_5 - Q_4)
\end{aligned} \tag{79}$$

The values of A, B, and C in (63) and (68) can be written in the form of the block matrices as below

$$x = (Q_1\ Q_2\ Q_3\ Q_4\ Q_5\ H_2\ H_3\ H_4)^T = (x_1\ x_2\ x_3\ x_4\ x_5\ x_6\ x_7\ x_8)^T$$

$$A' = \begin{bmatrix} N & 0 & 0 & 0 & 2M & 0 & 0 & 0 \\ 0 & N & 0 & 0 & 0 & M & 0 & 0 \\ 0 & 0 & N & 0 & -M & 0 & M & 0 \\ 0 & 0 & 0 & N & 0 & -M & 0 & M \\ -S & 0 & S & 0 & 0 & 0 & 0 & 0 \\ 0 & -S & 0 & S & 0 & 0 & 0 & 0 \\ 0 & 0 & -S & 0 & 0 & 0 & 0 & 0 \\ 0 & 0 & 0 & -S & 0 & 0 & 0 & 0 \end{bmatrix}$$

$$B' = \begin{bmatrix} 0 & 2M \\ 0 & M \\ 0 & 0 \\ 0 & 0 \\ 0 & 0 \\ 0 & 0 \\ S & 0 \\ 2S & 0 \end{bmatrix} \text{ and} \tag{80}$$

$$C' = \begin{bmatrix} 1 & 0 & 0 & 0 & 0 & 0 & 0 & 0 \\ 0 & 0 & 0 & 0 & 0 & 0 & 0 & 1 \end{bmatrix}$$

where N, M, S are defined as follows:

$$S = \frac{-a^2}{2gA\Delta x}$$

$$N = \frac{-f}{DA} \tag{81}$$

$$M = \frac{-Ag}{2\Delta x}$$

3.5.3. Case 3

The boundary conditions that can be controlled and measured are the flow rate and pressure head beginning of the pipeline. The input conditions are stated as

$$\begin{cases} Q(0,t) = Q_{in}(t) \\ H(0,t) = H_{in}(t) \end{cases} \tag{82}$$

and the output values are

$$\begin{cases} Q(\mathrm{L},t) = Q_{out}(t) \\ H(L,t) = H_{out}(t) \end{cases} \tag{83}$$

The vectors $u(t)$ and $y(t)$ contain the system forcing inputs and outputs respectively. The suggested model, along with inputs and outputs are $x = (\ Q_2\ Q_3\ Q_4\ \ Q_5\ \ H_2\ \ H_3\ \ H_4\ \ H_5\ )^T$, $u \coloneqq [\ Q_{in}\ H_{in}]^T = \ (Q_1\ \ H_1\ )^T$ and $y = (Q_5\ \ H_5\ )^T$, respectively.

$$\begin{aligned} \dot{Q}_2 &= \frac{-Ag}{2\Delta x}(H_3 - H_1) - \frac{f}{DA}Q_2 \\ \dot{Q}_3 &= \frac{-Ag}{2\Delta x}(H_4 - H_2) - \frac{f}{DA}Q_3 \\ \dot{Q}_4 &= \frac{-Ag}{2\Delta x}(H_5 - H_3) - \frac{f}{DA}Q_4 \\ \dot{Q}_5 &= \frac{-Ag}{\Delta x}(H_5 - H_4) - \frac{f}{DA}Q_5 \\ \dot{H}_2 &= \frac{-a^2}{2gA\Delta x}(Q_3 - Q_1) \\ \dot{H}_3 &= \frac{-a^2}{2gA\Delta x}(Q_4 - Q_2) \\ \dot{H}_4 &= \frac{-a^2}{2gA\Delta x}(Q_5 - Q_3) \\ \dot{H}_5 &= \frac{-a^2}{gA\Delta x}(Q_5 - Q_4) \end{aligned} \tag{84}$$

The values of A, B, and C in (63) and (68) can be written in the form of the block matrices as below

$$x = (\ Q_2\ Q_3\ Q_4\ Q_5\ \ H_2\ \ H_3\ \ H_4\ H_5)^T = (x_1\ x_2\ x_3\ x_4\ x_5\ \ x_6\ \ x_7\ \ x_8)^T$$

$$A' = \begin{bmatrix} N & 0 & 0 & 0 & 0 & -M & 0 & 0 \\ 0 & N & 0 & 0 & 0 & 0 & -M & 0 \\ 0 & 0 & N & 0 & M & 0 & 0 & -M \\ 0 & 0 & 0 & N & 0 & M & 0 & -M \\ 0 & -S & 0 & 0 & 0 & 0 & 0 & 0 \\ S & 0 & -S & 0 & 0 & 0 & 0 & 0 \\ 0 & S & 0 & -S & 0 & 0 & 0 & 0 \\ 0 & 0 & S & 0 & 0 & 0 & 0 & 0 \end{bmatrix}$$

$$B' = \begin{bmatrix} 0 & M \\ 0 & 0 \\ 0 & 0 \\ 0 & 0 \\ S & 0 \\ 0 & 0 \\ 0 & 0 \\ 0 & 0 \end{bmatrix} \text{ and} \qquad (85)$$

$$C' = \begin{bmatrix} 0 & 0 & 0 & 1 & 0 & 0 & 0 & 0 \\ 0 & 0 & 0 & 0 & 1 & 0 & 0 & 0 \end{bmatrix}$$

where N, M, S are defined as follows:

$$S = \frac{-a^2}{2gA\Delta x}$$

$$N = \frac{-f}{DA} \qquad (86)$$

$$M = \frac{-Ag}{2\Delta x}$$

3.5.4. Case 4

The boundary conditions that can be controlled and measured are the initial the flow rate in the beginning and pressure head in the end of the pipeline. The input conditions are stated

as

$$\begin{cases} Q(0,t) = Q_{in}(t) \\ H(L,t) = H_{out}(t) \end{cases} \tag{87}$$

and output value are

$$\begin{cases} H(0,t) = H_{in}(t) \\ Q(L,t) = Q_{out}(t) \end{cases} \tag{88}$$

The vectors $u(t)$ and $y(t)$ contain the system forcing inputs and outputs respectively. The suggested model, along with inputs and outputs are $x = (\,Q_2\ Q_3\ Q_4\ Q_5\ H_1\ H_2\ \ H_3\ \ H_4\,)^T$, $u \coloneqq [\,Q_{in}\ H_{out}]^T = \ (Q_1\ \ H_5\,)^T$ and $y = (Q_5\ \ H_1\,)^T$, respectively.

$$\begin{aligned}
\dot{Q}_2 &= \frac{-Ag}{2\Delta x}(H_3 - H_1) - \frac{f}{DA}Q_2 \\
\dot{Q}_3 &= \frac{-Ag}{2\Delta x}(H_4 - H_2) - \frac{f}{DA}Q_3 \\
\dot{Q}_4 &= \frac{-Ag}{2\Delta x}(H_5 - H_3) - \frac{f}{DA}Q_4 \\
\dot{Q}_5 &= \frac{-Ag}{\Delta x}(H_5 - H_4) - \frac{f}{DA}Q_5 \\
\dot{H}_1 &= \frac{-a^2}{2gA\Delta x}(Q_2 - Q_1) \\
\dot{H}_2 &= \frac{-a^2}{2gA\Delta x}(Q_3 - Q_1) \\
\dot{H}_3 &= \frac{-a^2}{2gA\Delta x}(Q_4 - Q_2) \\
\dot{H}_4 &= \frac{-a^2}{2gA\Delta x}(Q_5 - Q_3)
\end{aligned} \tag{89}$$

The values of A, B, and C in (63) and (68) can be written in the form of the block matrices as below

$$x = (Q_1\ Q_2\ Q_3\ Q_4\ Q_5\ \ H_2\ \ H_3\ \ H_4)^T = (x_1\ x_2\ x_3\ x_4\ x_5\ \ x_6\ \ x_7\ \ x_8)^T$$

$$A' = \begin{bmatrix} N & 0 & 0 & 0 & -M & 0 & M & 0 \\ 0 & N & 0 & 0 & 0 & -M & 0 & M \\ 0 & 0 & N & 0 & 0 & 0 & -M & 0 \\ 0 & 0 & 0 & N & 0 & 0 & 0 & -M \\ 2S & 0 & 0 & 0 & 0 & 0 & 0 & 0 \\ 0 & S & 0 & 0 & 0 & 0 & 0 & 0 \\ -S & 0 & S & 0 & 0 & 0 & 0 & 0 \\ 0 & -S & 0 & S & 0 & 0 & 0 & 0 \end{bmatrix}$$

$$B' = \begin{bmatrix} 0 & 0 \\ 0 & 0 \\ 0 & M \\ 0 & -2M \\ -2S & 0 \\ S & 0 \\ 0 & 0 \\ 0 & 0 \end{bmatrix} \tag{90}$$

and

$$C' = \begin{bmatrix} 0 & 0 & 0 & 1 & 0 & 0 & 0 & 0 \\ 0 & 0 & 0 & 0 & 1 & 0 & 0 & 0 \end{bmatrix}$$

where N, M, S are defined as follows:

$$S = \frac{-a^2}{2gA\Delta x}$$

$$N = \frac{-f}{DA} \tag{91}$$

$$M = \frac{-Ag}{2\Delta x}$$

3.5.5. Case 5

The initial and boundary conditions that can be controlled and measured are the flow rate in the beginning and end of the pipeline. The input conditions are stated as

$$\begin{cases} Q(0,t) = Q_{in}(t) \\ Q(L,t) = Q_{out}(t) \end{cases} \tag{92}$$

and output value are

$$\begin{cases} H(0,t) = H_{in}(t) \\ H(L,t) = H_{out}(t) \end{cases} \tag{93}$$

The vectors $u(t)$ and $y(t)$ contain the system forcing inputs and outputs respectively.

The suggested model, along with inputs and outputs are $x = (Q_2\ Q_3\ Q_4\ H_1\ H_2\ H_3\ H_4\ H_5)^T$, $u := [Q_{in}\ Q_{out}\ ]^T = (Q_1\ Q_5\ )^T$ and $y = (H_1\ H_5\ )^T$, respectively.

$$\begin{aligned}
\dot{Q}_2 &= \frac{-Ag}{2\Delta x}(H_3 - H_1) - \frac{f}{DA}Q_2 \\
\dot{Q}_3 &= \frac{-Ag}{2\Delta x}(H_4 - H_2) - \frac{f}{DA}Q_3 \\
\dot{Q}_4 &= \frac{-Ag}{2\Delta x}(H_5 - H_3) - \frac{f}{DA}Q_4 \\
\dot{H}_1 &= \frac{-a^2}{gA\Delta x}(Q_2 - Q_1) \\
\dot{H}_2 &= \frac{-a^2}{2gA\Delta x}(Q_3 - Q_1) \\
\dot{H}_3 &= \frac{-a^2}{2gA\Delta x}(Q_4 - Q_2) \\
\dot{H}_4 &= \frac{-a^2}{2gA\Delta x}(Q_5 - Q_3)
\end{aligned} \tag{94}$$

$$\dot{H}_5 = \frac{-a^2}{gA\Delta x}(Q_5 - Q_4)$$

The values of A, B, and C in (63) and (68)can be written in the form of the block matrices as below

$$x = (\, Q_2\ Q_3\ Q_4\ \ H_1\ \ H_2\ \ H_3\ \ H_4\ H_5)^T = (x_1\ x_2\ x_3\ x_4\ x_5\ \ x_6\ \ x_7\ \ x_8)^T$$

$$\mathrm{A} = \begin{bmatrix} \mathrm{N} & 0 & 0 & -\mathrm{M} & 0 & \mathrm{M} & 0 & 0 \\ 0 & \mathrm{N} & 0 & 0 & -\mathrm{M} & 0 & \mathrm{M} & 0 \\ 0 & 0 & \mathrm{N} & 0 & 0 & -\mathrm{M} & 0 & \mathrm{M} \\ 2\mathrm{S} & 0 & 0 & 0 & 0 & 0 & 0 & 0 \\ 0 & \mathrm{S} & 0 & 0 & 0 & 0 & 0 & 0 \\ -\mathrm{S} & 0 & \mathrm{S} & 0 & 0 & 0 & 0 & 0 \\ 0 & -\mathrm{S} & 0 & 0 & 0 & 0 & 0 & 0 \\ 0 & 0 & -\mathrm{S} & 0 & 0 & 0 & 0 & 0 \end{bmatrix}$$

$$\tilde{\mathrm{B}} = \begin{bmatrix} 0 & 0 \\ 0 & 0 \\ 0 & 0 \\ -2\mathrm{S} & 0 \\ -\mathrm{S} & 0 \\ 0 & 0 \\ 0 & \mathrm{S} \\ 0 & 2\mathrm{S} \end{bmatrix} \tag{95}$$

and

$$\tilde{\mathrm{c}} = \begin{bmatrix} 0 & 0 & 0 & 1 & 0 & 0 & 0 & 0 \\ 0 & 0 & 0 & 0 & 0 & 0 & 0 & 1 \end{bmatrix}$$

where N, M, S are defined as follows:

$$S = \frac{-a^2}{2gA\Delta x} \tag{96}$$

$$N = \frac{-f}{DA}$$

$$M = \frac{-Ag}{2\Delta x}$$

3.5.6. Case 6

The initial and boundary conditions that can be controlled and measured are the flow rate and pressure Head in the end of the pipeline. The input conditions are stated as

$$\begin{cases} Q(\mathrm{L}, t) = Q_{out}(t) \\ H(L, t) = H_{out}(t) \end{cases} \tag{97}$$

and output value are

$$\begin{cases} Q(0, t) = Q_{in}(t) \\ H(0, t) = H_{in}(t) \end{cases} \tag{98}$$

The vectors $u(t)$ and $y(t)$ contain the system forcing inputs and outputs respectively.

The suggested model, along with inputs and outputs are $x = (Q_1\ Q_2\ Q_3\ Q_4\ H_1\ H_2\ H_3\ H_4)^T$, $u := [Q_{out}\ H_{out}]^T = (Q_5\ H_5)^T$ and $y = (Q_1\ H_1)^T$, respectively.

$$\begin{aligned} \dot{Q}_1 &= \frac{-Ag}{\Delta x}(H_2 - H_1) - \frac{f}{DA}Q_1 \\ \dot{Q}_2 &= \frac{-Ag}{2\Delta x}(H_3 - H_1) - \frac{f}{DA}Q_2 \\ \dot{Q}_3 &= \frac{-Ag}{2\Delta x}(H_4 - H_2) - \frac{f}{DA}Q_3 \\ \dot{Q}_4 &= \frac{-Ag}{2\Delta x}(H_5 - H_3) - \frac{f}{DA}Q_4 \\ \dot{H}_1 &= \frac{-a^2}{gA\Delta x}(Q_2 - Q_1) \end{aligned} \tag{99}$$

$$\dot{H}_2 = \frac{-a^2}{2gA\Delta x}(Q_3 - Q_1)$$

$$\dot{H}_3 = \frac{-a^2}{2gA\Delta x}(Q_4 - Q_2)$$

$$\dot{H}_4 = \frac{-a^2}{2gA\Delta x}(Q_5 - Q_3)$$

The values of A, B, and C in (63) and (68)can be written in the form of the block matrices as below

$$x = (Q_1\ Q_2\ Q_3\ Q_4\ \ H_1\ \ H_2\ \ H_3\ \ H_4)^T = (x_1\ x_2\ x_3\ x_4\ x_5\ \ x_6\ \ x_7\ \ x_8)^T$$

$$\mathrm{A} = \begin{bmatrix} \mathrm{N} & 0 & 0 & 0 & -2\mathrm{M} & 2\mathrm{M} & 0 & 0 \\ 0 & \mathrm{N} & 0 & 0 & -\mathrm{M} & 0 & \mathrm{M} & 0 \\ 0 & 0 & \mathrm{N} & 0 & 0 & -\mathrm{M} & 0 & \mathrm{M} \\ 0 & 0 & 0 & \mathrm{N} & 0 & 0 & -\mathrm{M} & 0 \\ -2\mathrm{S} & 2\mathrm{S} & 0 & 0 & 0 & 0 & 0 & 0 \\ -\mathrm{S} & 0 & \mathrm{S} & 0 & 0 & 0 & 0 & 0 \\ 0 & -\mathrm{S} & 0 & \mathrm{S} & 0 & 0 & 0 & 0 \\ 0 & 0 & -\mathrm{S} & 0 & 0 & 0 & 0 & 0 \end{bmatrix}$$

$$\tilde{\mathrm{B}} = \begin{bmatrix} 0 & 0 \\ 0 & 0 \\ 0 & 0 \\ 0 & \mathrm{M} \\ 0 & 0 \\ 0 & 0 \\ 0 & 0 \\ \mathrm{S} & 0 \end{bmatrix} \qquad (100)$$

and

$$\tilde{\mathrm{c}} = \begin{bmatrix} 1 & 0 & 0 & 0 & 0 & 0 & 0 & 0 \\ 0 & 0 & 0 & 0 & 1 & 0 & 0 & 0 \end{bmatrix}$$

where N, M, S are defined as follows:

$$S = \frac{-a^2}{2gA\Delta x}$$

$$N = \frac{-f}{DA} \tag{101}$$

$$M = \frac{-Ag}{2\Delta x}$$

3.6. Observability and controllability

In this section the controllability and observability of the system is analyzed. The controllability and observability of the system is studied in Lemma 1 and Lemma 2 respectively.

For more information, details, and proofs reader is referred to these works [80], [81].

Lemma 1. For a linear system (54), (56) with N_u Control inputs, that is Head pressure and N_y out puts, that if measured flow rates, the controllability of matrix $\mathbb{C}_i$ is given by [80]:

$$\mathbb{C}_i(A, B) \coloneqq [B\ AB\ A^2B\ A^3B\ \ \ldots\ A^{i-1}B] \tag{102}$$

By the using the Cayley-Hamilton theorem, the rank of $\mathbb{C}_i$ is determined by the first $N \times N_u$ columns, where N is the state dimension and equal the dimension of Matrix A.

A linear system (or, equivalently, the matrix pair (A, B)) is called controllable if the controllability matrix has full row rank (i.e. $\{Rank(\mathbb{C}) = i$). where i is the state space dimension dim X.

Lemma 2. For linear system (63) and (68) described in Lemma.1. the observability matrix O_i can be defined as [81]:

$$\mathrm{O}_i(C,A) := \begin{bmatrix} C \\ CA \\ CA^2 \\ \vdots \\ CA^{i-1} \end{bmatrix} \tag{103}$$

Again by the Cayley-Hamilton theorem, the rank of O_i is determined by the first $N \times N_u$ rows, where N is the state dimension and equal the dimension of Matrix A. In Other words, $\ker(\mathrm{O}_\infty) = \ker(\mathrm{O}_i) = i \subset R^N$.

A linear system (or, equivalently, the matrix pair (A, C)) is called observable if the observability matrix has full columns rank (i.e. $Rank(O_i) = i$). where i is the number of independent columns in the observability matrix.

3.7. Simulation results

The simulations in this section are carried out using Matlab.

An illustration of the model is shown in Figure 1. In this figure the length of the pipeline is $L = 5.1 \times 10^3\, m$, the diameter of the pipe is $D = 0.56\, m$, the cross section is $A = 0.246\, m^2$, density is $\rho = 1000\, kg/m^3$, gravity is $g = 9.81\, m/s^2$ and the wave speed coefficient is $a = 1250\, m/s$ that are summarized in Table 3.1.

Table. 3.1. The proposed characteristics of the pipeline

L	$5.1 \times 10^3\, m$
D	$0.56\, m$
A	$0.246\, m^2$,
F	0.001
a	$1250\, m/s$
g	$9.81\, m/s^2$
ρ	$1000\, kg/m^3$

3.7.1. Case 1

Control variables according the case1 model are the pressures at the beginning and end of the pipe ($H_1\ and\ H_5$) and can be directly measured. Furthermore, the flow rates ($Q_1\ and\ Q_4$) are outputs of system. According to Lemmas 1 and 2, the rank of discriminant matrices is $rank\ \mathbb{C} = \ rank\ O\ = 16$, thus, the system is completely observable and controllable.

For case 1 the result will be Figure 3.2 displays the simulated pressure head at the inlet ($H\ (in) = H_1 = 10\ m$) and outlet ($H\ (out\ ) = H_5 = 7\ m$) of the pipe.

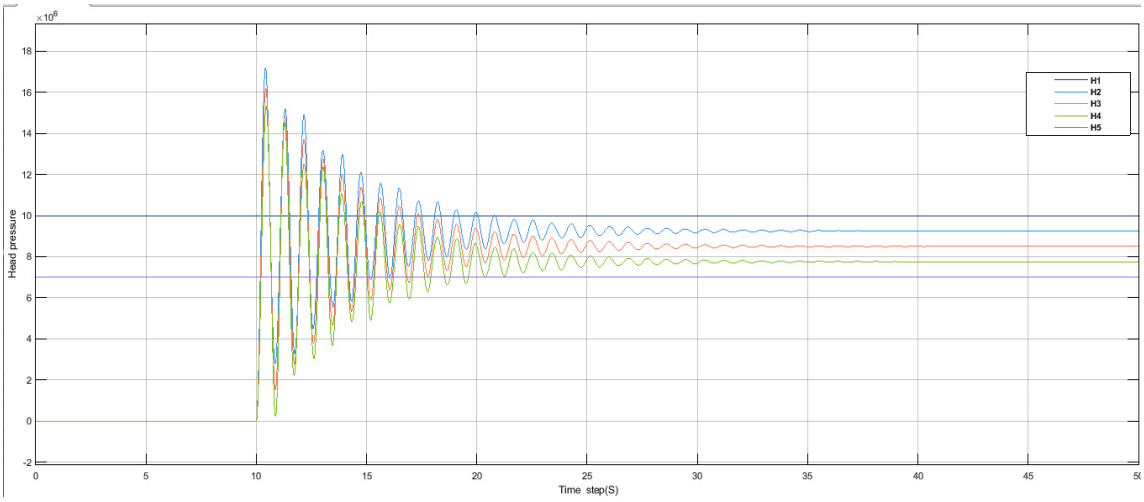

Figure 3.2 Pressure head variation for case 1

Figure 3.3 shows the evolution of the inflow and outflow, Q_1 and Q_5, respectively. It can be seen that after a few seconds the Q from the initial amount (0) is approaching the real amount. Therefore, the pipeline system is completely observable and controllable.

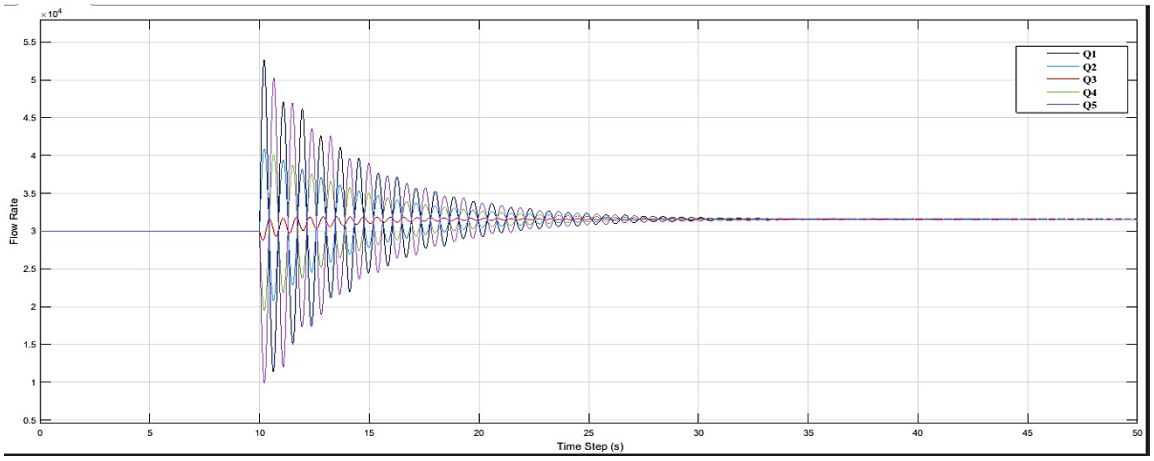

Figure 3.3 Output and input flow variation case 1

3.7.2. Case 2

Control variables according the case 2 are the pressures head at the beginning and flow rate at the end of the pipe (H_1 and Q_5) and can be directly measured. Furthermore, the flow rates (Q_1) and pressure head (H_n)are output of system. According to Lemma 1 and 2, the rank of discriminant matrices is $rank\ \mathbb{C} = \ rank\ O\ = 16$, thus, the system is completely observable and controllable.

For case 2 the result will be Figure 3.4 displays the simulated pressure head at the inlet ($H\ (in) = H_1 = 10\ m$) and Flow rate in outlet ($Q\ (out\ ) = H_5 = 3.2$) of the pipe.

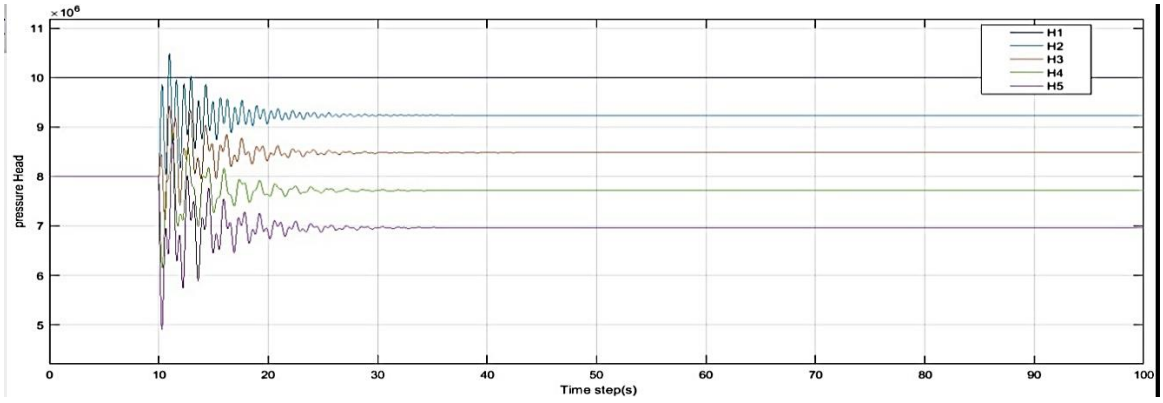

Figure 3.4 Pressure head variation for case 2

Figure 3.5 shows the evolution of the inflow and outflow, Q_1 and Q_5, respectively. It can be seen that after a few seconds the Q from the initial amount (0) is approaching the real amount. Therefore, the pipeline system is completely observable and controllable.

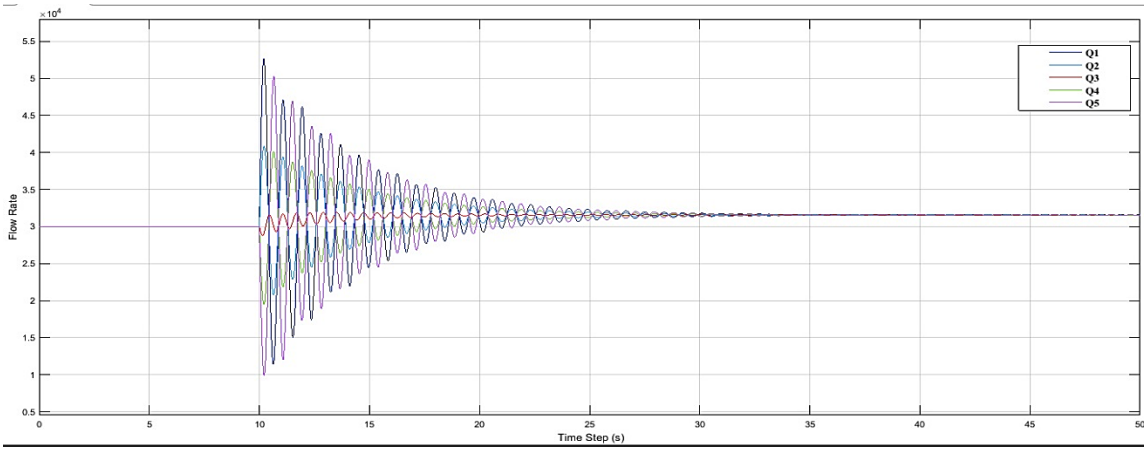

Figure 3.5 Flow rate for case 2

3.7.3. Case 3

Control variables according the case 3 are the pressures head and flow rate at the beginning of the pipe (Q_1 and H_1) and can be directly measured. Furthermore, the flow rates (Q_{n}) and pressure head (H_{n})are output of system. According to Lemma 1 and 2, the rank of discriminant matrices is $rank\ \mathbb{C} = \ rank\ O\ = 16$, thus, the system is completely observable and controllable.

For case 3 the result will be Figure 3.6 displays the simulated pressure head at the inlet ($H\ (in) = H_1 = 10\ m$) and the flow rate in outlet ($Q\ (out\ ) = H_5 = 3.2$) of the pipe.

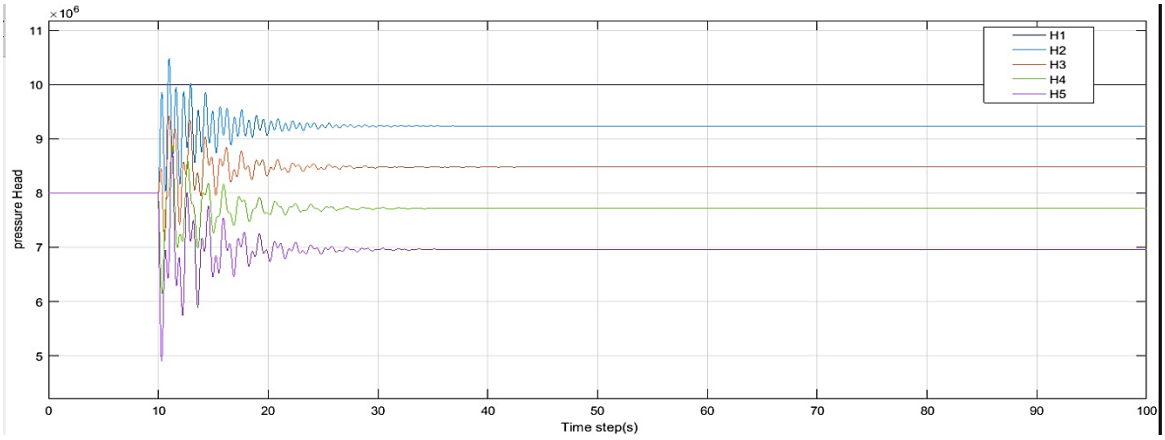

Figure 3.6 Pressure head variation forcase 3

Figure 3.7 shows the evolution of the inflow and outflow, Q_1 and Q_5, respectively. It can be seen that after a few seconds the Q from the initial amount (0) is approaching the real amount. Therefore, the pipeline system is completely observable and controllable.

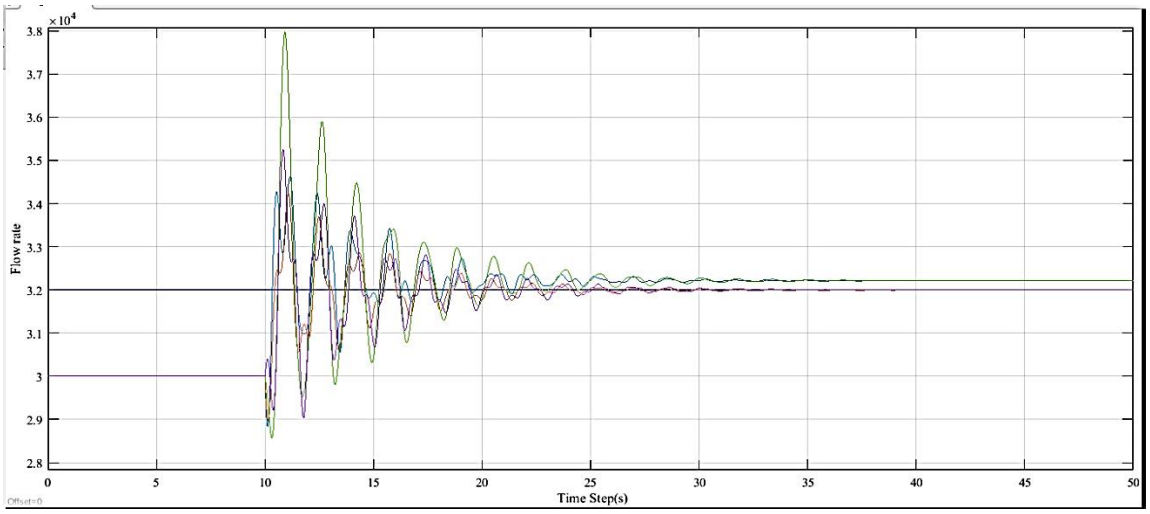

Figure 3.7 Flow rate for case 3

3.7.4. Case 4

Control variables according to case 4 are the flow rate at the beginning and pressures head at the end of the pipe (Q_1 and H_5) and can be directly measured. Furthermore, the flow rates

(Q_{n}) and the pressure head (H_1) are output of system. According to Lemmas 1 and 2, the rank of discriminant matrices is $rank\ \mathbb{C} = \ rank\ O\ = 16$, thus, the system is completely observable and controllable.

For case 2 the result will be Figure 3.8 which displays the simulated pressure head at the outlet ($H\ (out) = H_n = 7\ m$) and the flow rate in inlet ($Q\ (in\ ) = Q_1 = 3.2$) of the pipe.

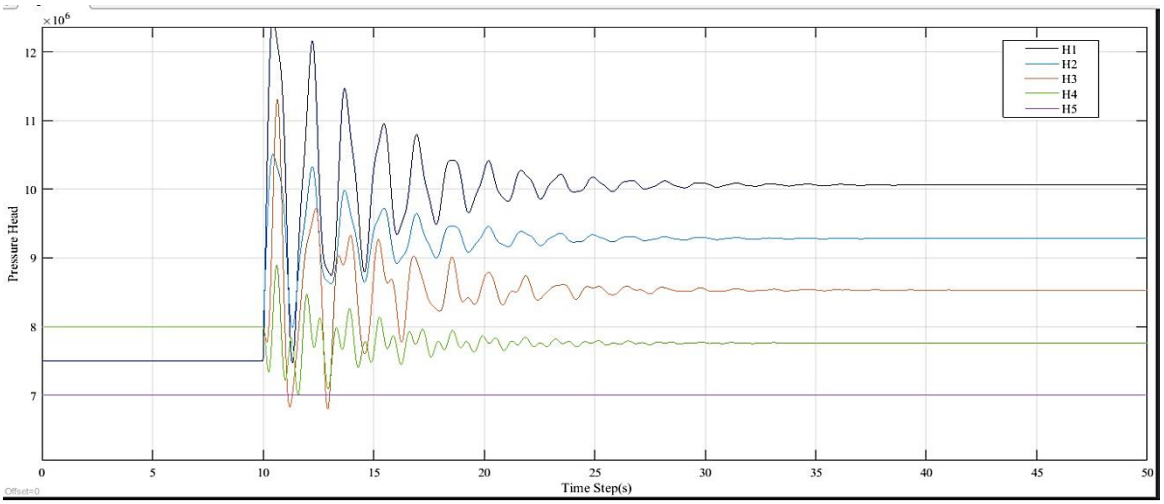

Figure 3.8 Pressure head variation for case 4

Figure 3.9 shows the evolution of the inflow and outflow, Q_1 and Q_5, respectively. It can be seen that after a few seconds the Q from the initial amount (0) is approaching the real amount. Therefore, the pipeline system is completely observable and controllable.

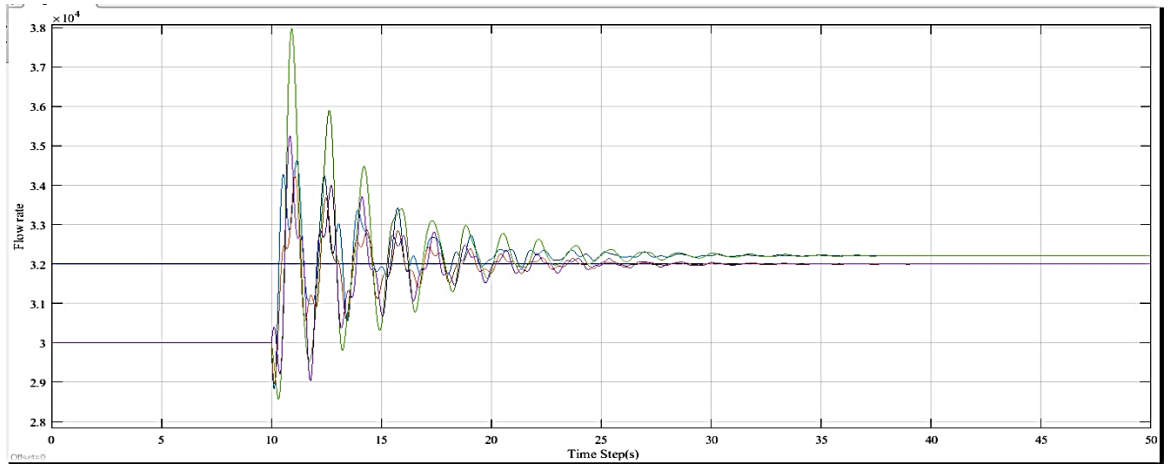

Figure 3.9 Flow rate for case 4

3.7.5. Case 5

Control variables according to case 5 are the flow rate at the beginning and end of the pipe (Q_1 and Q_5) and can be directly measured. Furthermore, the pressure head (H_1, H_n) are output of system. According to Lemmas 1 and 2, the rank of the discriminant matrices is $rank\ \mathbb{C} = \ rank\ O\ = 16$, thus, the system is completely observable and controllable.

For case 5 the result will be Figure 3.10 the displays the simulated flow rate at the outlet ($Q\ (out) = Q_n = 3.2$) and flow rate in inlet ($Q\ (in\ ) = Q_1 = 3.2$) of the pipe.

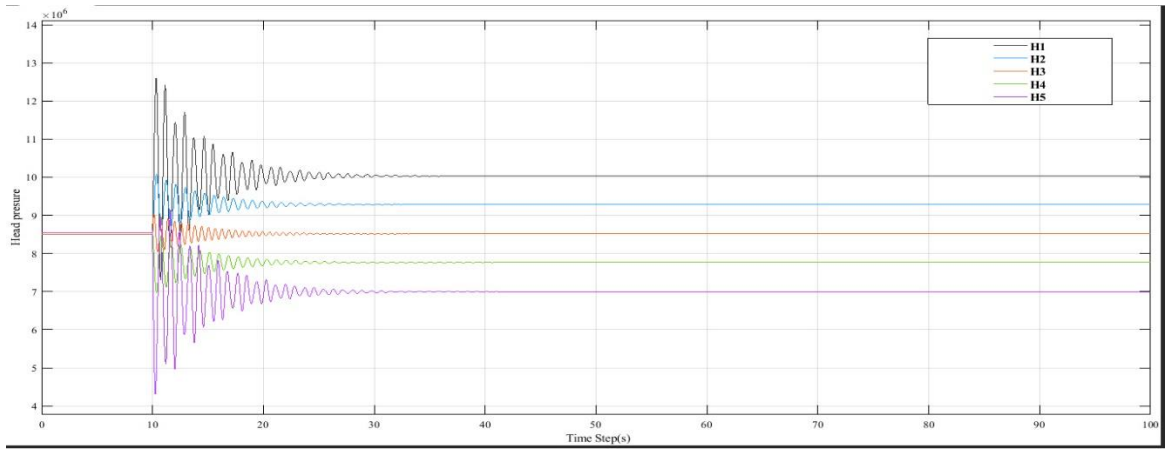

Figure 3.10 Pressure head variation for case 5

Figure 3.11 shows the evolution of the inflow and outflow, Q_1 and Q_5, respectively. It can be seen that after a few seconds the Q from the initial amount (0) is approaching the real amount. Therefore, the pipeline system is completely observable and controllable.

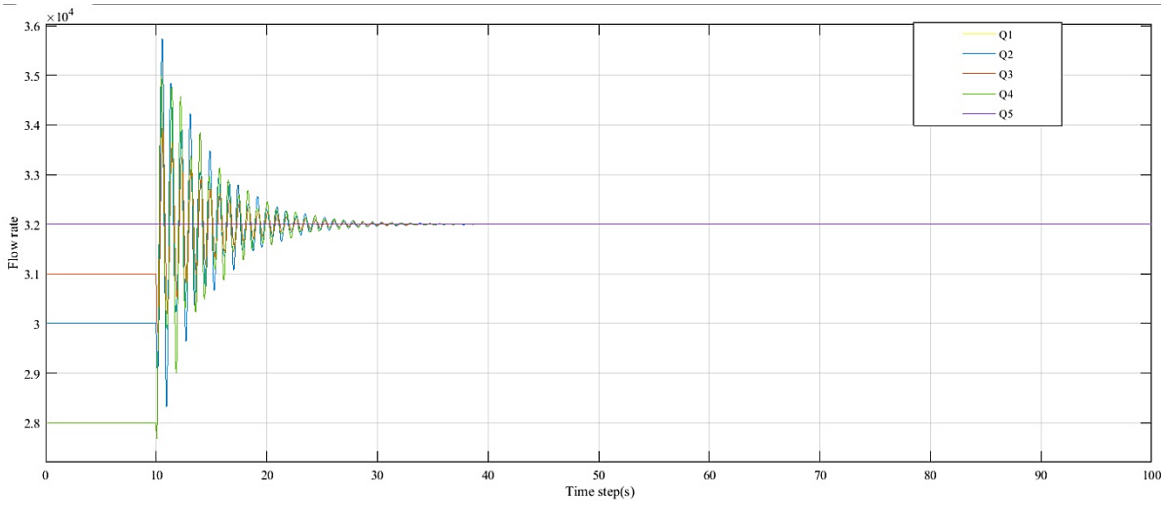

Figure 3.11 Flow rate for case 5

3.7.6. Case 6

Control variables according to case 6 are the flow rate and pressures head at the end of the pipe ($Q_5\ and\ H_5$) and can be directly measured. Furthermore, the flow rates (Q_1) and pressure head (H_1) are output of system. According to Lemmas 1 and 2, the rank of the discriminant matrices is $rank\ \mathbb{C} = \ rank\ O\ = 16$, thus, the system is completely observable and controllable.

For case 6 the result will be Figure 3.12 , which displays the simulated pressure head at the outlet ($H\ (in) = H_n = 7\ m$) and flow rate in outlet ($Q\ (in\ ) = Q_1 = 3.2$) of the pipe.

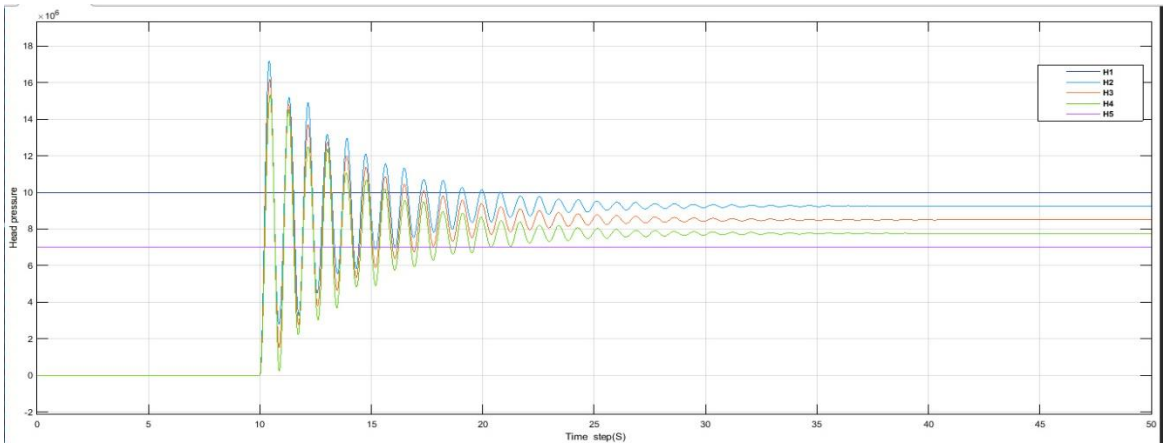

Figure 3.12 Pressure head variation case6

Figure 3.13 shows the evolution of the inflow and outflow, Q_1 and Q_5, respectively. It can be seen that after a few seconds the Q from the initial amount (0) is approaching the real amount. Therefore, the pipeline system is completely observable and controllable.

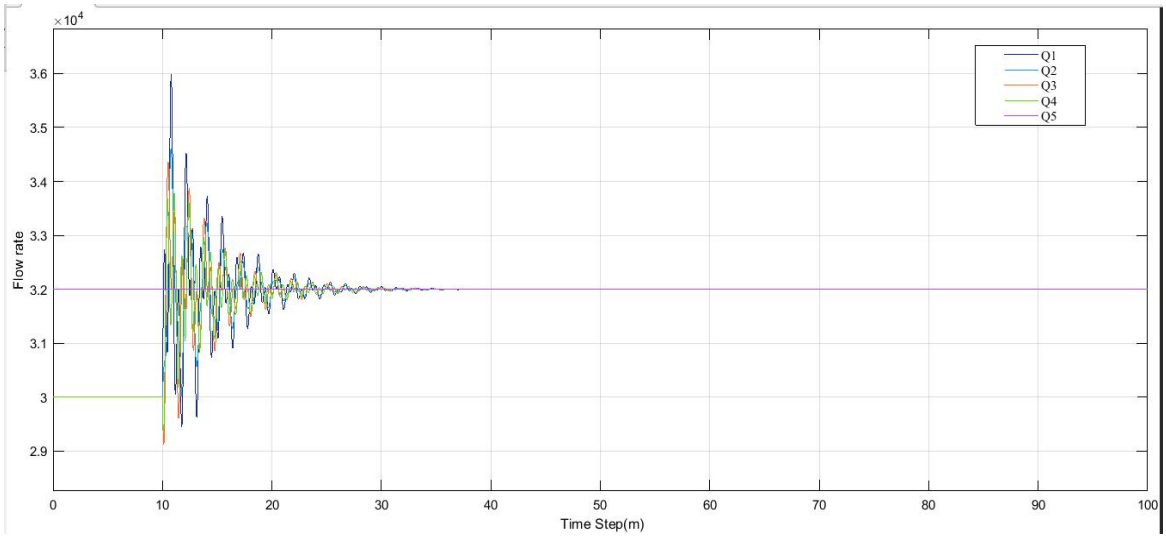

Figure 3.13 Flow rate for case 6

3.8. Conclusion

The objective of this chapter is analyzing the observability and controllability of the pipeline system. The system is stated by hyperbolic partial differential equations. In this chapter, the finite difference method is applied as it is a simple way to get a more convenient model in order to observe and control the structure of the nonlinear system. This method divides the entire pipeline into N number of sections. Some theorems and lemmas are presented in order to test the observability and controllability of the system. Future work is to study the stability of the pipeline system.

Chapter Four: Monitoring and modelling of pipeline leakage

4.1. Introduction

A leak is a way for fluid to escape a container or fluid-containing system, such as a tank or a ship's hull, through which the contents of the container can escape or outside matter can enter the container. Leaks are usually unintended and therefore undesired. The word leak usually refers to a gradual loss; a sudden loss is usually called a spill.

The matter leaking in or out can be gas, liquid, a highly viscous paste, or even a solid such as a powdered or granular solid or other solid particles.

Potable water is a critical resource to human society. Failure and inefficiencies in transporting drinking water to its final destination wastes resource and energy. With limited access to fresh water reserves and increasing demand of potable water, water shortage is becoming a critical challenge. So, addressing water losses during distribution presents significant opportunity for conservation.

Leaks are the major factor for unaccounted water losses in almost every water distribution network; old or modern. Vickers [82] reports water losses in US municipalities to range from 15 to 25 percent. The Canadian Water Research Institute [83] reports that on average, 20 percent of treated water is wasted due to losses during distribution and other unaccounted means. A study on leakage assessment in Riyadh, Saudi Arabia shows the average leak percentage of the ten studied areas to be 30 percent [84]**.** Losses through leaks represent a significant portion of the water supply, hence identification and elimination of leaks is imperative to efficient water resource management.

Fault detection and isolation (FDI) in real pipelines remains an important challenge for proper distribution of fluids, specifically in all aspects related to the opportune diagnosis of leaks and obstructions. Many of the FDI techniques rely on models which are themselves based on the fluid dynamics in the pipeline. Some of these techniques have been presented in Billman and Isermann [85], Benkherouf and Allidina [86], Verde [87], Besançon et al. [88] to cite a few.

A mathematical description of the pipeline dynamics was derived by theoretical modelling for gas pipelines [89] [90] and liquid pipelines [91]. Simplifying assumptions such as a

constant diameter D, a turbulent flow and isothermic conditions result in a common description for the gas and liquid flow dynamics. Assuming the fluid to be slightly compressible and the duct walls slightly deformable, the convective changes in velocity to be negligible, the cross section area of the pipe and the fluid density to be constant, then the dynamics of the pipeline fluid can be described in next section.

In the present chapter, the purpose is to summarize the modeling approach commonly used for the design of FDI techniques based on dynamical models.

4.2. Leak modeling

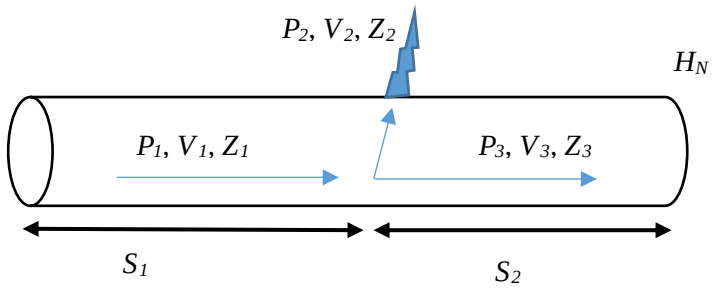

Figure 4.1 Scheme of a hole in a pipe

A mathematical expression for a leak can be deduced from Bernoulli's equation, which relates the pressure difference between the pipeline inside and outside.

Bernoulli's equation applies under the following considerations. [92]

- Non viscous flow
- Permanent or continuous flow
- Along the Pipe line
- Constant density

Let us consider a hole in a pipe as shown in Figure 4.1 Bernoulli's equation between points 1 and 2 is given by

$$\frac{p_1}{\gamma} + \frac{v_1^2}{2} + Z_1 = \frac{p_2}{\gamma} + \frac{v_2^2}{2} + Z_2 \tag{104}$$

where P is the pressure of the fluid load, v is the speed of the fluid, and Z is the elevation.

By taking into account that

$$Z_1 - Z_2 = 0, P_2 = p_{atm} = 0 \text{ and } H = \frac{p_1}{\gamma} + \frac{v_1}{2g} \tag{105}$$

reduces to

$$v_2 = \sqrt{2gH} \tag{106}$$

This represents the speed of the fluid outside the hole. Since the flow at such a point is given by the product of the output velocity and the hole area, we get

$$Q = A\sqrt{2gH} \tag{107}$$

where Q is the theoretical flow rate through the hole and A is the hole area.

Finally, the expression for the flow of a leak in a pipe at a point z_{leak} is given by

$$Q_{leak} = \lambda\sqrt{H(z_{leak}, t)} \tag{108}$$

with $\lambda \geq 0$.

4.3. The model modification of the pipeline with leakage

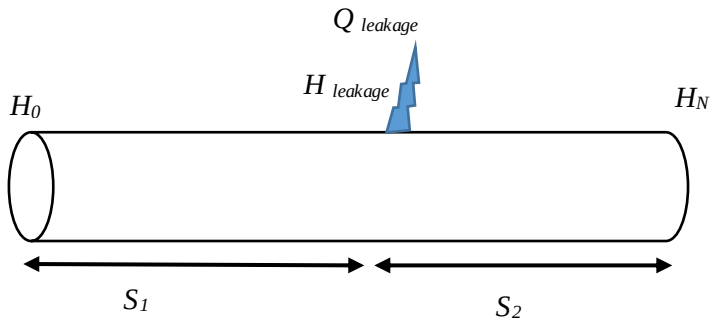

Figure 4.2 Schematic of pipeline with leakage

A leakage flow at some coordinate x_l in the pipeline, denoted by Q_l, is approximately proportional to the square root of the pressure head at this coordinate, H_l, according to:

$$Q_l(t) = \sqrt{\lambda H_l(t)} \tag{109}$$

Where λ denotes a constant that includes properties such as the cross-sectional area of the leak and a discharge coefficient and Q_l is the flow through the leak and H_l is pressure head at the leak point [93].

Each leak produces a discontinuity in the mass flow rate. The mass conservation at Q_l requires that:

$$Q_l = Q_0 - Q_N \tag{110}$$

where $Q_0$and Q_N are the flows in the beginning section of the pipeline and end of pipeline that leak respectively.

Now for the leak detection, the idea is to assume that one leak may occur at each section end, and include its influence in the above model via equations (54) and (56), with unknown magnitude. By designing an observer to reconstruct the magnitude for each leak of this kind, one can detect and isolate them, provided that they indeed occur close to the points a priori considered.

In order to be even more precise, one can further include the location of such possible leaks within the set of unknown variables to be reconstructed by the observer. Leak detection and isolation is then turned to a matter of amplitude and location estimations, and clearly this can in principle be done for any a priori given number of leaks to be detected.

Obviously larger the number of leaks is, the larger the excitation needed for the observer will be.

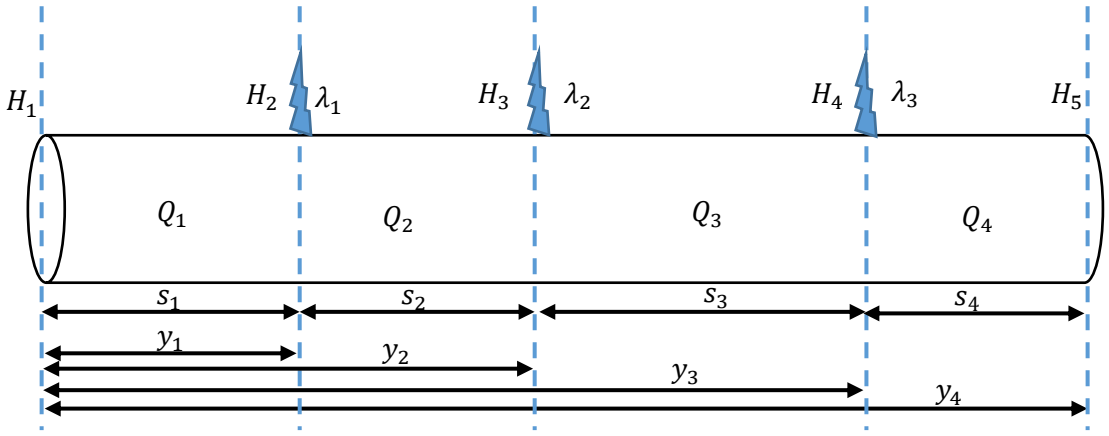

Figure 4.3 Schematic of pipeline with three leakage

In the above case of four-section model, one can consider three leaks along the pipeline, located at $y_{1\,leak} \coloneqq s_1$ and $y_{2\,leak} \coloneqq s_1 + s_2$ and $y_{3\,leak} \coloneqq s_1 + s_2 + s_3$ respectively, with $y_1$and y_2 and y_3 being unknown.

Of course if L denotes the total length of the pipeline, x_4 will be given by $s_4 = L - s_1 - s_2 - s_3$.

Assuming that the unknown amount (represented by coefficients λ_1 , λ_2 and λ_3 in (109) are constants, as well as the unknown locations (represented by with s_1, s_2 and s_3 via $y_{1\,leak}$, $y_{2\,leak}$ and $y_{3\,leak}$).

The equation (109) can be modified by including six additional state variables, $x_8 \coloneqq s_1, x_9 \coloneqq s_2, x_{10} \coloneqq s_3\ x_{11} \coloneqq \lambda_1\ x_{12} \coloneqq \lambda_2, x_{13} \coloneqq \lambda_3$ as follows:

$$\dot{Q}_1 = \frac{-Ag}{s_1}(H_2 - H_1) - \frac{f}{DA}Q_1$$

$$\dot{Q}_2 = \frac{-Ag}{s_2}(H_3 - H_2) - \frac{f}{DA}Q_2$$

$$\dot{Q}_3 = \frac{-Ag}{s_3}(H_4 - H_3) - \frac{f}{DA}Q_3$$

$$\dot{Q}_4 = \frac{-Ag}{L - s_1 - s_2 - s_3}(H_5 - H_4) - \frac{f}{DA}Q_4$$

$$\dot{H}_2 = \frac{-a^2}{gAs_1}(Q_2 - Q_1 - \sqrt{\lambda_1 H_2})$$

$$\dot{H}_3 = \frac{-a^2}{gAs_2}(Q_3 - Q_2 - \sqrt{\lambda_2 H_3}) \qquad (111)$$

$$\dot{H}_4 = \frac{-a^2}{gAs_3}(Q_4 - Q_3 - \sqrt{\lambda_3 H_4})$$

$$\dot{S}_1 = 0$$

$$\dot{S}_2 = 0$$

$$\dot{S}_3 = 0$$

$$\dot{\lambda}_1 = 0$$

$$\dot{\lambda}_2 = 0$$

$$\dot{\lambda}_3 = 0$$

Again we have to write this equation with element of x and the form of steady state is as

follows :

$$\dot{x}_1 = \frac{-Ag}{x_8}(x_5 - u_1) - \frac{f}{DA}x_1$$

$$\dot{x}_2 = \frac{-Ag}{x_9}(x_6 - x_5) - \frac{f}{DA}x_2$$

$$\dot{x}_3 = \frac{-Ag}{x_{10}}(x_7 - x_6) - \frac{f}{DA}x_3$$

$$\dot{x}_4 = \frac{-Ag}{l - x_8 - x_9 - x_{10}}(u_2 - x_7) - \frac{f}{DA}x_4$$

$$\dot{x}_5 = \frac{-a^2}{gAx_8}(x_2 - x_1 - \sqrt{x_{11}x_5})$$

$$\dot{x}_6 = \frac{-a^2}{gAx_9}(x_3 - x_2 - \sqrt{x_{12}x_6}) \qquad (112)$$

$$\dot{x}_7 = \frac{-a^2}{gAx_{10}}(x_4 - x_3 - \sqrt{x_{13}x_7})$$

$$\dot{x}_8 = 0$$

$$\dot{x}_9 = 0$$

$$\dot{x}_{10} = 0$$

$$\dot{x}_{11} = 0$$

$$\dot{x}_{12} = 0$$

$$\dot{x}_{13} = 0$$

Again for finding the state-space of the system the equations (54), (56) should be written in other form as flow [94]:

$$\dot{x}(t) = f(x(t) + g(x(t))u(t)) = f(x(t), u(t))$$
$$y(t) = h(x(t)) \tag{113}$$

where $x \in \mathbb{R}^n$ is the state, $u \in \mathbb{R}^m$ is the input, $y \in \mathbb{R}^p$ is the output and f, g, h are sufficiently differentiable vectors function.

4.4. Observer formulation

The problem of observer design naturally arises in a system approach, as soon as one needs some internal information from external (directly available) measurements.

In general indeed, it is clear that one cannot use as many sensors as signals of interest characterizing the system behavior (for cost reasons, technological constraints, etc.) [95]

In control theory, a state observer is a system that provides an estimate of the internal state of a given real system, from measurements of the input and output of the real system. It is typically computer-implemented, and provides the basis of many practical applications.

Knowing the system state is necessary to solve many control theory problems. In most practical cases, the physical state of the system cannot be determined by direct observation. Instead, indirect effects of the internal state are observed by way of the system outputs. A simple example is that of vehicles in a tunnel: the rates and velocities at which vehicles enter and leave the tunnel can be observed directly, but the exact state inside the tunnel can only be estimated. If a system is observable, it is possible to fully reconstruct the system state from its output measurements using the state observer. [96]

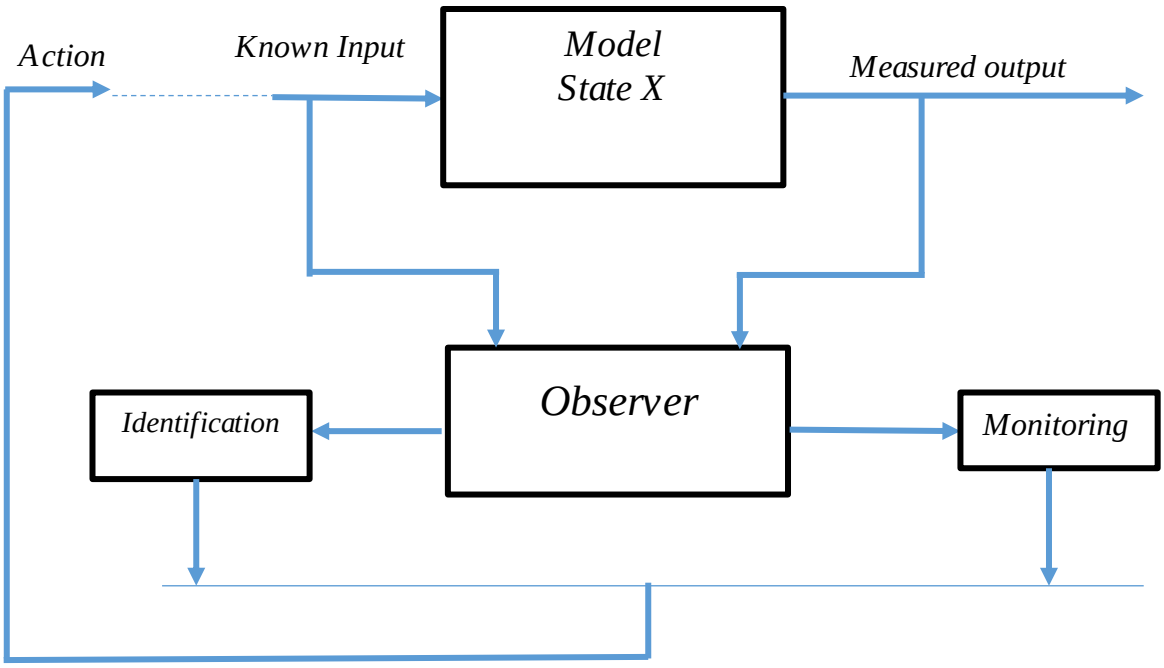

Figure 4.4 Observer model

The idea is to design an observer for the leak detection. The system under consideration will be considered to be described by a state-space representation generally of the following form:

$$\dot{x}(t) = f\big(x(t), u(t)\big) = f\big(x(t)\big) + g(x(t))u(t)$$
$$y(t) = [h_1(x), h_2(x)]^T = h(x(t)) \qquad (114)$$

where x denotes the state vector, u denotes the vector of known external inputs and y denotes the vector of measured outputs.

Functions f and h will in general be assumed to be C^∞ with respect to their arguments, and input functions $u(.)$ to be locally essentially bounded.

4.5. Luenberger observer

4.5.1. Linear approaches

Equation (54) and (56) resulting in (114) is in general nonlinear, and a very first approach could be to consider an approximate linearization around some fixed operation regime, giving rise to a standard linear time-invariant system of the form

$$\begin{aligned} \dot{x}(t) &= Ax(t) + Bu(t) \\ y(t) &= Cx(t) \end{aligned} \tag{115}$$

Under this form, it is well known that a simple observability condition on A, C guarantees that a so-called Luenberger observer [97]can solved for the state reconstruction issue, such as

$$\dot{\hat{x}}(t) = A\hat{x}(t) - K\big(C\hat{x}(t) - y(t)\big) + Bu(t) \tag{116}$$

for any matrix K such that $A - KC$ is Hurwitz (i.e., has all its eigenvalues with strictly negative real parts).

In fact, because of the great sensitivity of the operation point with respect to faults like leaks or obstructions, this approach is not successful in general. [98]

4.5.2. Nonlinear approaches Luenberger Extension

The most famous extension of the Luenberger observer is the so-called high-gain observer [99]which applies to systems when it is rewritten under the form

$$\begin{aligned} \dot{\xi}(t) &= A_0\xi(t) + \varphi\big(\xi(t), u(t)\big) \\ y(t) &= C_0\xi(t) \end{aligned} \tag{117}$$

Where $A_0 = \begin{bmatrix} 0 & I_p & & 0 \\ & \ddots & \ddots & \\ & & & I_p \\ 0 & \dots & & 0 \end{bmatrix}, C_0 = (I_p\ 0\ \cdots 0)$ and $\varphi(\xi, u)$ satisfies the Lipschitz condition in ξ uniformly in u and can be described by

$$\varphi(\xi, u) = \begin{bmatrix} \varphi_1(\xi_1, u) \\ \varphi_2(\xi_1, \xi_2, u) \\ \vdots \\ \varphi_{q-1}(\xi_1, \dots, \xi_{q-1}, u) \\ \varphi_q(\xi, u) \end{bmatrix} \text{ for } \xi = \begin{bmatrix} \xi_1 \\ \xi_2 \\ \\ \vdots \\ \xi_q \end{bmatrix} \tag{118}$$

with $\xi_i \in R^p$, if $y \in R^p$, and I_p stands for the $p \times p$ identity matrix.

This is possible under the uniform observability property [100] and an observer then takes the form

$$\dot{\hat{\xi}}(t) = A_0\hat{\xi}(t) + \varphi\left(\hat{\xi}(t), u(t)\right) - K_0[C_0\hat{\xi}(t) - y(t)] \tag{119}$$

where K_0 is such that $A_0 - K_0C_0$ is Hurwitz, and λ is to be chosen large enough to guaranty convergence, simultaneously allowing the tuning of the convergence rate.

4.6. Lie derivative

In differential geometry, the Lie derivative named after Sophus Lie, evaluates the change of a tensor field, along the flow of another vector field. This change is coordinate invariant and therefore the Lie derivative is defined on any differentiable manifold.

We now introduce a Lie derivative, which is virtually a directional derivative for

a scalar field $\lambda(x)$ with $x \in \mathbb{R}^n$ along the direction of an n-dimensional vector field

$f(x)$. The mathematical expression is given as

$$L_f\lambda(x) = \frac{\partial\lambda(x)}{\partial x} f(x) \tag{120}$$

Since $\frac{\partial \lambda(x)}{\partial x} x$ is a $1 \times n$ gradient vector of the scalar $\lambda(x)$and the norm of a gradient vector represents the maximum rate of function value changes, the product of the gradient and the vector field $f(x)$ in system becomes the directional derivative of $\lambda(x)$ along $f(x)$. Therefore, the Lie derivative of a scalar field defined by (120) is also a scalar field.

If each component of a vector field $h(x) \in \mathbb{R}^p$, p is considered to take a Lie derivative along $f(x) \in \mathbb{R}^n$, then all components can be acted on concurrently and the result is a vector field that has the same dimension as $h(x)$; its i th element is the Lie derivative of the $i - th$ component of $h(x)$. Namely, if $h(x) = [h_1(x), \dots, h_p(x)\ ]^T$ and each component $h_1(x), i = 1, \dots, p$ is a scalar field, then the Lie derivative of the vector field $h(x)$ is defined as

$$L_f h(x) = \begin{bmatrix} L_f h_1(x) \\ \vdots \\ L_f h_p(x) \end{bmatrix} \tag{121}$$

With the Lie derivative concept, we now define an observation space Ω over $\mathbb{R}^n$ as

$$\Omega = \text{span}\ \{\text{h(x)}, L_f h\ \ (x), \dots, L_f^{n-1} h\ \ (x)\ \} \tag{122}$$

In other words, this space is spanned by all up to order n Lie derivatives of the output function $h(x)$.

The system is observable if and only if $\dim(d\Omega\ ) = n$. For a proof. See [101]

4.7. Example (model for pipe with two sections)

Let us recall how such an approach can be applied to leak position and magnitude estimation by considering the model(54) (56)(54) reduced to two sections, that is Q_1, H_2, Q_2 with Q_1 and Q_2 measured variables and as state variables x_1, x_2, x_3. If this state is extended with a single leak at unknown position z (defined as state variable x_4) and the unknown coefficient

λ (defined as state variable x_5), and subject to inputs $u_1 = H_1$, $u_2 = H_3$, we have state-space representation under (54) and (56) and (114) as follows:

$$\begin{aligned} \dot{x}(t) &= f\big(x(t)\big) + g(x(t))u \\ y &= h(x(t)) \end{aligned} \tag{123}$$

With $x \coloneqq [Q_1\ H_2\ \ Q_2\ z\ \lambda]^T = [x_1\, x_2\, x_3\, x_4\, x_5\,]^T$.

Notice that under constant down stream pressure operation, as this will be considered $H_{out} = H_3$.

$$\begin{aligned} \begin{bmatrix} \dot{x_1} \\ \dot{x_2} \\ \dot{x_3} \\ \dot{x_4} \\ \dot{x_5} \end{bmatrix} = \begin{bmatrix} \dot{Q_1} \\ \dot{H_2} \\ \dot{Q_2} \\ \dot{z_1} \\ \dot{\lambda} \end{bmatrix} &= \begin{bmatrix} \dfrac{-gA}{z}(H_2 - H_1) \\ -\dfrac{b^2}{gAz}(Q_2 - Q_1 + \lambda\sqrt{H_2}) \\ -\dfrac{gA}{L-z}(H_3 - H_2) \\ 0 \\ 0 \end{bmatrix} \\ &= \begin{bmatrix} \dfrac{-gA}{x_4}(x_2 - u_1) \\ -\dfrac{b^2}{gAx_4}(x_3 - x_1 + x_4\sqrt{x_2}) \\ -\dfrac{gA}{L-x_4}(u_2 - x_2) \\ 0 \\ 0 \end{bmatrix} \end{aligned} \tag{124}$$

Let the vector of output derivatives $H(x)$, be defined as follows:

$$H(x) = \begin{pmatrix} h_1(x) \\ L_f h_1(x) \\ L_f^2 h_1(x) \\ h_2(x) \\ L_f h_2(x) \end{pmatrix} \tag{125}$$

Where $L_f^i h_j(x)$ represents the i −th Lie derivate of $h_j(x)$ in the f vector field direction. For system(123), the main objective is the estimation of the state x based on the output measurement y, its derivatives H(x) and state transformation from output derivatives space, ψ to the original space state, x, defined precisely by $\psi = H(x)$.

The existence of this transformation for (123) is determined by the observability rank condition [102]

$$rank\big(\mathcal{O}(x)\big) = n \tag{126}$$

From equation (118), the vector H(x) for the system is defined

$$H(x) = \begin{pmatrix} \xi_1 \\ \dot{\xi}_1 \\ \ddot{\xi}_1 \\ \xi_2 \\ \dot{\xi}_2 \end{pmatrix} = \begin{pmatrix} h_1(x) \\ L_f h_1(x) \\ L_f^2 h_1(x) \\ h_2(x) \\ L_f h_2(x) \end{pmatrix} = \begin{pmatrix} x_1 \\ -\frac{gA}{x_4}(x_2 - u_1) \\ \frac{b^2}{x_4^2}(x_3 - x_1 + x_5\sqrt{x_2} - \dot{u}_1) \\ x_3 \\ \frac{gA}{L - x_4}(u_2 - x_2) \end{pmatrix} \tag{127}$$

From (117) we can write observer system as follow

$$\begin{aligned} \dot{x}_1 &= x_1 \\ \dot{\hat{x}}_1 &= \frac{-gA}{\hat{x}_4}(\hat{x}_2 - u_1) \\ \ddot{\hat{x}}_1 &= \frac{b^2}{\hat{x}_4{}^2}(\hat{x}_3 - \hat{x}_1 - \hat{x}_5\sqrt{\hat{x}_2} - \dot{u}_1) \\ \hat{x}_2 &= \left(\frac{L - \hat{x}_4}{gA}\right)\hat{x}_3 + u_2 \\ \hat{x}_3 &= x_3 \end{aligned} \tag{128}$$

$$\hat{\dot{x}}_3 = \frac{gA}{L - \hat{x}_4}(u_4 - \hat{x}_2)$$

$$\hat{x}_4 = \frac{L\hat{\dot{x}}_3 - gA(u_1 - u_2)}{\hat{\dot{x}}_3 - \hat{\dot{x}}_1}$$

$$\hat{x}_5 = \frac{1}{\sqrt{\hat{x}_2}}\left[\frac{\hat{x}_4}{b^2}\hat{\dot{x}}_1\right] + \frac{1}{\sqrt{\hat{x}_2}}[x_1 - x_3 + \dot{u}_1]$$

4.8. Simulation

In this chapter, we present simulation results in order to evaluate the performance of designed leak detection and isolation scheme. The simulator has the same structure as the model system (112).

For those simulations, a pipeline was considered with similar characteristics as summarized in Table 4.1 below.

For the sake of illustration, here are reported the results for one example of single leak detection and another one for the case of three simultaneous leaks.

In all cases, the initial pressure head at upstream and downstream point of the pipeline were fixed in 16[m]and 2 [m], respectively. That $u_2 = 2\,m$, simple signal and $u_1 = 16\,m$. The simulator was initialized in steady state condition as follows:$Q_1(0) = Q_2(0) = 8.3 \times 10^{-3}\left[\frac{m^3}{s}\right]$since, in a free-leak-pipeline, the inflow is equal to out flow ; for one leak $z_1(0) = 0.5\,L\,[m]$ the discrete point is located in the middle of pipe length, $\lambda(0) = 0[m^{\frac{5}{2}}/s]$ since, at the beginning of the simulation, the pipe is not leaking.

Figure 4.5 presents the simulated pressure head at inlet ($H_{in} = H_1$) and outlet (H_{out}) of the pipe.

Table 4. 1. Pipeline Characteristics

L	120
D	0.150
A	0.01767
b	1250m/s
g	9.81 m/s^2
f	0

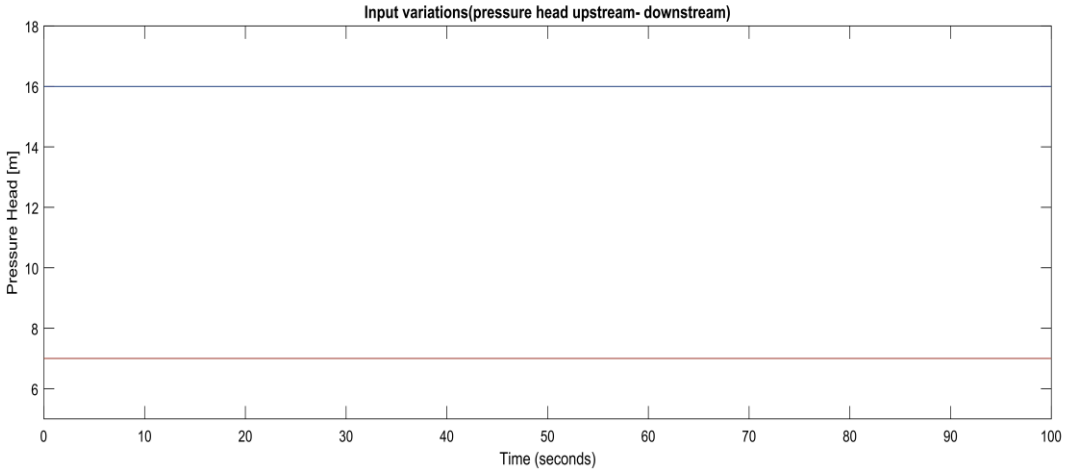

Figure 4.5 Pressure head at inlet and outlet of pipeline with leakage

Figure 4.6 shows the evolution of the inflow and outflow, Q_1 and Q_2 respectively. That shows after a few second the Q_1 from initial amount $Q(0)$ is reaching to real amount.

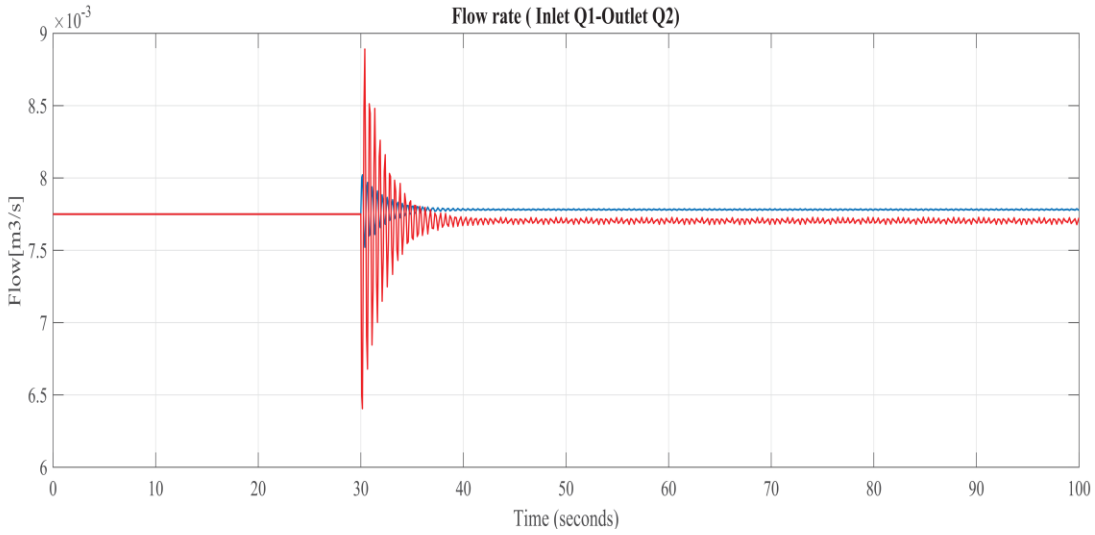

Figure 4.6 Flow rate at inlet and outlet of pipeline with leakage

In figure 4.7, the parameter valued λ are shown.

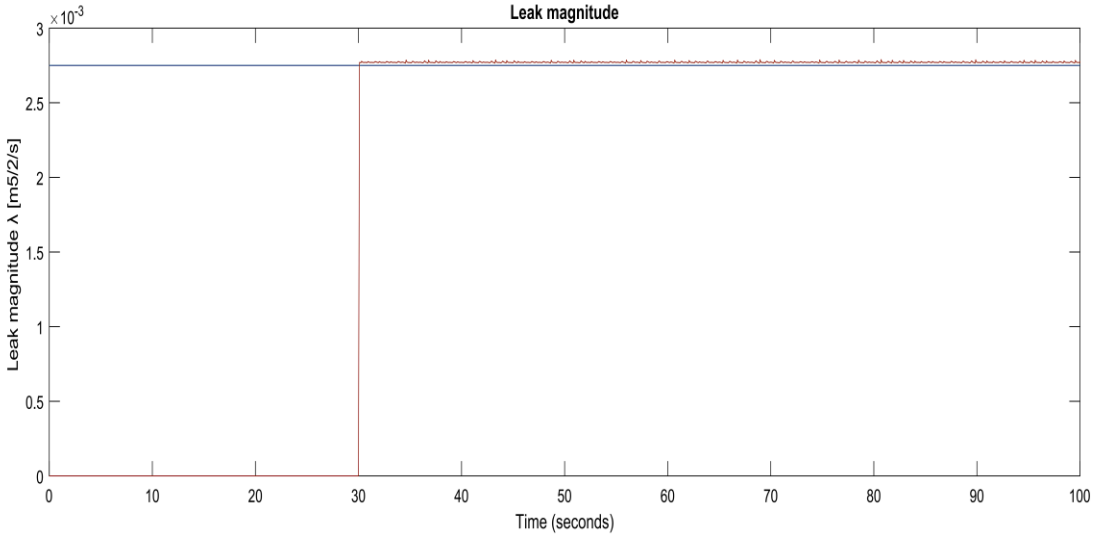

Figure 4.7 Leak magnitude

Finally, the leak position and pressure head is well estimated as seen in Figure 4.8.

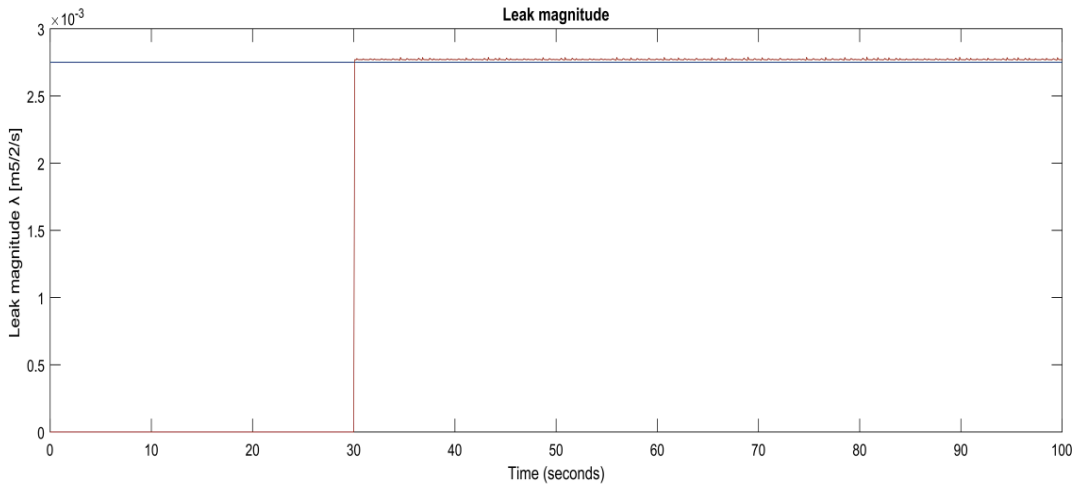

Figure 4.8 Leak position

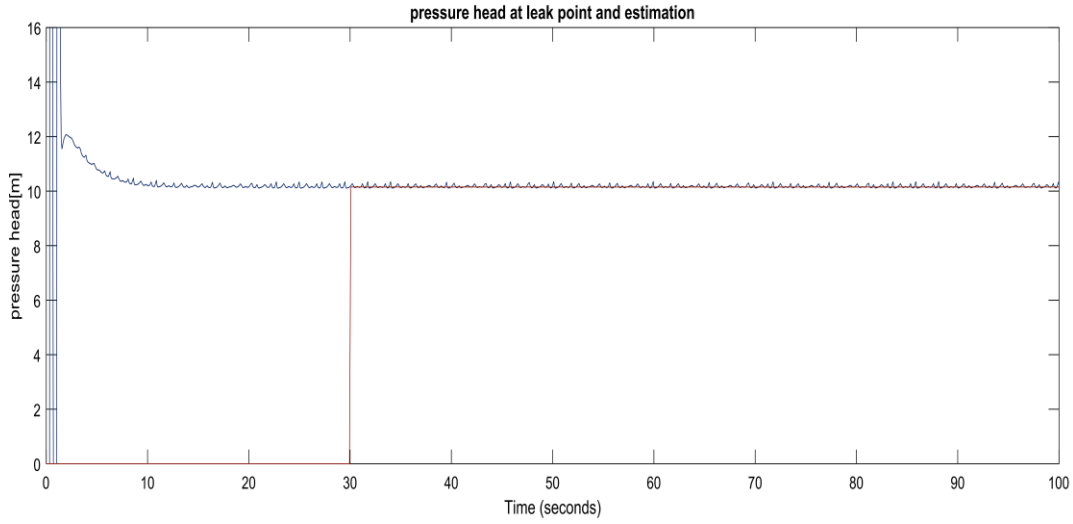

Figure 4.9 Pressure head at leak point (H2)

4.9. Conclusion

Pipelines and leak detection systems can be found in a wide variety of areas for various products. Accordingly, the challenges that the leak detection system faces vary depending on the application.

In this thesis is presented a model to confront the leak detection and location problem in a pipeline in which the position of the leaks are assumed unknown. The problem of leak detection and isolation in pipelines by means of nonlinear observers has been studied and tested in simulation. The detectability is guaranteed by appropriate excitation, chosen as a small varying input signal, via extensive simulations, and the results are quite promising.

It can be noticed that in the three-leak case which has been considered, the estimation performances could be improved by taking advantage of a first-step study on some equivalent single-leak location allowing to reduce the estimation problem.

But the fairly good results here obtained when directly facing the complete estimation problem are encouraging regarding its possible extension to detection of more leaks.

Chapter Five: Blockage

5.1. Introduction

Along with the development of industrial requirements, more and more long-distance pipelines have been built and served. According to the experiences, pipelines, as a means of transport, are the safest but this does not mean they are risk-free. Therefore, assuring the reliability of the gas pipeline infrastructure has become a critical need for the energy sector. Pipeline monitoring systems are indispensable in the areas of power plants petroleum and chemistry industries. When passing through the harsh environment, pipelines may be broken or blocked which would cause huge economic loss [103] [104] [105] [106].

Leaks and partial or complete blockages are common faults occurring in pipelines which cause problems. Leaks produce loss of fluid which leads to loss in pressure, production and economic cost, and in some cases it could affect the environment. Blockages impede flow leading to loss in pressure and hence increase the needed pumping force /cost to overcome the loss in pressure, and sometimes blockages could lead to complete stoppage of operation.

Early detection and accurate location of leaks or blockages could help to avoid the problems caused by such faults and foster the right timing decision for dealing with such faults in order to avoid or minimize production/operation interruption.

Blockages could arise from condensation, solid depositions, or un-intentionally partially closed inline valves.

Billman and Isermann in [107] introduced a new method for leak detection in pipelines. In recent years, there have been widespread studies based on frequency viewpoint analysis in the detection of deficiency in pipelines [108]. Mpesha et al. [109] proposed a frequency response model. Covas et al. [110] presented the standing wave difference method (SWDM) for leak detection.

Verde et al. [111] [112] [113] have done research in leak isolation and modeling observation in the detection of multi-leaking in the fluid pipeline.

Blockages are classified on the basis of their physical extent relative to the total length of the system. Localized constrictions that can be considered as point discontinuities are

referred to as discrete blockages, while blockages that have significant length relative to total pipe length are termed extended blockages. [114]

Unlike leaks within pipe systems, a blockage does not generate clear external indicators for its location such as the release and accumulation of fluids around the pipe. Often intrusive procedures using instruments, such as the insertion of a closed-circuit camera or a robotic pig, are required to determine the location of blockages. Insertion of camera or robotic pig may have some uncertainties regarding the travelling speed and travelling distance between the insertion point and the blockage, where in many cases the camera or the robotic pig get stuck into the blockage and causes a bigger problem in this case than the presence of the blockage only.

Over the last two decades researchers have tried to develop flow analysis based on techniques to detect blockages, methods that were developed using fluid transients depending on the response of the system to an injected transient for detecting, locating and sizing blockages; these non of intrusive methods have shown a promising development.

Adewumi, Eltohami and Ahmed [115], Adewumi, Eltohami and Solaja [116] proposed a time reflection method and conducted numerical experiments for detection of partial blockage of discrete and extended type in single pipeline for both single and multiple blockages. Vitovsky et al. [117] introduced an impulse response method for detection of leaks and partial blockages of discrete type in a single pipeline and the method was tested numerically. Wang, Lambert and Simpson [118] utilized the damping of fluid transients based on analytical solution and experimental verifications for detection of partial single discrete blockage in single pipeline. Sattar, Chaudry and Kassem [119] compared the numerical results with laboratory experiments which showed that blockage location could be obtained with almost no error, while the size detection had some errors.

The most current published researches are based on designing the observer, controller or fault diagnosis techniques. Nevertheless, investigating the observability as well as the controllability of the pipeline system is exceptionally significant. The classical techniques

for determining the observability as well as the controllability are in direct relation with the fullness of the rank of the discriminate matrices.

In this chapter, an intuitive technique is introduced for analyzing the observability as well as the controllability of the pipeline system. The parameters such as pressure and flow are maintained constant by implementing control valves depending on the different pressure and flow rate of the transmitting pipe.

In this chapter, an intuitive technique is introduced for analyzing the one-dimensional modeling of transients in a pipeline, commonly used for detection and location of blockage by means of model-based methods. The modeling starts with the discretization via finite-difference method of classical mass and continuity equations. The result of such a discretization is a system of ordinary differential equations, which is considered together with boundary conditions that represent faults and pipeline accessories.

We utilize the model demonstrated in [120], where the states of the system are considered to be flows, pressure heads, the blockage as well as a parameter related with the blockage intensity. In continuous time a nonlinear model is implemented in order to design observers. These observers are generally based on a transformation of the treated system into a triangular observable form hence, the variables which are directly approximated correspond to the output derivatives.

5.2. Pipeline modeling

In this paper, the convective change in velocity, as well as the compressibility in the line of length (L), are neglected, and the liquid density (ρ), the flow rate (Q), and pressure (P) at the inlet and outlet of the pipeline are measurable for evaluation. The cross-sectional area (A) of the pipe is constant throughout the pipe. The designed pipeline is shown in Figure 5.1.

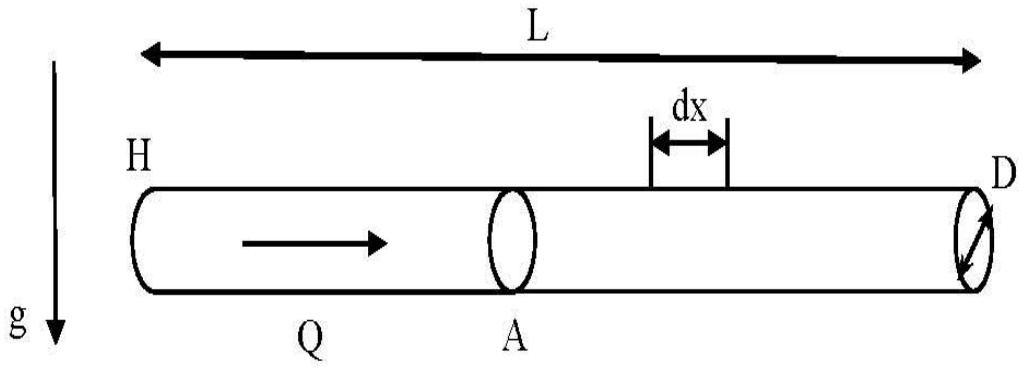

Figure 5.1 Schematic of pipeline

The dynamics of fluid in a pipeline is defined on the basis of the mass and momentum, and the conservation equations in hydrodynamics. In order to obtain the mass and momentum in hydrodynamics by implementing Newton's second law ($F = ma$) to a control volume in the continuum and body force pipe [121] ($s = \frac{f}{2D}v$) the following relation is given,

$$\frac{\partial v}{\partial t} + \frac{1}{\rho}\frac{\partial p}{\partial x} + \frac{f}{2D}v = 0 \tag{129}$$

By substituting $v = \frac{Q}{A}$, and $p = \rho g H$ in (1) the following relation is extracted,

$$\frac{\partial Q}{\partial t} + Ag\frac{\partial}{\partial x}H + \frac{fQ}{2DA} = 0 \tag{130}$$

where H is the pressure head (m), Q is the flow rate (m^3/s), x is the length coordinate (m), t is the time coordinate (s), g is the gravity(m/s^2), A is the section area (m^2), D is the diameter (m), and f is the friction coefficient.

In most of model friction coefficient is considered as a constant, even if it is sometimes updated known to depend on the so-called Reynolds number (Re) and the roughness coefficient of the pipe (e). The Swamee-Jain equation [122] describes this coefficient value for a pipe with a circular section of diameter (D) as:

$$f = \left(\frac{0.5}{\ln[0.27\left(\frac{e}{D}\right) + 5.74\frac{1}{Re^{0.9}}]} \right)^2 \quad (131)$$

where the Reynolds number can be calculated with:

$$Re = 4\frac{\rho Q}{\pi D \mu} = \frac{\rho V D}{\mu} \quad (132)$$

for ρ the fluid density and μ the fluid viscosity.

Equation (131) is valid for $10^{-8} < \frac{e}{D} < 0.01$ and$5000 < Re < 10^8$.

In order to derive the continuity equation, by applying the law of conservation of mass and using the Reynolds transport theorem to a control volume and simplifying, the following relation is obtained,

$$\frac{\partial p}{\partial t} + \rho a^2 \frac{\partial v}{\partial x} = 0 \quad (133)$$

By substituting the head pressure (H) and flow rate (Q) in (133) the following is obtained,

$$\frac{\partial H}{\partial t} + \frac{a^2}{gA}\frac{\partial Q}{\partial x} = 0 \quad (134)$$

in which a is the velocity of the pressure wave (m/s) in an elastic conduit filled with a slightly compressible fluid.

The pressure head (H) and flow rate (Q) are functions of position and time $H(x,t)$ and $Q(x,t)$, where $x \in [0, L]$.

For the system with small changes in the flow rate Q, the momentum equation from the nonlinear system can be linearized as below

$$\frac{\partial Q}{\partial t} + Ag\frac{\partial}{\partial x}H + \frac{fQ}{DA} = 0 \quad (135)$$

The pipeline model is designed based on (135) and (134). Obtaining the solutions of these equations is complex. However, several methods are utilized in order to numerically integrate them. Some of the main methods such as characteristics and finite difference

techniques are proposed by Wylie [123]. In this work, the finite difference method is applied since it is a simple way to get a more convenient model in order to observe and control the structure of the nonlinear system. The finite difference method is a discretization technique which divides the entire pipeline into N number of sections [124].

5.3. Blockage modeling

Blockages are also common faults in pipes and pipeline networks. They could be formed by the accumulation of the transported fluid or they can be caused by the partial closure of a valve. Blockages reduce the efficiency of pipeline systems, but can also cause serious damage in the security of the plant. Hereafter three types of blockages in a pipeline are presented. Figure.5.2 represents a blockage that occurs in a pipe.

A blocked is a reduced cross-sectional area of the pipe with significant length λ. To model the blocked stretch, the lockage area, denoted by A_b, is quantified as a percentage of the pipeline area A.

Pressure H_1 changes because of the blockage and such a changed pressure are given by H_{1b}.

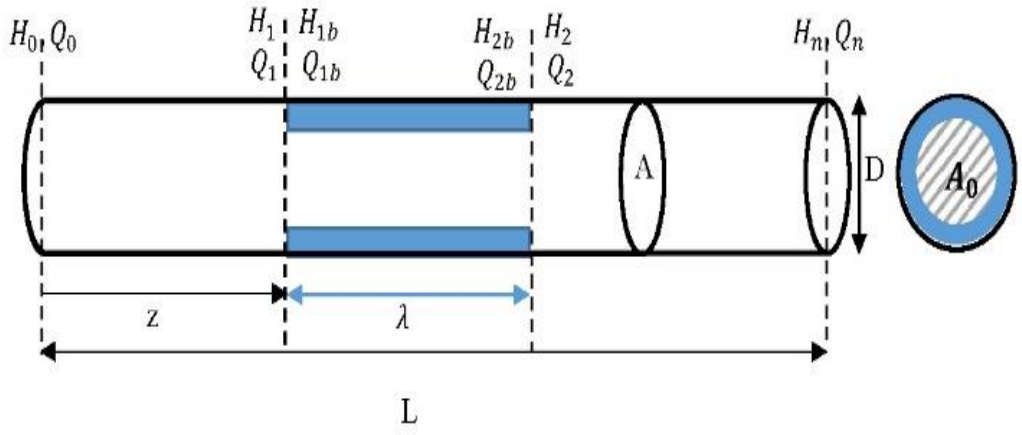

Figure 5.2 Blockage in pipeline

If Bernoulli's and continuity equations are both applied between point 1 (before the blockage) and point 1b (after the blockage), one has

$$H_1 + \frac{V_1^2}{2g} + Z_1 + h_w - h_L = H_{1b} + \frac{V_{1b}^2}{2g} + Z_{1b} \quad (136)$$

where H is the pressure head of the fluid, V is the fluid flow speed, ρ is the density of the fluid, Z is the elevation at points blockage,h_w represents energy inputs by pumps or turbines, and $h_L$represents pressure losses in the pipeline section. As levels Z_1 and Z_{1b} are equal, and energy inputs by pumps and/or turbines are zero (in this case), then one gets

$$H_1 + \frac{V_1^2}{2g} - h_L = H_{1b} + \frac{V_{1b}^2}{2g} \quad (137)$$

By continuity of conservation of mass,

$$\rho V_1 A_! = \rho V_{1b} A_{1b} \quad (138)$$

where A is the cross-sectional area of the pipe and A_b is the cross-sectional area at the blockage. Therefore, $V_{1b} = \frac{V_1 A}{A_b}$.

By substituting equation (138) in equation (137) we have

$$H_{1b} = H_1 + \frac{V_1^2}{2g}\left(1 - \left(\frac{A}{A_b}\right)^2\right) - h_L \quad (139)$$

It may be difficult to analytically obtain h_L, since it is a function of the flow and the blockage geometry. Therefore, for practical purposes, the following expression that includes a discharge coefficient η can be used:

$$H_{1b} = H_1 + \frac{A_b^2 V_1^2 - A^2 V_1^2}{2g\eta A_b^2} \quad (140)$$

which, expressed in terms of the volumetric flow $Q = VA$, becomes

$$H_{1b} = H_1 + \frac{A_b^2 Q_1^2 - A^2 Q_1^2}{2g\eta A^2 A_b^2} \quad (141)$$

This model takes into account the two phenomena occurring at the two edges of the blocked section: a contraction appearing upstream of the blockage (from A to A_0) and an expansion occurring downstream (from A_0 to A),

The following equations describe the dynamics of pressures head and flows before blockage (H_1, Q_1) and after it (H_{1b}, Q_{1b}) respectively

The flow dynamics are then described via the flow rate in each section and the pressures head at the end of each section.

$$\begin{aligned}
\dot{Q}_0 &= -Ag\frac{H_1 - H_0}{z} - \frac{f}{2DA}Q_0 \\
\dot{Q}_1 &= -Ag\frac{H_1 - H_0}{z} - \frac{f}{2DA}Q_1 \\
\dot{Q}_{2b} &= -A_b g\frac{(H_{2b} - H_{1b})}{\lambda} - \frac{f_b}{2DA_b}Q_{2b} \\
\dot{Q}_N &= -Ag\frac{(H_N - H_2)}{(L - z - \lambda)} - \frac{f}{2DA}Q_N \\
\dot{H}_0 &= -\frac{a^2}{gA}\frac{Q_1 - Q_0}{z} \\
\dot{H}_1 &= -\frac{a^2}{gA}\frac{Q_1 - Q_0}{z} \\
\dot{H}_{2b} &= -\frac{a^2}{gA_b}\frac{(Q_{2b} - Q_{1b})}{\lambda} \\
\dot{H}_N &= -\frac{a^2}{gA}\frac{(Q_N - Q_2)}{(L - z - \lambda)}
\end{aligned} \tag{142}$$

where $H_{1b}$and H_2 are calculated using Bernoulli's and continuity equation

$$\begin{aligned}
H_{1b} &= H_1 + \frac{A_b^2 Q_1^2 - A^2\, Q_1^2}{2g\eta A^2 A_b^2} \\
H_2 &= H_{2b} + \frac{A^2\, Q_{2b}^2 - A_b^2 Q_{2b}^2}{2g\eta A^2 A_b^2}
\end{aligned} \tag{143}$$

and at the point of the blockage the flow rate before and after of it are equal $Q_1 = Q_{1b}$ an $Q_{2b} = Q_2$

For example, with one blockage that are depicted in Figure 5.2, the variables are $H_0, H_1, H_2, H_\mathrm{n}$ for Head pressure and $Q_0, Q_1, Q_2, Q_\mathrm{n}$ are flow rates.

The idea in this chapter is to design an observer and controller for the systems mentioned in (134) and (135). A General non-linearized model is stated as

$$\frac{dx_i}{dt} = f(x,t) + g(x,t) \tag{144}$$

$$y = h(x,t) \tag{145}$$

where x is the state vector containing the i unknown flow perturbation quantities at each point.

Control variables in different case can be present by the Pressures Head and Flow rates at the beginning and end of the pipe.

The solution of discretized models, by any method, requires defining some boundary conditions, which represent known values of the variables at the border of the studied domain. Boundary conditions can only be Pressures Head, only Flows, or a combination of both. The choice of boundary conditions changes the structure of the model and can even vary the number of equations in which the discretized model is subdivided.

In real systems, boundary conditions are given by the elements available in the hydraulic system

Figure 3 represents the possible boundary conditions in a scheme of a discretized pipeline.

Therefore, we have six case for the modelling, based on the choose of the control variables

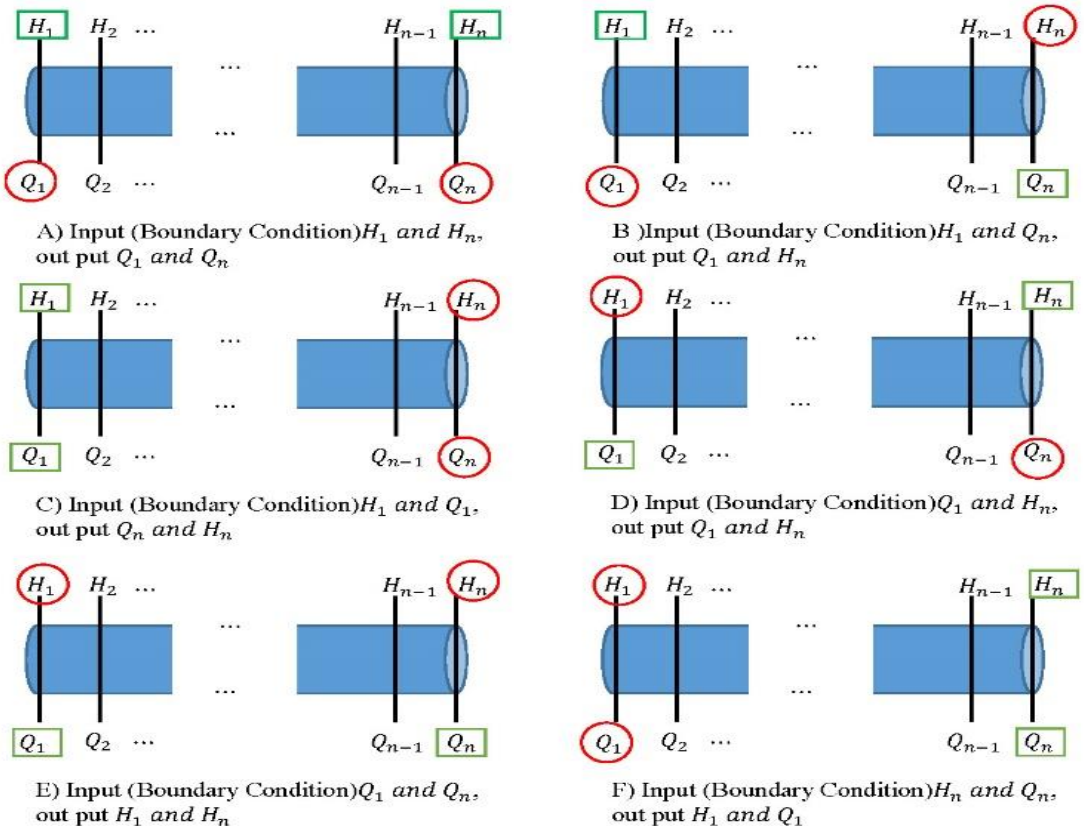

Figure 5.3 Boundary conditions

5.3.1 Case 1

The initial and boundary conditions that can be controlled and measured are the pressure heads in the beginning and end of the pipeline. The input conditions are stated as

$$\begin{cases} H(0,t) = H_{in}(t) \\ H(L,t) = H_{out}(t) \end{cases} \tag{146}$$

and output value are

$$\begin{cases} Q(0,t) = Q_{in}(t) \\ Q(L,t) = Q_{out}(t) \end{cases} \tag{147}$$

The vectors $u(t)$ and $y(t)$ contain the system forcing inputs and outputs respectively.

The suggested model, along with inputs and outputs are $x = (Q_0\ Q_1\ Q_{2\mathrm{b}}\ Q_{\mathrm{n}}\ H_1\ H_{2\mathrm{b}}\ \lambda\ \mathrm{z}\ A_b)^T$,$u \coloneqq [H_{in}\ H_{out}]^T = (H_0\ H_{\mathrm{n}})^T$ and $y = (Q_0\ Q_{\mathrm{n}})^T$, respectively.

$$\dot{Q}_0 = -Ag\frac{H_1 - H_0}{z} - \frac{f}{2DA}Q_0$$

$$\dot{Q}_1 = -Ag\frac{H_1 - H_0}{z} - \frac{f}{2DA}Q_1$$

$$\dot{Q}_{2b} = -A_b g\frac{(H_{2b} - H_{1b})}{\lambda} - \frac{f_b}{2DA_b}Q_{2b}$$

$$\dot{Q}_n = -Ag\frac{(H_n - H_2)}{(L - z - \lambda)} - \frac{f}{2DA}Q_n$$

$$\dot{H}_1 = -\frac{a^2}{gA}\frac{Q_1 - Q_0}{z} \tag{148}$$

$$\dot{H}_{2b} = -\frac{a^2}{gA_b}\frac{(Q_{2b} - Q_{1b})}{\lambda}$$

$$\dot{\lambda} = 0$$

$$\dot{z} = 0$$

$$\dot{A}_b = 0$$

where $H_{1b}$and H_2 are calculated using Bernoulli's and continuity equation

$$H_{1b} = H_1 + \frac{A_b^2 Q_1^2 - A^2\ Q_1^2}{2g\eta A^2 A_b^2}$$

$$H_2 = H_{2b} + \frac{A^2\ Q_{2b}^2 - A_b^2 Q_{2b}^2}{2g\eta A^2 A_b^2} \tag{149}$$

5.3.2. Case 2

The boundary conditions that can be controlled and measured are the initial the flow rate in the beginning and pressure head in the end of the pipeline. The input conditions are stated as

$$\begin{cases} Q(0,t) = Q_{in}(t) \\ H(L,t) = H_{out}(t) \end{cases} \tag{150}$$

and output value are

$$\begin{cases} H(0,t) = H_{in}(t) \\ Q(L,t) = Q_{out}(t) \end{cases} \tag{151}$$

The vectors $u(t)$ and $y(t)$ contain the system forcing inputs and outputs respectively.

The suggested model, along with inputs and outputs are $x = (\,Q_1\ Q_{2\mathrm{b}}\ Q_{\mathrm{n}}\ H_0\ H_1\ H_{2\mathrm{b}}\ \lambda\ \mathrm{z}\ A_b)^T$, $u \coloneqq [\,Q_{in}\ H_{out}]^T = (Q_0\ H_{\mathrm{n}}\,)^T$ and $y = (Q_n\ H_0\,)^T$, respectively.

$$\dot{Q}_1 = -Ag\frac{H_1 - H_0}{z} - \frac{f}{2DA}Q_1$$

$$\dot{Q}_{2b} = -A_b g\frac{(H_{2b} - H_{1b})}{\lambda} - \frac{f_b}{2DA_b}Q_{2b}$$

$$\dot{Q}_n = -Ag\frac{(H_n - H_2)}{(L - z - \lambda)} - \frac{f}{2DA}Q_n$$

$$\dot{H}_0 = -\frac{a^2}{gA}\frac{Q_1 - Q_0}{z} \tag{152}$$

$$\dot{H}_1 = -\frac{a^2}{gA}\frac{Q_1 - Q_0}{z}$$

$$\dot{H}_{2b} = -\frac{a^2}{gA_b}\frac{(Q_{2b} - Q_{1b})}{\lambda}$$

$$\dot{\lambda} = 0$$

$$\dot{z} = 0$$

$$\dot{A}_b = 0$$

where $H_{1b}$and H_2 are calculated using Bernoulli's and continuity equation

$$\begin{aligned} H_{1b} &= H_1 + \frac{A_b^2 Q_1^2 - A^2\, Q_1^2}{2g\eta A^2 A_b^2} \\ H_2 &= H_{2b} + \frac{A^2\, Q_{2b}^2 - A_b^2 Q_{2b}^2}{2g\eta A^2 A_b^2} \end{aligned} \tag{153}$$

5.3.3. Case 3

The initial and boundary conditions that can be controlled and measured are the flow rate and pressure head in the beginning of the pipeline. The input conditions are stated as

$$\begin{cases} H(0,t) = H_{in}(t) \\ Q(0,t) = Q_{in}(t) \end{cases} \tag{154}$$

and output value are

$$\begin{cases} Q(L,t) = Q_{out}(t) \\ H(L,t) = H_{out}(t) \end{cases} \tag{155}$$

The vectors $u(t)$ and $y(t)$ contain the system forcing inputs and outputs respectively.

The suggested model, along with inputs and outputs are $x = (\,Q_1\ Q_{2\mathrm{b}}\ Q_n\ H_1\ H_{2\mathrm{b}}\ H_n\ \lambda\ \mathrm{z}\ A_b)^T$,$u \coloneqq [H_{in}\ Q_{in}\,]^T = (Q_0\ \ H_0\,)^T$ and $y = (Q_{\mathrm{n}}\ H_n\,)^T$, respectively.

$$\begin{aligned} \dot{Q}_1 &= -Ag\,\frac{H_1 - H_0}{z} - \frac{f}{2DA}\,Q_1 \\ \dot{Q}_{2b} &= -A_b g\,\frac{(H_{2b} - H_{1b})}{\lambda} - \frac{f_b}{2DA_b}\,Q_{2b} \end{aligned} \tag{156}$$

$$\dot{Q}_n = -Ag\frac{(H_n - H_2)}{(L - z - \lambda)} - \frac{f}{2DA}Q_n$$

$$\dot{H}_1 = -\frac{a^2}{gA}\frac{Q_1 - Q_0}{z}$$

$$\dot{H}_{2b} = -\frac{a^2}{gA_b}\frac{(Q_{2b} - Q_{1b})}{\lambda}$$

$$\dot{H}_n = -\frac{a^2}{gA}\frac{(Q_n - Q_2)}{(L - z - \lambda)}$$

$$\dot{\lambda} = 0$$

$$\dot{z} = 0$$

$$\dot{A}_b = 0$$

where $H_{1b}$and H_2 are calculated using Bernoulli's and continuity equation

$$\begin{aligned} H_{1b} &= H_1 + \frac{A_b^2 Q_1^2 - A^2\, Q_1^2}{2g\eta A^2 A_b^2} \\ H_2 &= H_{2b} + \frac{A^2\, Q_{2b}^2 - A_b^2 Q_{2b}^2}{2g\eta A^2 A_b^2} \end{aligned} \tag{157}$$

5.3.4. Case 4

The initial and boundary conditions that can be controlled and measured are the flow rate in the beginning and pressure rate in end of the pipeline. The input conditions are stated as

$$\begin{cases} H(\mathrm{L}, t) = H_{out}(t) \\ Q(0, t) = Q_{in}(t) \end{cases} \tag{158}$$

and output value are

$$\begin{cases} Q(L, t) = Q_{out}(t) \\ H(0, t) = H_{in}(t) \end{cases} \tag{159}$$

The vectors $u(t)$ and $y(t)$ contain the system forcing inputs and outputs respectively.

The suggested model, along with inputs and outputs are $x = (\,Q_1\ Q_{2\mathrm{b}}\ Q_n\ H_0\ H_1\ H_{2\mathrm{b}}\ \lambda\ \mathrm{z}\ A_b)^T$,$u \coloneqq [H_{out}\ Q_{in}\,]^T = (\,H_n\ Q_0)^T$ and $y = (Q_{\mathrm{n}}\ H_0\,)^T$, respectively.

$$\dot{Q}_1 = -Ag\frac{H_1 - H_0}{z} - \frac{f}{2DA}Q_1$$

$$\dot{Q}_{2b} = -A_b g\frac{(H_{2b} - H_{1b})}{\lambda} - \frac{f_b}{2DA_b}Q_{2b}$$

$$\dot{Q}_N = -Ag\frac{(H_n - H_2)}{(L - z - \lambda)} - \frac{f}{2DA}Q_n$$

$$\dot{H}_0 = -\frac{a^2}{gA}\frac{Q_1 - Q_0}{z}$$

$$\dot{H}_1 = -\frac{a^2}{gA}\frac{Q_1 - Q_0}{z} \qquad (160)$$

$$\dot{H}_{2b} = -\frac{a^2}{gA_b}\frac{(Q_{2b} - Q_{1b})}{\lambda}$$

$$\dot{\lambda} = 0$$

$$\dot{z} = 0$$

$$\dot{A}_b = 0$$

where $H_{1b}$and H_2 are calculated using Bernoulli's and continuity equation

$$H_{1b} = H_1 + \frac{A_b^2 Q_1^2 - A^2\ Q_1^2}{2g\eta A^2 A_b^2} \qquad (161)$$

$$H_2 = H_{2b} + \frac{A^2\ Q_{2b}^2 - A_b^2 Q_{2b}^2}{2g\eta A^2 A_b^2}$$

5.3.5 Case 5

The initial and boundary conditions that can be controlled and measured are the flow rate in the beginning and end of the pipeline. The input conditions are stated as

$$\begin{cases} Q(0,t) = Q_{in}(t) \\ Q(L,t) = Q_{out}(t) \end{cases} \tag{162}$$

and output value are

$$\begin{cases} H(0,t) = H_{in}(t) \\ H(L,t) = H_{out}(t) \end{cases} \tag{163}$$

The vectors $u(t)$ and $y(t)$ contain the system forcing inputs and outputs respectively.

The suggested model, along with inputs and outputs are $x = (\,Q_1\ Q_{2\mathrm{b}}\ H_0\ H_1\ H_{2\mathrm{b}}\ H_n\ \lambda\ \mathrm{z}\ A_b)^T$,$u \coloneqq [Q_{in}\ Q_{out}\,]^T = (Q_0\ \ Q_n\,)^T$ and $y = (H_0\ \ H_n\,)^T$, respectively.

$$\dot{Q}_1 = -Ag\frac{H_1 - H_0}{z} - \frac{f}{2DA}Q_1$$

$$\dot{Q}_{2b} = -A_b g\frac{(H_{2b} - H_{1b})}{\lambda} - \frac{f_b}{2DA_b}Q_{2b}$$

$$\dot{H}_0 = -\frac{a^2}{gA}\frac{Q_1 - Q_0}{z}$$

$$\dot{H}_1 = -\frac{a^2}{gA}\frac{Q_1 - Q_0}{z} \tag{164}$$

$$\dot{H}_{2b} = -\frac{a^2}{gA_b}\frac{(Q_{2b} - Q_{1b})}{\lambda}$$

$$\dot{H}_n = -\frac{a^2}{gA}\frac{(Q_n - Q_2)}{(L - z - \lambda)}$$

$$\dot{\lambda} = 0$$

$$\dot{z} = 0$$

$$\dot{A}_b = 0$$

where $H_{1b}$and H_2 are calculated using Bernoulli's and continuity equation

$$\begin{aligned} H_{1b} &= H_1 + \frac{A_b^2 Q_1^2 - A^2\, Q_1^2}{2g\eta A^2 A_b^2} \\ H_2 &= H_{2b} + \frac{A^2\, Q_{2b}^2 - A_b^2 Q_{2b}^2}{2g\eta A^2 A_b^2} \end{aligned} \tag{165}$$

5.3.6 Case 6

The boundary conditions that can be controlled and measured are the pressure head and the flow rate in the end of the pipeline. The input conditions are stated as

$$\begin{cases} Q(L,t) = Q_{out}(t) \\ H(\mathrm{L},t) = H_{out}(t) \end{cases} \tag{166}$$

and output value are

$$\begin{cases} Q(0,t) = Q_{in}(t) \\ H(L,t) = H_{in}(t) \end{cases} \tag{167}$$

The vectors $u(t)$ and $y(t)$ contain the system forcing inputs and outputs respectively.

The suggested model, along with inputs and outputs are $x = (\,Q_1\ Q_{2\mathrm{b}}\ Q_n\ H_1\ H_{2\mathrm{b}}\ H_n\,\lambda\,\mathrm{z}\,A_b)^T$,$u \coloneqq [H_{out}\ Q_{out}\,]^T = (Q_{\mathrm{n}}\ H_n\,)^T$ and $y = (Q_0\ H_0\,)^T$, respectively.

$$\begin{aligned} \dot{Q}_0 &= -Ag\,\frac{H_1 - H_0}{z} - \frac{f}{2DA}\,Q_0 \\ \dot{Q}_1 &= -Ag\,\frac{H_1 - H_0}{z} - \frac{f}{2DA}\,Q_1 \\ \dot{Q}_{2b} &= -A_b g\,\frac{(H_{2b} - H_{1b})}{\lambda} - \frac{f_b}{2DA_b}\,Q_{2b} \\ \dot{H}_0 &= -\frac{a^2}{gA}\,\frac{Q_1 - Q_0}{z} \end{aligned} \tag{168}$$

$$\dot{H}_1 = -\frac{a^2}{gA}\frac{Q_1 - Q_0}{z}$$

$$\dot{H}_{2b} = -\frac{a^2}{gA_b}\frac{(Q_{2b} - Q_{1b})}{\lambda}$$

$$\dot{\lambda} = 0$$

$$\dot{z} = 0$$

$$\dot{A}_b = 0$$

where $H_{1b}$and H_2 are calculated using Bernoulli's and continuity equation

$$H_{1b} = H_1 + \frac{A_b^2 Q_1^2 - A^2\, Q_1^2}{2g\eta A^2 A_b^2}$$

$$H_2 = H_{2b} + \frac{A^2\, Q_{2b}^2 - A_b^2 Q_{2b}^2}{2g\eta A^2 A_b^2} \tag{169}$$

5.4. Observer design by using the extended Kalman filter

The idea considered here for the purpose of blockage detection problem is the leak parameter estimation z, λ and A_0, by using an extended kalman filter as a state observer. To that end, the model previously described by (148) can be extended with the dynamics of such parameters, and a nonlinear observer can be designed for the extended system [125]. This requires that available measurements, as well as input variables, be specified. Here, for different cases assumed that can directly measured only be pressures head, only flows, or a combination of both flow rates at the beginning or end of pipeline. For case 1 flow rates at the pipeline ends are directly measured

$$y = [Q_0\ Q_n]^T \tag{170}$$

and that the pressure heads at the same locations are known inputs:

$$u = [H_0\ H_n]^T \tag{171}$$

Finally, considering extensions

$$\dot{z} = 0; \dot{\lambda} = 0; \dot{A}_b = 0 \tag{172}$$

for leak parameters $z, \lambda$and A_b, whose derivative can be taken as zero since their variation is small. Then, the extended model of (148), is:

$$\begin{bmatrix} \dot{Q}_0 \\ \dot{Q}_1 \\ \dot{Q}_{2b} \\ \dot{Q}_n \\ \dot{H}_1 \\ \dot{H}_{2b} \\ \dot{\lambda} \\ \dot{z} \\ \dot{A}_b \end{bmatrix} = \begin{bmatrix} -Ag\dfrac{H_1 - H_0}{z} - \dfrac{f}{2DA}Q_0 \\ -Ag\dfrac{H_1 - H_0}{z} - \dfrac{f}{2DA}Q_1 \\ -A_b g\dfrac{(H_{2b} - H_{1b})}{\lambda} - \dfrac{f_b}{2DA_b}Q_{2b} \\ -Ag\dfrac{(H_n - H_2)}{(L - z - \lambda)} - \dfrac{f}{2DA}Q_n \\ -\dfrac{a^2}{gA}\dfrac{Q_1 - Q_0}{z} \\ -\dfrac{a^2}{gA_b}\dfrac{(Q_{2b} - Q_{1b})}{\lambda} \\ 0 \\ 0 \\ 0 \end{bmatrix} \tag{173}$$

Hence, the model (173) can be written in compact form as:

$$\dot{x} = \phi(x, u) \tag{174}$$

with $x = (\, Q_1\ Q_{2\mathrm{b}}\ \ Q_n\ \ H_0\ H_1\ \ H_{2\mathrm{b}}\ \lambda\ \mathrm{z}\ A_b)^T$and $\phi(x, u)$ a nonlinear function.

Now, to estimate the leak parameters z, λ and A_0, a discrete-time Extended Kalman Filter is designed for nonlinear model (173). To do that, this model is discretized by using the Heun's method. In this method, the solution for initial value problem:

$$\dot{x} = \phi\big(x(t), u(t)\big), x(t_0) = \ x_0 \tag{175}$$

is given by [126]

$$x^{i+1} = x^i + \frac{\Delta t}{2}[\phi\big(x^i, u^i\big) + \phi\big(x^i + \Delta t\phi\big(x^i, u^i\big), u^{i+1}\big)] \tag{176}$$

Where Δt is the time step and i is the index of discrete time. Finally the ordinary differential equations in (173) are transformed by using (176), into following difference equations:

$$Q_0^{i+1} = Q_0^i + \frac{\Delta t}{2}\left(-Ag\frac{H_1^i - H_0^i}{z^i} - \frac{f}{2DA}Q_0^i - Ag\frac{\widehat{H}_1^{i+1} - H_0^{i+1}}{z^{i+1}}\right) - \frac{f}{2DA}\widehat{Q}_0^{i+1}$$

$$Q_1^{i+1} = Q_1^i + \frac{\Delta t}{2}\left(-Ag\frac{H_1^i - H_0^i}{z^i} - \frac{f}{2DA}Q_1^i - Ag\frac{\widehat{H}_1^{i+1} - H_0^{i+1}}{z^{i+1}}\right) - \frac{f}{2DA}\widehat{Q}_1^{i+1}$$

$$Q_{2b}^{i+1} = Q_{2b}^i + \frac{\Delta t}{2}\left(-A_b g\frac{\widehat{H}_{2b}^i - \widehat{H}_{1b}^i}{\lambda^i} - \frac{f_b}{2DA_b}Q_{2b}^i - Ag\frac{\widehat{H}_{2b}^{i+1} - \widehat{H}_{1b}^{i+1}}{\lambda^{i+1}}\right) - \frac{f}{2DA}\widehat{Q}_{2b}^{i+1}$$

$$Q_n^{i+1} = Q_n^i + \frac{\Delta t}{2}\left(-Ag\frac{\widehat{H}_n^i - \widehat{H}_2^i}{(L - z^i - \lambda^i)} - \frac{f}{2DA}Q_n^i - Ag\frac{\widehat{H}_n^{i+1} - \widehat{H}_2^{i+1}}{(L - z^{i+1} - \lambda^{i+1})}\right) - \frac{f}{2DA}\widehat{Q}_n^{i+1} \quad (177)$$

$$H_1^{i+1} = H_n^i + \frac{\Delta t}{2}\left(-\frac{a^2}{gA}\frac{Q_1^i - Q_0^i}{z^i} - \frac{a^2}{gA}\frac{\widehat{Q}_1^{i+1} - \widehat{Q}_0^{i+1}}{z^{i+1}}\right)$$

$$H_{2b}^{i+1} = H_{2b}^i + \frac{\Delta t}{2}\left(-\frac{a^2}{gA_b}\frac{Q_1^i - Q_0^i}{\lambda^i} - \frac{a^2}{gA}\frac{\widehat{Q}_1^{i+1} - \widehat{Q}_0^{i+1}}{\lambda^{i+1}}\right)$$

$$\lambda^{i+1} = \lambda^i$$

$$z^{i+1} = z^i$$

$${A_b}^{i+1} = {A_b}^i$$

in compact form:

$$x^{i+1} = \phi\left(x^i, u^{i+1}, u^i\right);\ y^i = Hx^i \tag{178}$$

Where

$$x^i = \left[Q_0^i\ Q_1^i\ Q_{2b}^i\ Q_n^i H_n^i\ H_{2b}^i\ \lambda^i\ z^i\ {A_b}^i\right]^T;$$

$$u^i = [H_0^i\ H_n^i]^T \tag{179}$$

$$H = \begin{bmatrix} 1 & 0 & 0 & 0 & 0 & 0 & 0 & 0 & 0 \\ 0 & 0 & 0 & 1 & 0 & 0 & 0 & 0 & 0 \end{bmatrix}$$

5.5. Observer scheme

A discrete-time extended Kalman filter as state observer for the system (173) can be chosen as [127]

$$\hat{x}^i = \hat{x}^{\tilde{\imath}} + \kappa^i(y^i - H\hat{x}^{\tilde{\imath}}) \tag{180}$$

where $\hat{x}^{\tilde{\imath}}$ is the a priori estimate of x^i:

$$\hat{x}^{\tilde{\imath}} = \phi(\hat{x}^{i-1}, u^{i-1}) \tag{181}$$

$\kappa^i$is the Kalman gain:

$$\kappa^i = P^{\tilde{\imath}} H^T (H P^{\tilde{\imath}} H^T + R)^{-1} \tag{182}$$

$P^{\tilde{\imath}}$ is the a priori covariance matrix:

$$P^{\tilde{\imath}} = J^i P^{i-1} (J^i)^{-1} + Q \tag{183}$$

P^i is the posteriori covariance matrix:

$$P^i = (I - K^i H) P^{\tilde{\imath}} \tag{184}$$

J^i is the Jacobian matrix:

$$J^i = \frac{\partial \phi(x, u)}{\partial x}\Big|_{x=\hat{x}^i} \tag{185}$$

Finally, R and D are known as the covariance matrices of measure and process noises, respectively. Notice that:

$$\hat{x}^i = (\hat{Q}_1^i\ \hat{Q}_{2b}^i \hat{Q}_n^i\ \hat{H}_0^i\ \hat{H}_1^i\ \hat{H}_{2b}^i \hat{\lambda}^i\ \ \hat{z}^i\ \hat{A}_b^i) \quad (186)$$

With $P^{\tilde{0}} = \left(P^{\tilde{0}}\right)^T > 0, R = R^T > 0\ and\ D = D^T > 0.$

5.6. Simulation results

In this section are reported simulations results for two case with different boundary condition. Various cases of blockage appearing at different couples of times along the pipeline were simulated, with detection blockage under appropriate conditions and excitation.

The model have been realized on pipeline, with the following physical parameters:

In this Figure the length of the pipeline is $L = 1.2 \times 10^3\ m$, the diameter of pipe is $D = 0.56\ m$, the cross section is $A = 0.246\ m^2$, density is $\rho = 1000\ kg/m^3$, gravity is $g = 9.81\ m/s^2$, friction factor of pipe is $f = 0.006$ and for blockage part is $f_b = 0.016$ and the wave speed is $a = 1250\ m/s$ that are summarized in Table 5.1.

Table.5.1. The proposed characteristics of the pipeline

L	$1.2 \times 10^3\ m$
D	$0.56\ m$
A	$0.246\ m^2$,
f	0.006
f_b	0.016
a	$1250\ m/s$
g	$9.81\ m/s^2$
ρ	$1000\ kg/m^3$

5.6.1. Simulation for case 1

Control variables according the case1 model are the pressures head at the beginning and end of the pipe (H_0 and H_n) and can be directly measured. Furthermore, the flow rates (Q_0 and Q_n) are output of the system. According to Lemma 1 and 2, the rank of discriminant matrices is $rank\,\mathbb{C} = \text{rank}\,O = 18$, thus, the system is completely observable and controllable.

Figure 5.4 displays the simulated pressure head at the inlet ($H\ (in) = H_0 = 14\,m$) and outlet ($H\ (out\ ) = H_n = 7.3\,m$) of the pipe.

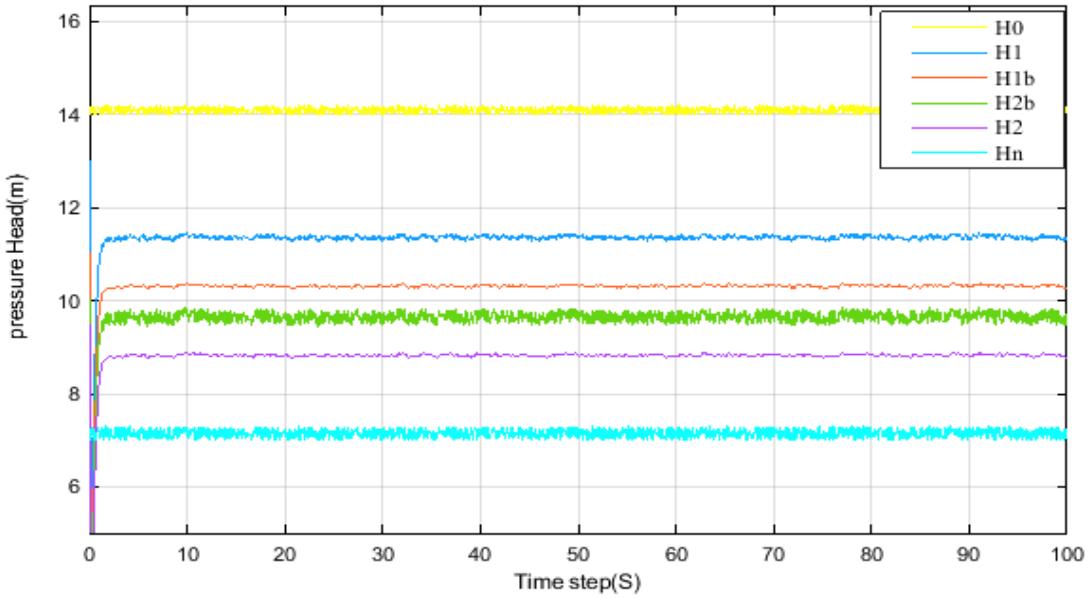

Figure 5.4 pressure head in pipeline case1

Figure 5.5, 5.6 and 5.7 estimate the position, length and area of blockage in pipeline

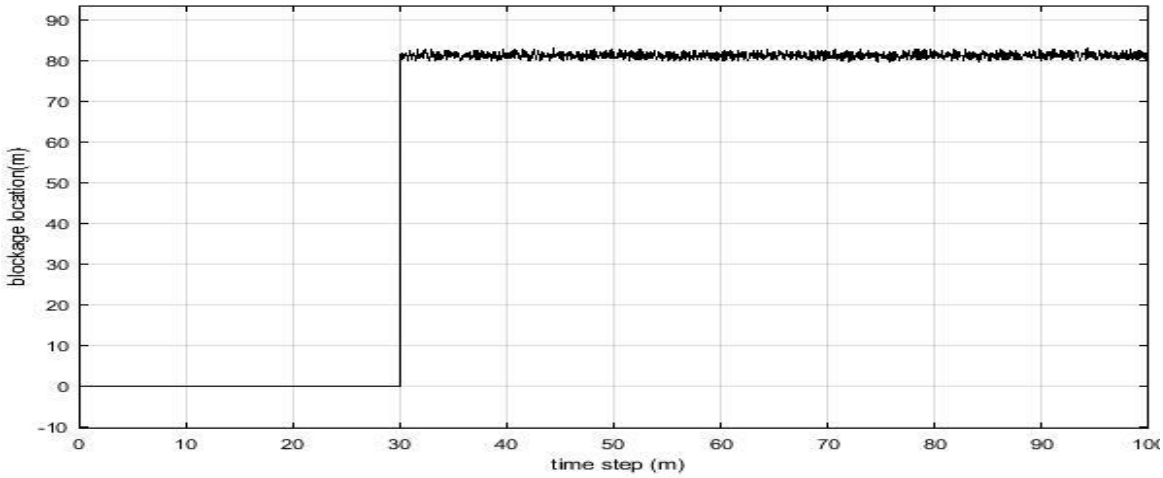

Figure 5.5 Position of blockage

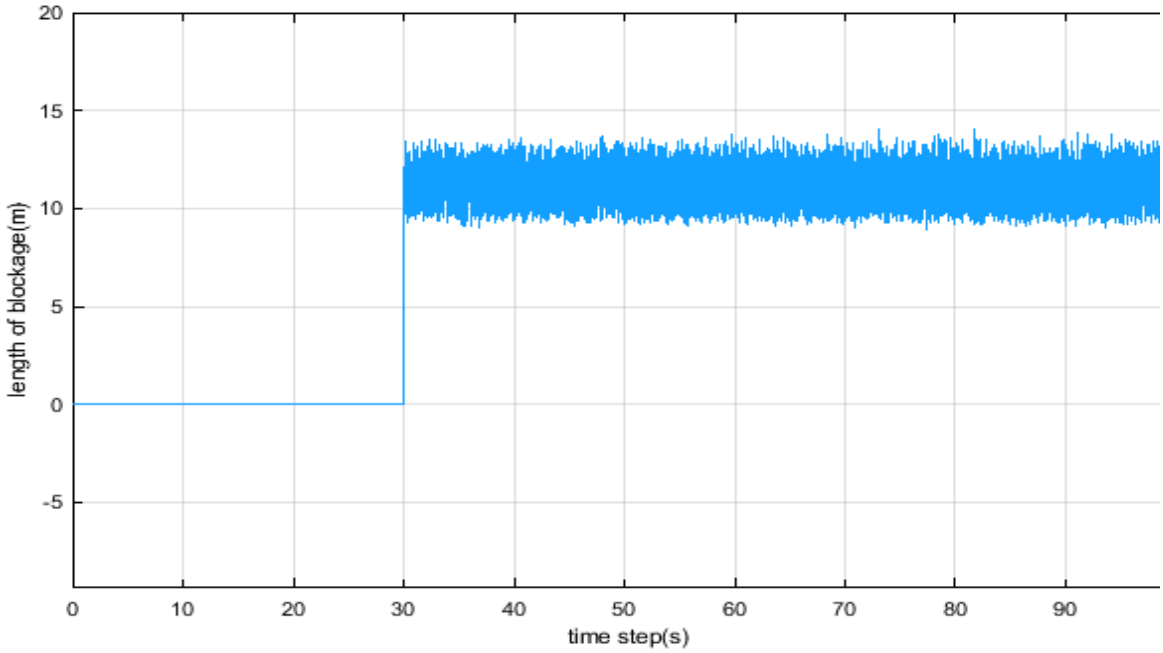

Figure 5.6 Length of blockage

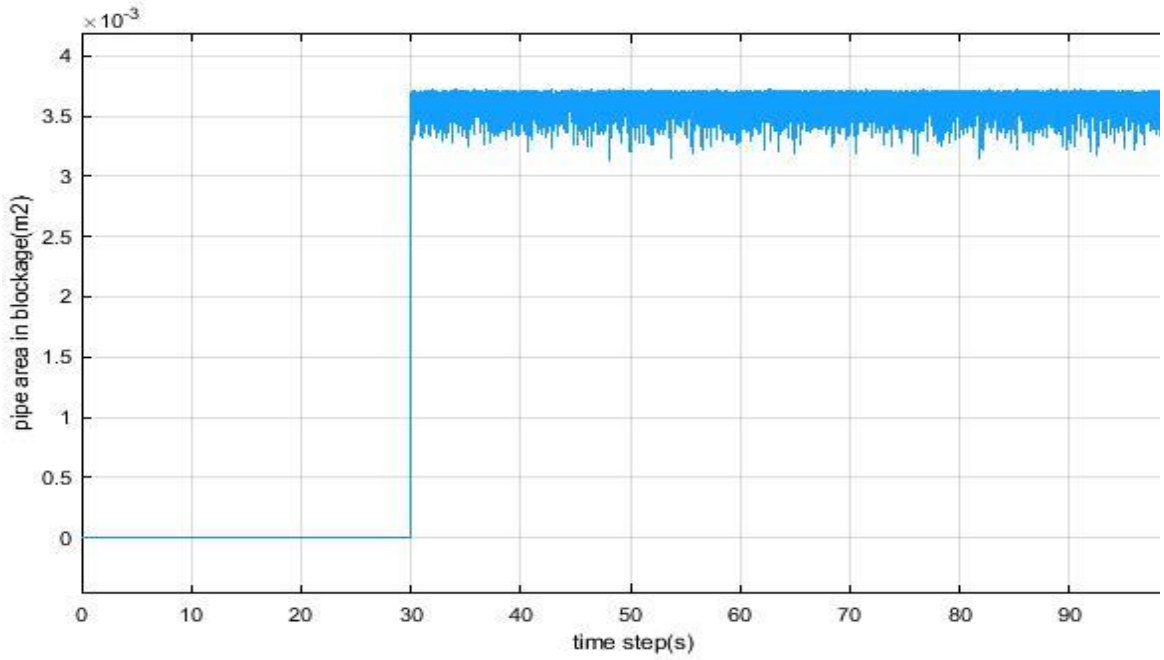

Figure 5.7 Pipe area in blockage

5.7. Conclusion

The objective of this paper is to analyzed and model the blockage detection in a pipeline system. The system is stated by hyperbolic partial differential equations. In this work, the finite difference method is applied as it is a simple way to get a more convenient model in order to observe and control the structure of the nonlinear system. This method divides the entire pipeline into N number of sections. Flow and pressure head estimations have been well estimated in presence of a blockage. Future work is to study the case of multi blockage estimation of the pipeline system.

Chapter Six: Flow control of fluid in pipelines using PID &PD controllers

6.1. Introduction

Classic PID approaches as well as controllers have been updated and expanded during the years, from the primary controllers on the basis of the relays as well as synchronous electric motors or pneumatic or hydraulic systems to current microprocessors. Currently, many techniques for the tuning as well as design of PI and PID controllers are proposed [128]. The method proposed in [129] is the most widely utilized PID parameter tuning methodology in chemical industry and is considered as a conventional technique. Basilio and Matos [130] suggested a new method with less complexity in order to tune the parameters of PI controllers of the plant with monotonic step response. The methodology of internal mode principle is utilized in [131] and [132] in order to extract the gains of PID and PI controllers. Exhaustive investigation [133] [134] [135] [136] revealed that the outcomes of P control are very sensitive to the sensing location as well as the quantity of phase shift. By suitable selections of these variables, the P control can be completely efficient in annihilating the vortex shedding or minimizing its strength. Furthermore, it is demonstrated that the increment in the proportional gain can result in the decrement of the velocity fluctuations in the wake and the strength of vortex shedding. Nevertheless, a large gain causes instability in the system [137] [138] [139].

In order to implement the control law, the primary step is to determine a desired output response of a particular system to an arbitrary input over a time interval, that can be carried out by system identification [140]. Generally, it is feasible to generate a model on the basis of a complete physical illustration of the system. Nevertheless, this model contains complexity, also has high calculation costs [141]. The secondary step is to define the parameters of the PID controller. There exist various works associated with the methodologies for the tuning of PID controllers applied in various controller structures [142].

Flow control is a rapidly evolving field of fluid mechanics. There have been various concepts of flow control in drag reduction, lift enhancement, mixing enhancement, etc. [143] [144] [145]. Fadlun et al. [146] implemented the concept of [147] to a finite-difference methodology where a staggered grid is used. In [148] a digital pulse feedback flow control system utilizing microcontroller as well as feedback sensing element is developed. Surprisingly, even though the

flow control methods are widely spread, investigating the stability of the control system is very rare. In [149] [150] [151] the P, PI and PID controls are proposed for flow over a cylinder with a Reynolds number below 200. The aim of control in these studies is the attenuation or annihilation of vortex shedding behind a bluff body. The only investigation on the implementation of PI and PID controls to the flow over a bluff body is carried out in [151].

This chapter deals with the modeling and control of flow rate in heavy-oil pipelines. For this aim, the PID control algorithm is utilized to control the flow mechanism in pipelines. A torsional actuator is placed on the motor-pump in order to control the vibration on the motor. The stability of the PID controller is verified using Lyapunov stability analysis. The stability analysis of the controller results in a theorem which validates that the system states are bounded. The theoretical concepts are validated using numerical simulations and analysis, which proves the effectiveness of the PID controller in the control of flow rates in pipelines. Further, it is the first attempt to place a torsional actuator on the motor-pump in order to control the vibration on the motor and hence control the flow rates in pipelines.

This chapter is structured as follows. Firstly, in Section 2 the pump model system is established. The PID control method is described in Section 3. In this section, sufficient conditions for the controller under the Lyapunov stability theorem are designed. A numerical example is presented in Section IV to illustrate the results. Finally, the conclusions are provided in Section V.

6.2. Feedback Control

The success of feedback control is because this system makes everything faster, more precise and less sensitive to disturbances. The open loop control, regarding its simplicity, it's only advised when the outputs and inputs are known and in which there is no disturbance associated.

In a system with feedback control there is a big disadvantage which is the probability of the system get unstable, for that the correct controller must be chosen, and it must be perfect for the system that is being monitored.

The basic structure of conventional feedback control systems is shown in Fig.6.1, using a block diagram representation. The purpose is to make the variable y to follow the Set-point r. For that,

the variable *u* is manipulated at the command of the controller. The variable *d* is considered as disturbances. The disturbance may be any factor that influences the process variable.

6.2.1 PID Controller

Feedback loops have been controlling continuous processes since 1700's [152]. Today, there are several more controllers, but most of all derivate from the PID controller. "The PID controller is by far the most common control algorithm. Most feedback loops are controlled by this algorithm or minor variations of it. It is implemented in many different forms, as a stand-alone controller or as part of a DDC (Direct Digital Control) package. Many thousands of instrument and control engineers worldwide are using such controllers in their daily work." [153]

A PID controller is a controller that includes the proportional element,"*P element"*, the integral element, "*I element"* and the derivative element,"*D element"*.

Defining $u(t)$ as the controller output, the final form of the PID algorithm is:

$$u(t) = K_p e(t) + K_i \int_0^t e(\tau)d\tau + K_d \frac{d}{dt} e(t) \qquad (187)$$

Where:

P_{out}: Proportional term of output

K_p: Proportional gain, a tuning parameter

K_i: Integral gain, a tuning parameter

K_d: Derivative gain, a tuning parameter

e: Error = $SP - PV$

t: Time or instantaneous time (the present)

MV: Manipulated variable

The figure 6.1 show the simple structure of a PID controller.

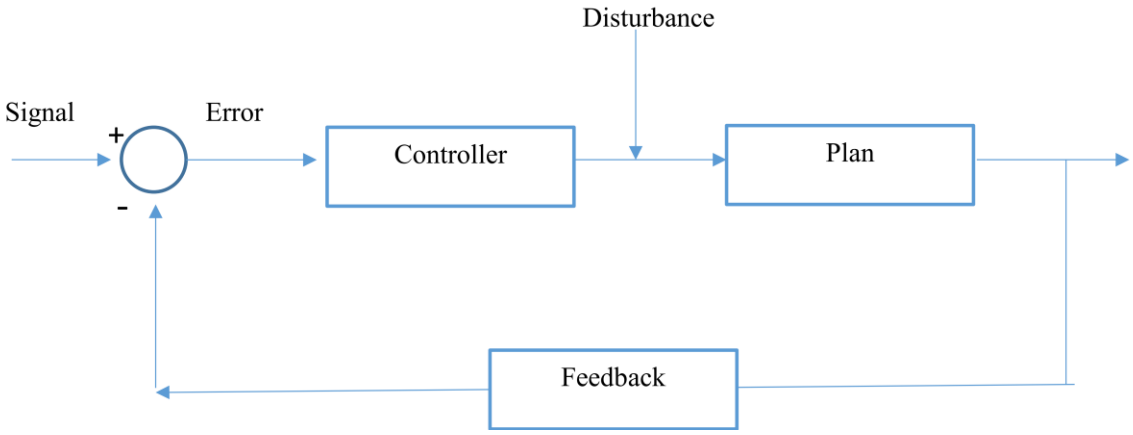

Figure 6.1 PID controller structure

6.2.2 Proportional term

The proportional influence is proportional to the generated error [154].

The proportional term is given by:

$$P_{out} = K_p e(t) \tag{188}$$

The higher the error the higher the proportional control which is clearly seen in the equation. That conclusion leads us to another one that is that: the proportional control leads the system to a fast Set Point. But it has a disadvantage, it has steady-state error, and that error can lead to an overshoot when the system gets to the Set Point. One way to avoid it is to increase the proportional term, but that can led to an unstable system.

6.2.3 Integral term

The integral influence is proportional to the variation of the error on time.

The integral term is given by:

$$I_{out} = K_i \int_0^t e(\tau) d\tau \tag{189}$$

The most important benefit is that this term eliminates the steady-state error, but it has a disadvantage which is the fact that the stability of the system is affected. Regarding the upper equation we can conclude that this integral term depends on past values of the error.

6.2.4 Derivative term

The derivative term is proportional to the rate of change of the error, as we can see on the equation below.

The derivative term is given by:

$$D = K_d \frac{d}{dx} e(x,t) \tag{190}$$

This term makes an estimation of the future error and by that it can increase or decrease the speed of correction, because it can work in an early way when there are detected any changes on the error. This term is very sensitive to disturbances.

If the derivative term only changes with the rate of change of the error, if the error does not change then we don't have derivative influence.

6.3. Materials and methods for modelling of the system

Flow control loop system is basically a feedback control system. The structure of the pump model system is shown in Figure. 6.2 which is an open loop system. If there is unwanted vibration in the motor, the stability of the flow rate will hamper. Therefore, it is important to change the open loop system to a closed loop system by implementing a controller so as to control the stability of the flow rate by controlling the vibration in the motor.

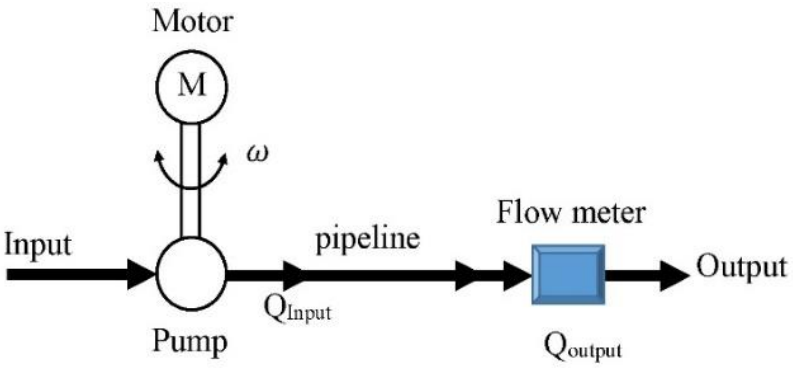

Figure 6.2 Scheme of open loop model

6.4. Modelling

6.4.1. Modelling of the pipeline

The proposed model consists of an induction motor, which causes a rotation in the pump and consequently can lead to flow of heavy-oil in pipelines as shown in Figure.1. This flow model can be illustrated in the form of a partial differential equation (PDE) [155].

The linear global theory associated with flow stability is rooted in eigendecompositions of the linearized flow operators. The direct as well as adjoint eigendecompositions associated with these kinds of operators generate information related to the stability of the operator, the acceptance of initial conditions as well as external forcing, also the sensitivity to spatially localized disturbances.

From the viewpoint of incompressible, constant-density, constant-viscosity flows associated with Newtonian fluids, the nonlinear Navier–Stokes equation is defined for a nondimensional velocity field $v(x,t)$: $\mathbb{R}^n \times \mathbb{R} \to \mathbb{R}^n$, pressure field $p(x,t)$: $\mathbb{R}^n \times \mathbb{R} \to \mathbb{R}^n$ and Reynolds number $Re > 0$ as,

$$\frac{\partial u}{\partial t} = -\frac{\nabla p}{\rho} - u.\nabla u + F_f \qquad (191)$$

where,

ρ is the density in $\frac{kg}{m^3}$

u is the flow velocity in $\frac{m}{s}$,

∇ is the divergence,

p is the pressure in $\frac{kg}{m.s^2}$,

t is time in s,

F_f is termed as the summation of external force and body forces

By implementing the mass balance into Equation (191) the following is concluded [156],

$$\nabla . u = 0 \tag{192}$$

Equation (191) can be rewritten as,

$$\frac{\partial u}{\partial t} = -\frac{1}{\rho}\frac{\partial p}{\partial x} + F_f \tag{193}$$

Let $\frac{\partial p}{\partial x}$ be the change of pressure in two different points, moreover for achieving a numerical stability of computation, it is essential to partition the pipeline into various segment, hence the flow in the pipeline can be stated as,

$$\frac{\partial u_i}{\partial t} = -\frac{1}{\rho L}(p_i - p_{i-1}) + F_f, i = 1, \dots, n \tag{194}$$

where L is taken to be the distance between the two sections. Now let,

$$\alpha p_i = p_{i-1}, i = 1, \dots, n \tag{195}$$

where α is termed as the coefficient of pressure changes in sections

$$\frac{\partial u_i}{\partial t} = -\frac{1}{\rho L}(1 - \alpha)p_i + F_f, i = 1, \dots, n \tag{196}$$

The loss of the friction under the conditions of laminar flow conforms with the Hagen–Poiseuille equation [157] [158]. For a circular pipe having a fluid of density (ρ) and kinematic viscosity υ, the hydraulic slope F_f can be described as,

$$F_f = \frac{64}{Re}\frac{u^2}{2gD} + F_b = \frac{64v}{2g}\frac{u}{D^2} + F_b \tag{197}$$

where g is the gravity, D is the diameter of the pipes and F_b is the shape force vector in pipes. By substitution of (197) in (196), the following equation can be extracted,

$$\frac{\partial u_i}{\partial t} = -\frac{1}{\rho L}(1-\alpha)p_i + \frac{64v}{2g}\frac{u}{D^2} + F_b, \quad i = 1, \dots, n \tag{198}$$

The pressure $p(x,t)$ in the pipeline can be described as,

$$p = \frac{F}{A} \tag{199}$$

where F is the force inside the pipeline, also A is the cross section in the pipe.

By taking into consideration $F = ma = m\frac{d^2x}{d^2t}$, and $u = \frac{dx}{dt}$, also by substitution of (199) in (198) the following equation is obtained,

$$\frac{\partial}{\partial t}\frac{\partial x_i}{\partial t} = -\frac{(1-\alpha)}{\rho AL}\frac{\partial^2 x_i}{\partial t^2} + \frac{64v}{2gD^2}\frac{\partial x_i}{\partial t} + F_b \tag{200}$$

Therefore,

$$-\frac{(1-\alpha)+\rho AL}{\rho AL}\frac{\partial^2 x_i}{\partial t^2} + \frac{64v}{2gD^2}\frac{\partial x_i}{\partial t} + F_b = 0 \tag{201}$$

If an external force, f_p generated by the pump, (201) can be rewritten as follows,

$$\Gamma\ddot{x} + \Phi\dot{x} + f_b = f_p \tag{202}$$

where $x \in \mathbb{R}^2$, $\Gamma \in \mathbb{R}^{2\times2}$,$\Phi \in \mathbb{R}^{2\times2}$, $f_b = [f_{b1}\ f_{b2}]^T \in \mathbb{R}^{2\times1}$,$f_p = [f_{p1}\ f_{p2}]^T \in \mathbb{R}^{2\times1}$.

Since in this work two pipelines are used, (202) can be rewritten as,

$$\gamma_1\ddot{x}_1 + \varphi_1\dot{x} + f_{b1} = f_{p1} \tag{203}$$

$$\gamma_2 \ddot{x}_1 + \varphi_2 \dot{x} + f_{b2} = f_{p2}$$

Since the pump is supplying pressure to the pipes for the maintaining of the flow rates, so the pipes will have the same external force, $f_{p1} = f_{p2}$.

6.4.2. Modelling of the actuator

In order to reduce the vibrations of the motor caused by the external forces (f_p) a torsional actuator is placed on the motor, see Figure 6.3.

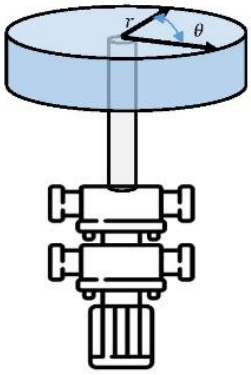

Figure 6.3 Torsional actuator with motor-pump arrangement

The motor and the pump are interconnected with the help of a shaft. The main purpose of the motor is to drive the pump. The pump with the help of the motor initiate a flow of fluid in the pipe. Any unwanted vibration in the motor will result in the vibration in the pump, which will result in improper flows in the pipe. Therefore, it is important to control the vibration in the motor, so as to control the vibration in the pump for making a stable flow of fluid in the pipelines. For this purpose, a torsional actuator having a motor and disk arrangement as shown in figure 3 is placed on the top base of the pump The main intention of the torsional actuator is to control the vibration on motor and consequently controlling the flow rates in pipelines.

The inertia moment of the torsional actuator is defined as,

$$J_t = m_t r_t^2 \tag{204}$$

where m_t is considered to be the mass of the disc, and r_t is the radius of the disc. The torque produced by means of the disc is defined as

$$u_\theta = J_t(\ddot{\theta}_t + \ddot{\theta}) \tag{205}$$

where $\ddot{\theta}$ is taken to be the angular acceleration of the motor and $\ddot{\theta}_t$ is taken to be the angular acceleration of the torsional actuator.

In order to reduce the torsional response, the directions of $\ddot{\theta}_t$ as well as $\ddot{\theta}$ are taken to be different. The friction of the torsional actuator is defined as [159],

$$f_d = c\dot{\theta}_t + F_c \tanh(\beta\dot{\theta}_t) \tag{206}$$

where c is taken to be the torsional viscous friction coefficient, β is the motor constant, F_c is taken to be the coulomb friction torque, also tanh is considered to be the hyperbolic tangent which depends on β and motor speed. The final torsion control is expressed as,

$$u_\theta = J_t\left(\ddot{\theta}_t + \ddot{\theta}\right) - f_d \tag{207}$$

6.4.3. Modelling of the pump

The general equation of the pump supplying pressure to the pipe for flow control can be demonstrated as [160],

$$T\dot{\omega} = \tau - (\tau_p - n\omega) \tag{208}$$

where

ω is angular velocity,

τ is motor torque,

τ_p is frictional torque of the motor,

n is load constant,

T is rotations inertia time constant.

The equation (208) can be modified as follows,

$$\ddot{x}_p = \frac{\tau - (\tau_p - nx_p)}{T} \tag{209}$$

Where $\ddot{x}_p$ is the flow acceleration of the pump. Since $\tau, T, \tau_p,$ and n are known quantities of pump so $\ddot{x}_p$ can be estimated.

The external force generated by the pump is

$$f_p = m_p \ddot{x}_p \tag{210}$$

where $\ddot{x}_p$ is the acceleration of the motor and m_p is volumetric mass of the pump.

The shape force vector f_b can be modeled as a linear or a nonlinear model.

From (202), by considering the shape force vector f_b as a non-linear model, the following analysis is illustrated:

In simple non-linear case, (202) becomes

$$\Gamma \ddot{X} + \Phi \dot{X} + f_b = f_p \tag{211}$$

where f_b is taken to be non-linear.

6.5. Control using PD method

Since 1700's the control of continuous process has been carried out by utilizing feedback loop [161] [162]. The system with a feedback control has a drawback which is related to the instability of the system. In order to resolve this problem an appropriate controller should be chosen and also it must be ideal for the monitoring system.

The control mechanism is demonstrated in Figure 6.4 which shows the entire control process of the flow rate of the heavy-oil in pipelines.

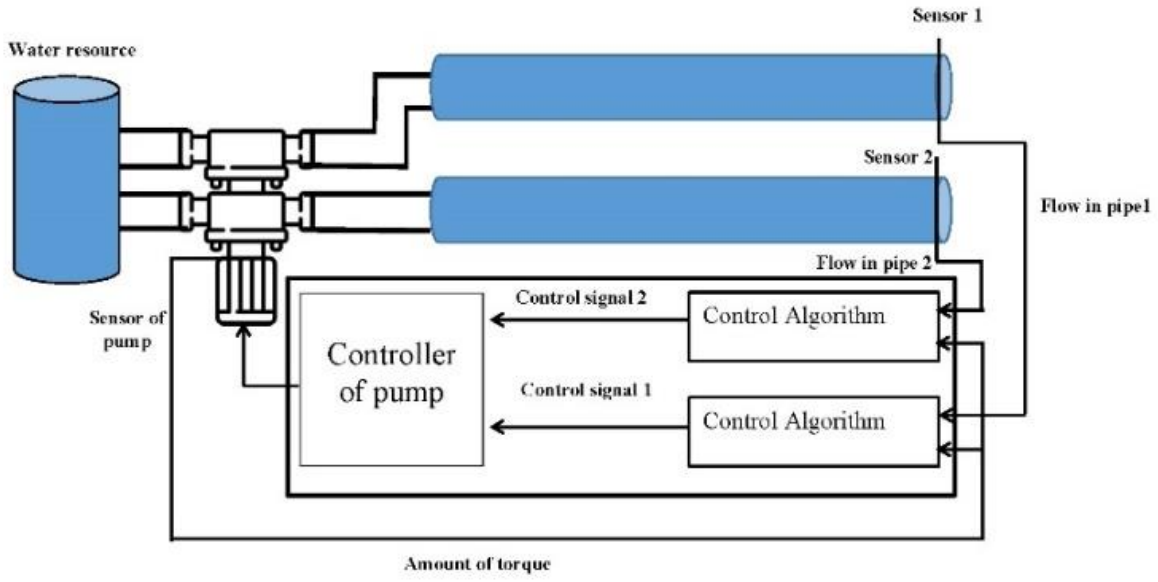

Figure 6.4. Structure of system

The proportional feedback is a simplified control and it is easy to implement. Other advantage of using P controller can be mentioned as minimized dead time, rise time, peak error and integrated error. Furthermore, its outcome is notably sensitive for the sensing location and feedback gain. The drawbacks of P control are:

•Abnormal variations in output upset operators

• Abnormal variations in output upset other loops

•Amplification of noise

A PD controller consists of the proportional element and the derivative element. The PD control is a control law based only the output which available for feedback, and is a usually common and practical control methodology utilized in the control community.

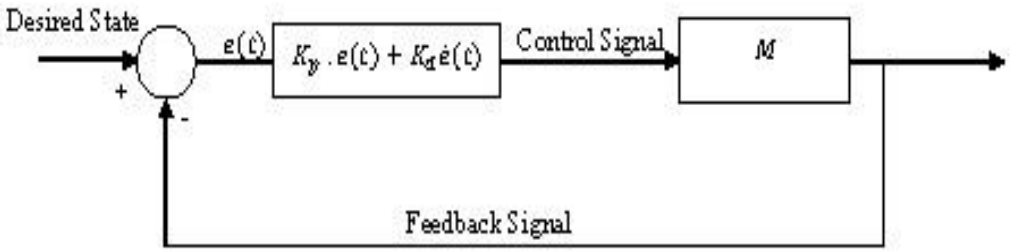

Figure 6.5 PD controller

In the PD control (Figure 6.5), the controller is composed of a simple gain as illustrated below [163] [164]:

$$\Psi(t) = -k_p e(t) - k_d \dot{e}(t) \tag{212}$$

where Ψ is the control input, $e(t)$ is the error, k_p is the proportional gain and k_d is the differential gain.

The proportional part $k_p\big(e(t)\big)$ in the PD control tunes the output signal in straight proportion to the controller input which is the error signal. In the case that there is an increment in the proportional gain k_p, the system under observation results in a fast response, minute steady-state errors as well as an extremely oscillatory response. The differential part ($k_d \dot{e}(t)$) utilizes the amount of variation of the error signal. It presents an element of prediction into the control action, and is capable of making the error to diminish to zero without oscillations with extreme amplitudes. The PD control is designed based on the choosing of proper gains k_p and k_d, mentioned in (212), in such a manner that the closed-loop system be stable, also superior performances can be obtained.

The closed-loop system mentioned in (202) along with the PD control shown in (212) is defined as,

$$\Gamma \ddot{X} + \Phi \dot{X} + f_b = f_p - k_p e(t) - k_d \dot{e}(t) \tag{213}$$

In this case, $\mathrm{e}(t) = x - x^d$, and x^d is the desired reference. For the flow control $x^d = 0$. k_p as well as k_d are positive constant which correspond to the proportional and derivative gains respectively.

In (213) the term $(f_b - f_p)$ can be considered as uncertainties, and is assumed to satisfy in a Lipschitz condition.

The closed-loop system mentioned in (213) with a PD control is,

$$\Gamma\ddot{X} + \Phi\dot{X} + F_g = -k_p e(t) - k_d \dot{e}(t) \tag{214}$$

where $F_g = f_b - f_p - f_d$.

In order to decrease the regulation error, the derivative gain should be increased. The utilization of large derivative gain results in slow temporary performance. It is notable that, if the derivative gain approaches towards infinity, the regulation error approaches to zero [165]. So it is advised to utilize a smaller derivative gain if the system is embedded with high-frequency noise signals.

6.5.1. Theorem

By taking into account the flow system defined in (202) and controlled utilizing the PD controller (214), the closed-loop system stated in (213) is stable under the consideration that the control gains are positive. So the regulation errors approach to the below mentioned residual,

$$\dot{D} = \{\dot{X}, \left\|\dot{X}\right\|^2 \leq \mu\} \tag{215}$$

where ${F_g}^T \Lambda^{-1} F_g \leq \mu$ and $\Phi - \Lambda > 0$, Λ is any positive matrix.

6.5.2. Proof

Using (202) and (212) the new closed loop system is

$$\Gamma\ddot{X} + \Phi\dot{X} + F_g = -k_p X - k_d \dot{X} \tag{216}$$

For the purpose of stability analysis, a Lyapunov candidate is selected as stated in (217). The first the term of equation denotes the kinetic energy and also the second term signifies the elastic potential energy. Since Γ as well as k_p are positive definite, therefore $V \geq 0$.

$$V = \frac{1}{2}\dot{X}^T \Gamma \dot{X} + \frac{1}{2}\dot{X}^T k_p X \tag{217}$$

The derivative of (217) is defined as,

$$\dot{V} = \dot{X}^T \Gamma \ddot{X} + \dot{X}^T k_p X = \dot{X}^T \left(-\Phi \dot{X} - F_g - k_p X - k_d \dot{X}\right) + \dot{X}^T k_p X$$
$$= -\dot{X}^T (\Phi + k_d)\dot{X} - \dot{X}^T F_g \tag{218}$$

For equation (218) the matrix inequality is validated in [166],

$$A^T B + B^T A \leq A^T \Lambda A + B^T \Lambda^{-1} B \tag{219}$$

The inequality of (219) is valid for any $A, B \in \mathbb{R}^{n \times m}$and any $0 < \Lambda = \Lambda^T \in \mathbb{R}^{n \times n}$, hence the scalar variable $\dot{X}^T F_g$ can be stated as,

$$\dot{X}^T F_g = \frac{1}{2}\dot{X}^T F_g + \frac{1}{2} {F_g}^T \dot{X} \leq \dot{X}^T \Lambda \dot{X} + {F_g}^T \Lambda^{-1} F_g \tag{220}$$

where Λ is stated as,

$$\Phi > \Lambda > 0 \tag{221}$$

By applying (221) in (220), the following relation is obtained,

$$\dot{V} \leq -\dot{X}^T (\Phi + k_d - \Lambda)\dot{X} + {F_g}^T \Lambda^{-1} F_g \tag{222}$$

If $k_d > 0$ and $\Phi > 0$, then,

$$\dot{V} \leq -\dot{X}^T \Pi \dot{X} + \mu \leq -\lambda \Pi \left\|\dot{X}\right\|^2 + {F_g}^T \Lambda^{-1} F_g \tag{223}$$

where $\Pi = \Phi + k_d - \Lambda > 0$.

The boundedness of ${F_g}^T \Lambda^{-1} F_g \leq \mu$ signifies that the regulation error $\left\|\dot{X}\right\|$ is bounded [167], so

$$\left\|\dot{X}\right\|^2 > \mu \; \forall t \in [0, T] \tag{224}$$

Therefore it can be concluded that $\dot{V} < 0$ when $\left\|\dot{X}\right\|^2 > \mu$.then The next step is to demonstrate that the total time during which $\left\|\dot{X}\right\|^2 > \mu$ is finite.

Suppose T signifies the time interval during which $\|\dot{X}\|^2 > \mu$. Then $\|\dot{X}\|^2 > \mu$ is inside the circle if $\|\dot{X}\|^2 > \mu$ is outside the circle of radius μ for finite time and afterward re-enters the circle. Furthermore, as the total time $\|\dot{X}\|^2 > \mu$ is finite, $\sum_{k=1}^{\infty} T_k < \infty$, then,

$$\lim_{k\to\infty} T_k = 0 \tag{225}$$

Therefore, $\|\dot{X}\|^2$is bounded with an invariant set argument. Furthermore, by utilizing (223) it can be proved that $\|\dot{X}\|$ is likewise bounded. Assume $\|\dot{X}\|^2$to be the greatest tracking error throughout the T_k interval. Therefore, by utilizing (218) and since $\|\dot{X}\|^2$ is bounded we have,

$$\lim_{k\to\infty}[\|\dot{X}\|^2 - \mu] = 0 \tag{226}$$

Hence, $\|\dot{x}\|^2$ approaches μ_{f_b}, thus, the derivative of the regulation error x approaches to the residual set,

$$\dot{D} = \{\dot{X}, \|\dot{X}\|^2 \leq \mu\} \tag{227}$$

Besides, for $\|\dot{X}\|^2 > \mu$ the total time is finite, therefore $V = \frac{1}{2}\dot{X}^T\Gamma\dot{X} + \frac{1}{2}\dot{X}^T k_p X$ is bounded, thus the regulation error $\dot{X}$ is bounded.

6.6. The tuning method based on a PID controller

System with feedback control parameters drawback which is related to the instability of the system. In order to resolve this problem an appropriate controller should be chosen and also it must be ideal for the monitoring system. The proportional feedback control is uncomplicated and relatively easy to implement. Nevertheless, its outcome is completely sensitive to the sensing location as well as feedback gain. It is concluded from the control theory that these drawbacks of the P control should be overcome by adopting I as well as D controls. Nevertheless, there exist very few studies investigating the application of the PID control for fluid-mechanics problems. In addition, there are a very limited number of studies dealing with the P control and PI controller for pipeline. Due to this lack of investigations, this section aims to develop a PID control for flow rate in the pipeline.

The control mechanism is shown in Figure. 6.4 which shows the entire control process of the flow rate of the heavy-oil in pipelines.

The PID control is considered as a control law in which the existence of output for feedback is essential. This practical control method is widely utilized in the control community. In the PID control, the controller is made of a simple gain (P control), an integrator (I control), a differentiator (D control) or some weighted composition of these possibilities [168], see Figure 6.6.

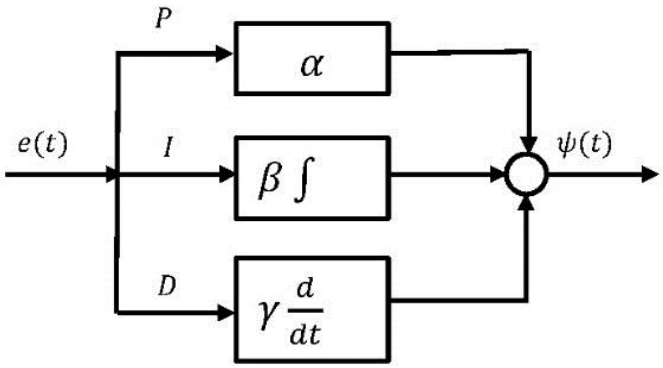

Figure 6.6 PID controller

The PID control is expressed as,

$$\Psi(t) = -\kappa_p e(t) - \kappa_i \int_0^t e(t)d\tau - \kappa_d \dot{e}(t) \tag{228}$$

where k_p, k_i, as well as k_d are positive definite and k_i is the integration gain. For the flow control, X^d is desired reference and also $X^d = \dot{X}^d = 0$. Hence, equation (228) is rewritten as below,

$$\Psi(t) = -\kappa_p X - \kappa_i \int_0^t X d\tau - \kappa_d \dot{X} \tag{229}$$

For analyzing the PID controller, equation (228) can be stated as below,

$$\Psi(t) = -\kappa_p X - \kappa_d \dot{X} - \vartheta$$
$$\vartheta = \kappa_i \int_0^t X d\tau \ , \vartheta(0) = 0 \tag{230}$$

The closed-loop system of equation (202) along with the PID control (equation (229)) is demonstrated as below,

$$\Gamma \ddot{x} + \Phi \dot{x} + F_g = -\kappa_p X - \kappa_d \dot{X} - \vartheta$$
$$\dot{\vartheta} = \kappa_i X \tag{231}$$

In matrix form, the closed-loop system is defined as,

$$\frac{d}{dt}\begin{bmatrix} \vartheta \\ X \\ \dot{X} \end{bmatrix} = \begin{bmatrix} \kappa_i X \\ \dot{X} \\ -\Gamma^{-1}(\Phi \dot{X} + F_g + k_p X + k_d \dot{X} + \vartheta) \end{bmatrix} \tag{232}$$

Here the stability of the PID control demonstrated by equation (229) is analyzed. The equilibrium of equation (232) is presented by $[\vartheta \quad X \quad \dot{X}] = [\hat{\vartheta} \quad 0 \quad 0]$. As at equilibrium point $X = 0$ as well as $\dot{X} = 0$, the equilibrium is $[f(0), \quad 0, \quad 0]$. For moving the equilibrium to the origin, the following is defined,

$$\hat{\vartheta} = \vartheta - f(0) \tag{233}$$

Therefore, the final closed-loop equation is defined as,

$$\Gamma \ddot{X} + \Phi \dot{X} + F_g = -\kappa_p X - \kappa_d \dot{X} - \vartheta + f(0)$$
$$\vartheta = \kappa_i x \tag{234}$$

For analyzing the stability of equations (234) and (234) and (234), the following properties are required,

Property 1. The positive definite matrix Γ should satisfy the condition below

$$0 < \lambda_{min}(\Gamma) \leq \|\Gamma\| \leq \lambda_{Max}(\Gamma) \leq \bar{\gamma} \tag{235}$$

such that $\lambda_{min}(\Gamma)$ as well as $\lambda_{Max}(\Gamma)$ are considered as the minimum and maximum eigenvalues of the matrix Γ, respectively and $\bar{\gamma} > 0$ is taken to be the upper bound.

Property 2. f is taken to be Lipschitz over $\tilde{x}$ and $\tilde{y}$ if

$$\|f(\tilde{x}) - f(\tilde{y})\| \leq \Omega\|\tilde{x} - \tilde{y}\| \tag{236}$$

As F_g is a first-order continuous function it also satisfies Lipschitz condition, Property 2 is hereby established.

The lower bound of F_g can be calculated as below,

$$\int_0^t f dx = \int_0^t F_g dx + \int_0^t d_u dx \tag{237}$$

The lower bound of $\int_0^t F_g dx$ is stated as $-\hat{F}_g$ and the lower bound of $\int_0^t d_u dx$ as -$\hat{D}_u$. Therefore, the lower bound of Ω is defined as,

$$\Omega = -\hat{F}_g - \hat{D}_u \tag{238}$$

The stability analysis of PID control approach is given by the theorem mentioned below.

6.6.1. Theorem

By taking into consideration the structural system of equations (202) controlled by the PID control approach of equation (228), the closed-loop system of equations (234) is taken to be asymptotically stable at the equilibriums $\left[\vartheta - f(0), X, \dot{X}\right]^T = 0$, if the following gains are satisfied,

$$\lambda_{min}(\kappa_d) \geq \frac{1}{4}\left(\frac{1}{3}\lambda_{min}(\Gamma)\lambda_{min}(\kappa_p)\right)^{1/2}\left[1 + \frac{k_e}{\lambda_{Max}(\Gamma)}\right] - \lambda_{min}(\Phi)$$

$$\lambda_{Max}(\kappa_i) \leq \frac{1}{6}\left(\frac{1}{3}\lambda_{min}(\Gamma)\lambda_{min}(\kappa_p)\right)^{1/2}\left[\frac{\lambda_{min}(\kappa_p)}{\lambda_{Max}(\Gamma)}\right] \tag{239}$$

$$\lambda_{min}(\kappa_p) \geq \frac{3}{2}[\Omega + \Xi]$$

6.6.2. Proof

The Lyapunov function can be stated as below,

$$V = \frac{1}{2}\dot{X}^T\Gamma\dot{X} + \frac{1}{2}X^T\kappa_p X + \frac{\sigma}{4}\vartheta^T\kappa_i^{-1}\vartheta + X^T\vartheta + \frac{\sigma}{2}X^T\kappa_d X + \frac{\sigma}{4}X^T\kappa_d X + \int_0^t F_g dx - \Omega \tag{240}$$

where $V(0) = 0$. For prove that $V \geq 0$, we divide it into three parts, $V = V_1 + V_2 + V_3$, where,

$$V_1 = \frac{1}{6}X^T\kappa_p X + \frac{\sigma}{4}X^T\kappa_d X + \int_0^t F_g dx - \Omega \geq 0, \kappa_p > 0, \kappa_d > 0 \tag{241}$$

$$V_2 = \frac{1}{6}X^T\kappa_p X + \frac{\sigma}{4}\vartheta^T\kappa_i^{-1}\vartheta + X^T\vartheta \geq \frac{1}{2}\frac{1}{3}\lambda_m(\kappa_p)\|x\|^2 + \frac{\sigma\lambda_{min}(\kappa_i^{-1})}{4}\|\vartheta\|^2 - \|x\|\|\vartheta\| \tag{242}$$

In case that $\sigma \geq \frac{3}{(\lambda_{min}(\kappa_i^{-1})\lambda_{min}(\kappa_p))}$, the following is obtained,

$$V_2 \geq \frac{1}{2}\left(\sqrt{\frac{\lambda_{min}(\kappa_p)}{3}}\|x\| - \sqrt{\frac{3}{4(\lambda_{min}(\kappa_p))}}\|\xi\|\right)^2 \geq 0 \tag{243}$$

Also,

$$V_3 \geq \frac{1}{6}X^T k_p X + \frac{1}{2}\dot{X}^T\Gamma\dot{X} + \frac{\sigma}{2}X^T\Gamma\dot{X} \tag{244}$$

Since

$$X^T AX \geq \|X\|\|AX\| \geq \|X\|\|A\|\|X\| \geq \lambda_{Max}(A)\|X\|^2 \tag{245}$$

in a case that $\sigma \leq \frac{1}{2}\frac{\sqrt{\frac{1}{3}\lambda_{min}(\Gamma)\lambda_m(\kappa_p)}}{\lambda_{Max}(\Phi)}$, the following is obtained,

$$V_3 \geq \frac{1}{2}\begin{pmatrix}\frac{1}{3}\lambda_{min}(\kappa_p)\|X\|^2 + \lambda_{min}(\Gamma)\left\|\dot{X}\right\|^2 \\ +\sigma\lambda_{Max}(\Gamma)\|X\|\left\|\dot{X}\right\|\end{pmatrix}$$
$$= \frac{1}{2}\left(\sqrt{\frac{\lambda_{min}(\kappa_p)}{3}}\|X\| + \sqrt{\lambda_{Max}(\Gamma)}\left\|\dot{X}\right\|\right)^2 \geq 0 \tag{246}$$

Therefore,

$$\frac{1}{2}\frac{\sqrt{\frac{1}{3}\lambda_{min}(\Gamma)\lambda_m(\kappa_p)}}{\lambda_{Max}(\Gamma)} \geq \sigma \geq \frac{3}{(\lambda_{min}(\kappa_i^{-1})\lambda_{min}(\kappa_p))} \tag{247}$$

The derivative of equation (232) is obtained as below,

$$\dot{V} = \dot{X}^T\Gamma\ddot{X} + \dot{X}^T\kappa_p X + \frac{\sigma}{2}\vartheta^T\kappa_i^{-1}\vartheta + \dot{X}^T\vartheta + \dot{X}^T\vartheta + X^T\vartheta + \frac{\sigma}{2}\dot{X}^T\Gamma\dot{X}$$
$$+ \frac{\sigma}{2}X^T\Gamma\ddot{X} + \sigma\dot{X}^T\kappa_d X + \dot{X}^T F_g \tag{248}$$

The matrix inequality of the equation below is validated in [166],

$$A^TB + B^TA \leq A^T\Lambda A + B^T\Lambda^{-1}B \tag{249}$$

The inequality of (248) is valid for any $A, B \in \mathbb{R}^{n\times m}$and any $0 < \Lambda = \Lambda^T \in \mathbb{R}^{n\times n}$, hence the scalar variable $\dot{X}^T F_g$ can be stated as,

$$\dot{X}^T F_g = \frac{1}{2}\dot{X}^T F_g + \frac{1}{2}{F_g}^T\dot{X} \leq \dot{X}^T\Lambda_{F_g}\dot{X} + {F_g}^T\Lambda_{F_g}^{-1}F_g \tag{250}$$

Utilizing equation (248) the following is obtained,

$$-\frac{\sigma}{2}X^T\Phi\dot{X} \leq \frac{\sigma}{2}\Xi_\Phi\left(X^Tx + \dot{X}^T\dot{X}\right) \tag{251}$$

where $\|\Phi\| \leq \Xi_\Phi$. Therefore, $\vartheta = k_i, \vartheta^T k_i^{-1}\vartheta$ becomes $x^T\vartheta$ also $x^T\vartheta$ becomes $x^T k_i$. Utilizing equation (251) the following is extracted,

$$\dot{V} = -\dot{X}^T\left[\Phi + \kappa_d - \frac{\sigma}{2}\Gamma - \frac{\sigma}{2}\Xi\right]\dot{X} - X^T\left[\frac{\sigma}{2}\kappa_p - \kappa_i - \frac{\sigma}{2}\Xi\right]X - \frac{\sigma}{2}X^T\left[F_g - f(0)\right] + \dot{X}^T f(0) \tag{252}$$

By applying the Lipschitz condition of equation (236) the following is obtained,

$$\frac{\sigma}{2}X^T\left[f(0) - F_g\right] \leq \frac{\sigma}{2}\kappa_f\|X\|^2 \tag{253}$$

$$-\frac{\sigma}{2}X^T[F_g - f(0)] \leq X^T\frac{\sigma}{2}\Omega X \tag{254}$$

From equation (248) we have,

$$\dot{X}^T f(0) \geq -f^T(0)\Lambda^{-1}f(0) \tag{255}$$

by utilizing equation (244)

$$\dot{V} = -\dot{X}^T\left[\Phi + \kappa_d - \frac{\sigma}{2}\Gamma - \frac{\sigma}{2}\Xi\right]\dot{X} - X^T\left[\frac{\sigma}{2}\kappa_p - \kappa_i - \frac{\sigma}{2}\Xi - \frac{\sigma}{2}\kappa_f\right]X + \dot{X}^T f(0) \tag{256}$$

then

$$\dot{V} \leq -\dot{X}^T\left[\lambda_{min}(\Phi) + \lambda_{min}(\kappa_d) - \frac{\sigma}{2}\lambda_{Max}(\Gamma) - \frac{\sigma}{2}\Xi\right]\dot{X} - X^T\left[\frac{\sigma}{2}\lambda_{min}(\kappa_p) - \lambda_{min}(\kappa_i) - \frac{\sigma}{2}\Xi - \frac{\sigma}{2}\Omega\right]X \tag{257}$$

Therefore, $\dot{V} \leq 0, \|X\|$ diminishes if the following conditions are held:

$$\lambda_{min}(\Phi) + \lambda_{min}(\kappa_d) \geq \frac{\sigma}{2}[\lambda_{Max}(\Gamma) + \kappa_c]$$

$$\lambda_{min}(k_p) \geq \frac{2}{\sigma}\lambda_{Max}(k_i) + \Xi + \Omega \tag{258}$$

By utilizing equation (247) as well as $\lambda_{min}(\kappa_i^{-1}) = \frac{1}{\lambda_{Max}(\kappa_i)}$, the following is obtained,

$$\lambda_{min}(\kappa_d) \geq \frac{1}{4}\left(\frac{1}{3}\lambda_{min}(\Gamma)\lambda_m(\kappa_p)\right)^{1/2}\left[1 + \frac{\Xi}{\lambda_{Max}(\Gamma)}\right] - \lambda_{min}(\Phi) \tag{259}$$

Again $\frac{2}{\sigma}\lambda_{Max}(k_i) = \frac{2}{3}\lambda_{min}(k_p)$. Thus,

$$\lambda_{Max}(\kappa_i) \leq \frac{1}{6}\left(\frac{1}{3}\lambda_{min}(\Gamma)\,\lambda_{min}(\kappa_p)\right)^{1/2}\frac{\lambda_{min}(\kappa_p)}{\lambda_{Max}(\Gamma)} \tag{260}$$

Furthermore,

$$\lambda_{min}(\kappa_p) \geq \frac{3}{2}[\Omega + \Xi] \tag{261}$$

This theorem suggests that the closed-loop system is asymptotically stable. □

6.7. Numerical results

For the numerical analysis purpose and for the validation of the novel control strategy, the various parameters associated with the flow control are described in Table 6.1:

Table 6.1. Parameters associated with the flow control

ρ	1240	kg/m^3
υ	1.604×10^{-3}	m^2/s
g	9.81	m/s^2
L	100	m
α	0.95	-
D	0.05	m
A	1.96×10^{-3}	m^2
r_t	0.3	m
m_t	1.5	kg

The implemented software in this paper is Matlab/Simulink. Simulations are presented to show that the motor vibration can be attenuated to a significant level by using the torsional actuator with the developed controllers thus validating the effectiveness of the proposed control approach using PID controllers. A simulation period of 20s is considered for evaluation. For the simulation purposes, the weight of the torsional actuator is considered to be 5% of the motor and pump weight in combination.

Since the maximum flow rate of the pipeline is $13\,m^3/s$ so the other non linear force associated with Ω has to be less than $13\,m^3/s$. Hence, we select the value of $\Omega = 13\,m^3/s$, and

$$\lambda_{min}(\gamma_1) = 1.0002, \lambda_{min}(\gamma_2) = 1.000206, \lambda_{min}(\Xi_1) = 2.09, \lambda_{min}(\Xi_2) = 2.09$$

For pipe 1 (see Figure 6.4) the gain values are present as

$$\lambda_{min}(k_{p1}) \geq 453, \lambda_{min}(k_{d1}) \geq 8, \tag{262}$$

Also for pipe 2 (see Figure 6.4) the gain values are present as

$$\lambda_{min}(k_{p2}) \geq 453, \lambda_{min}(k_{d2}) \geq 8, \tag{263}$$

For the ranges mentioned in (262) and (263), and with several trials for PD controller the best value of gains are selected as,

$$k_{p1} = 510, k_{d1} = 73, k_{p2} = 520, k_{d2} = 83 \tag{264}$$

Two subsystem blocks of milling model, one without control system and other with control system are created in order to compare the results. The flow rate from the pump is the input to the flow model. Numerical integrators are used to compute the velocity and position from the acceleration signal. The control signal from the controller subsystem block is fed to the torsional actuator simulation block to generate the required control forces.

Figure. 6.7 and Figure. 6.8 represent the attenuated vibration in motor. As can be concluded from these figures, the PD controller has high performance in minimizing vibration. Figure. 6.9 and Figure 6.10 represent the flow rate in pipelines 1 and 2, respectively. These figures demonstrate that with PD controller, the flowrates initiate from zero and maintain a stable flow rate which proves the effectiveness of the PD controller.

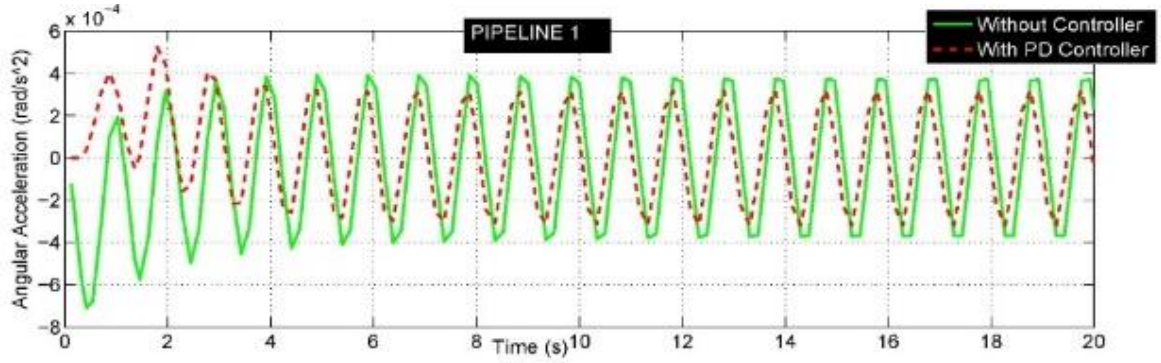

Figure.6.7 Comparison of motor vibration attenuation using PD controller for pipeline 1

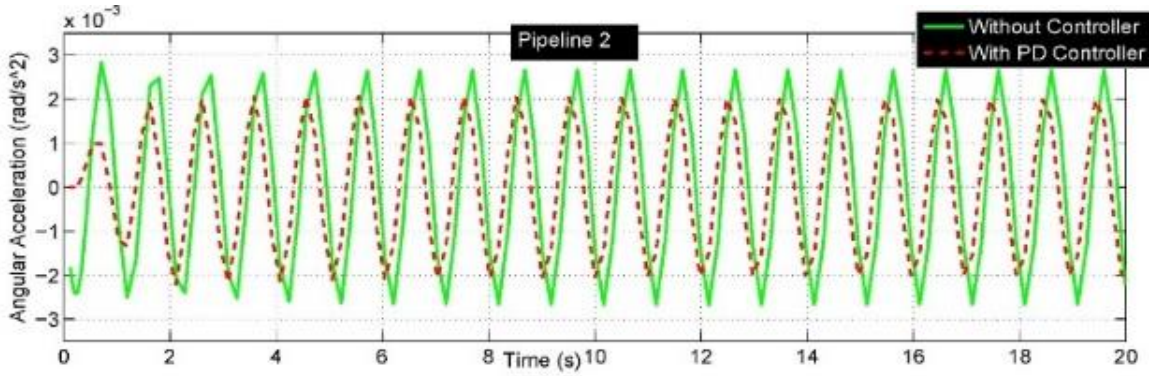

Figure. 6.8 Comparison of motor vibration attenuation using PD controller for pipeline 2

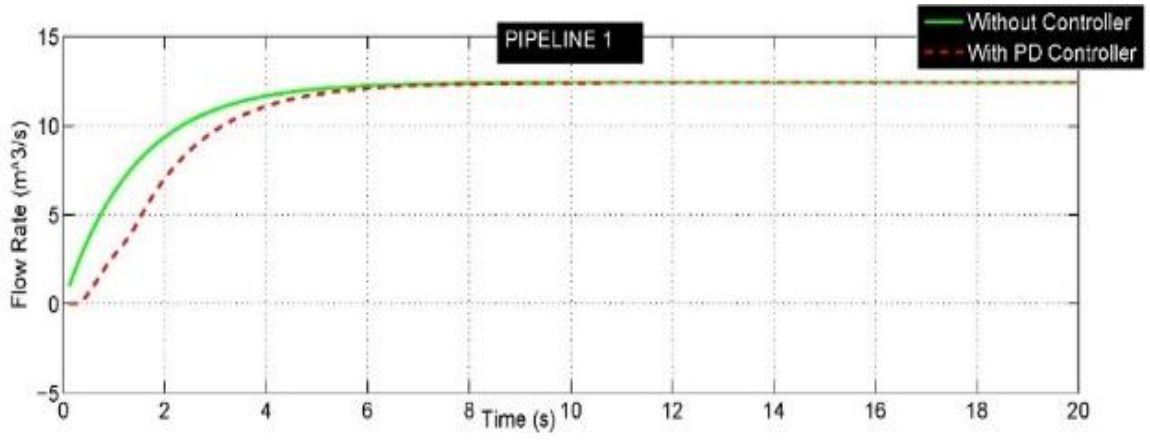

Figure. 6.9. Stability of flow rate using a PD controller in pipeline 1

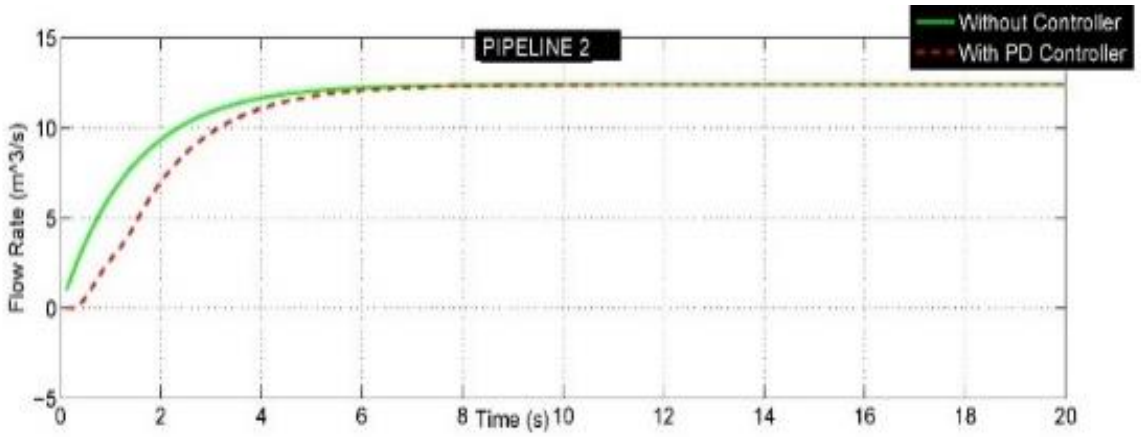

Figure 6.10 Stability of flow rate using a PD controller in pipeline 2

The theorem proposed in this paper generates sufficient conditions for the minimum amounts of the proportional as well as the derivative gains. This theorem validates that both proportional and derivative gains must be positive as negative gains can make the systems unstable. The PID gains are selected within the stable range by the stability analysis in order to ensure the efficiency.

Since the maximum flow rate of the pipeline is $13\,m^3/s$ so the other non linear force associated with Ω has to be less than $13\,m^3/s$. Hence, we select $\Omega = 13\,m^3/s$, and

$$\lambda_{min}(\gamma_1) = 1.0002, \lambda_{min}(\gamma_2) = 1.000206, \lambda_{min}(\Xi_1) = 2.09, \lambda_{min}(\Xi_2) = 2.09 \quad (265)$$

From Theorem 2, we use the following PID gains

$$\lambda_{min}(\kappa_{p1}) \geq 453, \lambda_{min}(\kappa_{d1}) \geq 8, \lambda_{Max}(\kappa_{i1}) \leq 928 \quad (266)$$

Also for pipe 2 we have,

$$\lambda_{min}(\kappa_{p2}) \geq 453, \lambda_{min}(\kappa_{d2}) \geq 8, \lambda_{Max}(\kappa_{i2}) \leq 928 \quad (267)$$

For the ranges mentioned in equation (266) and (267), the best values of gains are

$$\kappa_{p1} = 458, \kappa_{d1} = 110, \kappa_{i1} = 650, \kappa_{p2} = 480,$$

$$\kappa_{d2} = 115, \kappa_{i2} = 645$$

Two subsystem blocks of model, one in the absence of a control mechanism as open loop system and another with a control mechanism are generated for comparing the outcomes. The flow rate from the pump is the input to the flow model. Numerical integrators are utilized in order to calculate the velocity as well as the position from the acceleration signal. The control signal from the controller subsystem block is given to the torsional actuator simulation block in order to produce the essential control forces.

Figures 6.11 and 6.12 represent the attenuated vibration in motor. From these figures, it can be concluded that the PID controller is performing good in minimizing the vibration. Figures 6.13 and 6.14 represents the flow rate in pipeline 1 and pipeline 2. when PID controller are used, the flow rates initiate from zero and maintain a stable flow rate, which proves the effectiveness the of PID controller.

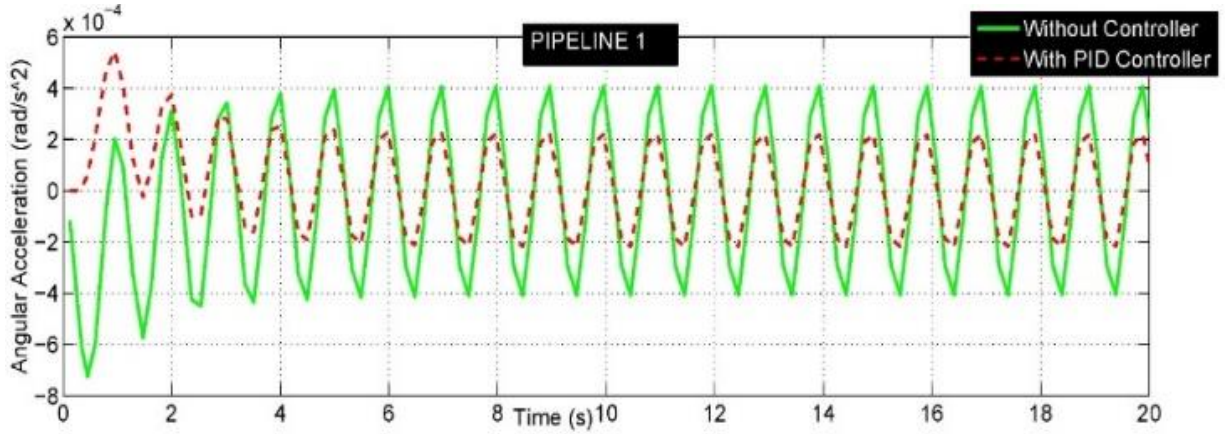

Figure 6.11 Comparison of motor vibration attenuation using a PID controller for pipeline 1

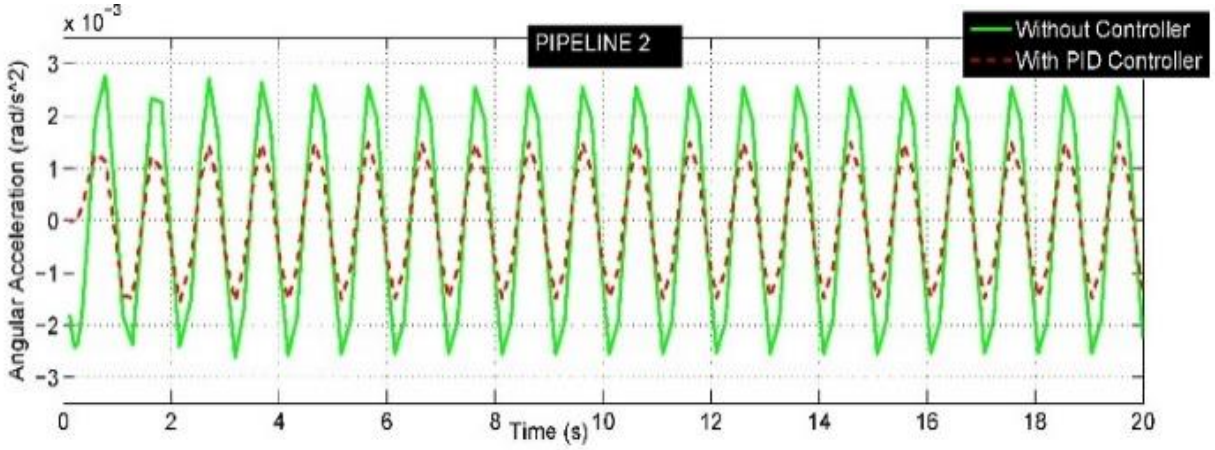

Figure 6.12 Comparison of motor vibration attenuation using a PID controller for pipeline 2

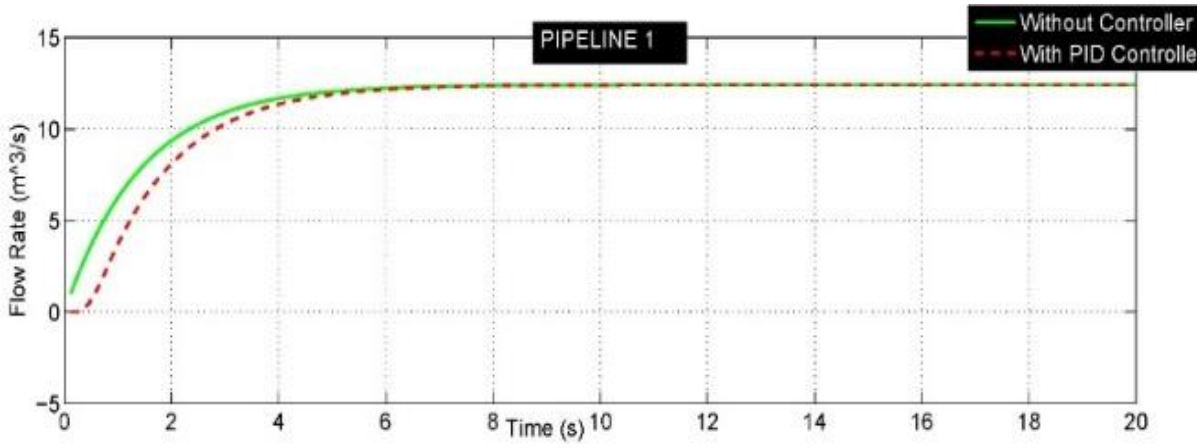

Figure. 6.13 Stability of flow rate using a PID controller in pipeline 1

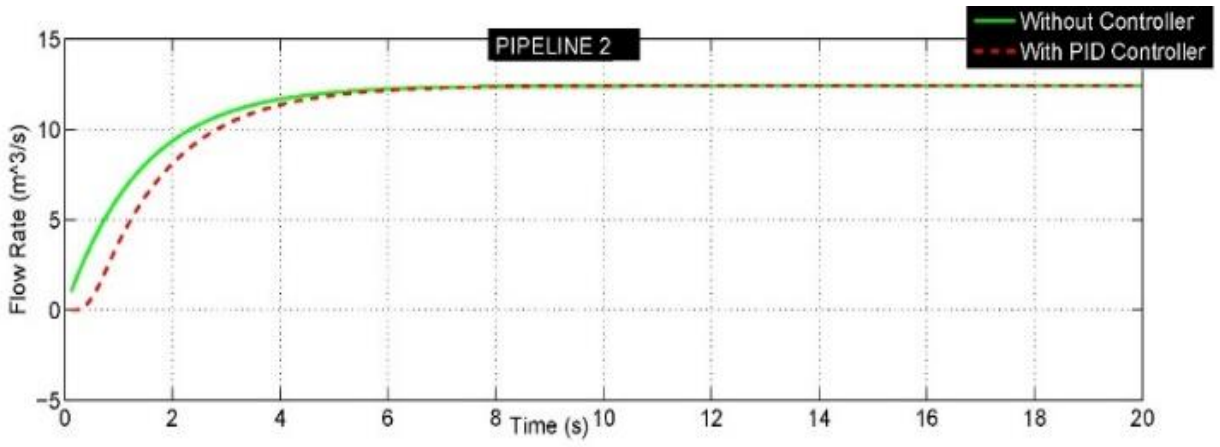

Figure 6.14 Stability of flow rate using a PID controller in pipeline 2

6.7. Conclusions

A novel active control strategy for the attenuation of motor vibration hence the flow rate control process is proposed. The important theoretical contribution associated with the stability analysis for the PD and PID controller was developed. The required stability conditions were obtained for

the purpose of tuning the PD/PID gains on the basis of proposed theorems. By utilizing Lyapunov stability analysis, the minimum values of the proportional and derivative gains and the maximum values of the integral gains were computed. The numerical simulation and analysis validates the effectiveness of PD and PID controllers in the minimization of motor vibration to control the flow rate in pipelines. The main contributions of this chapter are:

1) In this work, the stability of PID and PD controller is validated which has not been given importance in earlier researches considering the flow rate control.

2) The technique of using torsional actuator on the motor-pump arrangement is entirely a new concept.

Future work is intended towards the development of the experimental setup for further investigation and the improvement of the controller by fuzzy methods

Chapter Seven: Conclusions

7.1. Conclusion

Pipelines and leak detection systems can be found in a wide variety of areas for various products. Accordingly, the challenges that the leak detection system faces vary depending on the application.

In this thesis, it is presented a model to confront the leak and blockage detection and location problem in a pipeline in which the position of the leaks or blockage are assumed unknown.

The problem of leak detection and isolation in pipelines by means of nonlinear observers has been studied and tested in simulation. The detectability is guaranteed by appropriate excitation, chosen as a small varying input signal, via extensive simulations, and the results are quite promising.

It can be noticed that in the three-leak case which has been considered, the estimation performances could be improved by taking advantage of a first-step study on some equivalent single-leak location allowing to reduce the estimation problem.

But the fairly good results here obtained when directly facing the complete estimation problem are encouraging regarding its possible extension to detection of more leaks.

Future work

Future work will be concerned with the application of ANNs for automatically detecting the occurrence of leakages and blockage in pipelines, replacing the human operator, which monitors the online trends from the acoustic sensors. The data for network training will generate by a computer code expressly developed for simulating flow in pipelines with and without leaks.

The data for ANN development should consist of field measurements of process variables (pressure, flow rate, temperature) performing where there are leaks. A leak and block detection system for pipelines will be developed by using artificial neural networks (ANN) for leak sizing and location and by processing the field data

Moreover, future work will be dedicated to studying the applicability of the method to estimate and locate more leaks. This however increases the dimension of the estimation problem, which might make the appropriate excitation more difficult to obtain.

References

References

[1] Z. Huaguag, "Oil Pipeline Leak Detection and Location Using Double Sensors Pressure," *Fifth World Congress on Intelligent Controland Automation*, 2004.

[2] J. Fiedler, AN OVERVIEW OF PIPELINE LEAK DETECTION TECHNOLOGIES, krohne,Inc, 7 dearborn road.

[3] B .Jervey, Americas Natural Gas Pipelines-A Closer Look At This Gigantic Pipeline System,, DESMOG , 2011..

[4] Duguid C, Pipelines and Platforms, Oil and Gas Infrastructure, Oil and Gas Guidance, 2016.

[5] "U.S Department of Transportation, Federal Aviation Administration, Flight Standards Service-Aviation Maintenance Technical Handbook-Airframe," vol. 2, no. Chapter 12 and 14, FAA-H-8083-31., 2012.

[6] S.M. Folga , "Natural Gas Pipeline Technology Overview, Argonne National Laboratory, ANL/EVS/TM/08-5," pp. 1-12, 2007.

[7] T. Chris., A. Saguna, " Pipeline Leak Detection Techniques," *Annals. Computer Science Series5th Tome 1st Fasc*, 2007.

[8] M. Barker., R.R. Fessler., R. Biztek, "Pipeline Corrosion, Final Report, U.S. Department of Transportation, Pipeline and Hazardous Materials Safety Administration Office of Pipeline and Safety, Integrity Management Program, Under Delivery Order DTRS56- 02-D-70," 2008.

[9] J. Machell., S. Mounce., J. B. Boxall , "Online Modelling of Water Distribution Systems: A UK Case Study, Drinking Water Engineering and Science," 2010.

[10] A. Edson, " Gas pipeline blast kills 8, 4 others hurt. The Montreal Gazette," 1962.

[11] A. Edson, "Gas pipeline blast kills," *others hurt The Montreal Gazette*, vol. 8, no. 4, 1965.

[12] H. Eldon, Pipeline Explosion Kills Two Men, Sundre, Canada: Ottawa Citizen, 1965.

[13] D.M Gordon, Pipeline Explosion In Mexico Kills 52, The Telegraph, November 3,.

[14] The Associate Press, 26 Killed in Mexico pipeline fire, CBCNEWS WORLD, 2012..

[15] M.Clayton , West Virginia gas pipeline explosion-just a drop in the disaster bucket, The Christain Science Monitor, 2012.

[16] Pipeline Accident Report, Natural Gas-Fuelled Building Explosion and Resulting Fire, New York City: National Transportation Safety Board, 2015.

[17] C. Madrazo, 12 Lose Lives In Vast Lake Of Blazing Oil, New York: The Sydney Morning Gerald, 1959.

[18] A. Lannon, Eight Settle Claims Over Kanawha County Gas Pipeline Explosion., News Work: TriStateupdate, 2013.

[19] P. Shea , Nat Gas Pipeline Explosion, Oklahoma: The ValueWalk, 2013.

[20] A. Emmanuel , Preventable Errors Led to Pipeline Spill, Inquire Finds, Michigan: the New York Times, 2012.

[21] K. Millage , Timeline of Bellingham Pipeline Explosion., The Bellingham Herald., 2009.

[22] A. Cooper., C. Boyette , Feds: Operator Knew of Pipeline Problems Years Before, Michigan Oil Spill, 2012.

[23] M. Gollom , Pipeline Rupture: Alberta Resident Unaware of 2009 Blast., CBC News. , 2014.

[24] J.M Foster , Natural Gas Pipeline Explosion Levels Homes, Kentucky Town: CLIMATEPROGRESS, 2014.

[25] D. China , Chinese Oil Pipeline Explosion, November 23: Reuters, 2013.

[26] Nigerian Pipeline Fire Kills as Many as 100, the Seattle Times, Associated Press and the New York Times, 2008.

[27] A. Sider , "High-Tech Monitors Often Miss Oil Pipeline Leaks," *The Wall Street Journal,* 2014.

[28] Warda H.A, Adam G and Rashad A.B, "A Practical Implementation of Pressure Transient Analysis in Leak Localization in Pipelines," *International Pipeline Conference,* 2004.

[29] M. Willcox .,G. Downes, " A Brief Description of NDT Techniques," *Insight NDT Limited,* 2000-2003.

[30] H.F. Duan., P.J. Lee, " Experimental Investigation of Wave Scattering Effect of Pipe Blockages on Transient Analysis," *16th Conference on Water Distribution System Analysis,,* vol. 891, pp. 314-1320, 2014.

[31] A. Lazhar., L. Hadj-Taieb., E. Hadj-Taieb, "Two leaks detection in viscoelastic pipeline systems by means of transient," *Journal of Loss Prevention in the Process Industries.,* vol. 26, pp. 1341-1351, 2013 .

[32] H.-F. Duan., P. Lee., and Ghidaoui.M. , "Transient wave-blockage interaction in pressurized water pipelines," *12th International Conference on Computing and Control for the Water Industry, CCW12013. Science Direct. ,* vol. 70, p. 573– 582, 2014.

[33] A. Kaliatka., M. Vaisnoras., M. Valincius, " Modelling of valve induced water hammer phenomena in a district heating system," *Journal of Computer and Fluids,* vol. 94, no. 14, pp. 30-36, 2014.

[34] S. Riedelmeier., S. Becker., E. Schlucker, " Measurements of junction coupling during water hammer in piping systems," *Journal of Fluids and Structures ,* vol. 48, pp. 156-168, 2014.

[35] A.S. Tijsseling, " Water hammer with fluid-structure interaction in thick-walled pipes," *Computers and Structures ,* vol. 85, pp. 884-851, 2007.

[36] A.S, Tijsseling., M.F. Lambert ., A.R. Simpson.,M.L. Stephens., J.P. Vitkovsky., A. Bergant, "Skalak's extended theory of water hammer," *Journal of Sound and Vibration,* vol. 310, pp. 718-728, 2008.

[37] R,Wang., Z. Wang., X. Wang ,H. Yang., J. Sun , "Water hammer assessment techniques for water distribution systems," *Procedia Engineering ,* vol. 70, pp. 1717-1725, 2014.

[38] M.H. Afshar., M. Rohani , " Water hammer simulation by implicit method of characteristic," *International Journal of Pressure Vessels and Piping,* 2008.

[39] J.N. Delgado.,N.M.C. Martins., D.I.C. Covas , " Uncertainties in hydraulic transient modelling in raising pipe systems; laboratory case studies," *Science Direct Procedia Engineering,* vol. 70, p. 487 – 496, 2014.

[40] C. Nayak, "Fault detection in fluid flowing pipes using acoustic method," *International Journal of Applied Engineering Research, ISSN 0973-4562,* vol. 9, no. 1, pp. 23-28, 2014.

[41] H. Fuchs., R. Riehle, " Ten Years of Experience with Leak Detection by Acoustic Signal Analysis," *Elsevier Science Publishers Ltd,* 1990.

[42] D.B. Sharp., D.M. Campbell , " Leak detection in pipes using acoustic pulse reflectometry. Acustica, 83(3), 560-566, 1997.".

[43] K.A.Papadopoulou., M.N. Shamount., B. Lennox., D. Mackay, J.T . Turner., X. Wang, " An evaluation of acoustic reflectometry for leakage and blockage detection," *IMechE ,* 2008.

[44] W. Duan.,R. Kirby. , J. Prisutova, K.V. Horoshenkov, "On the use of power reflection ratio and phase change to determine the geometry of blockage in a pipe," *Journal of Applied Acoustics,* vol. 87, pp. 190-197, 2015.

[45] O. Hunaidi., A. Wang , "A new system for locating leaks in urban water distribution pipes,," *International Journal of Management of Environmental Quality,* vol. 17, no. 4, pp. 450-466, 2006.

[46] H.F. Duan., P.J. Lee., M.S. Ghidaoui., J. Tuck, " Transient wave-blockage interaction and extended blockage detection in elastic water pipelines.," *Journal of Fluids and Structures,* vol. 46, pp. 2-16, 2014.

[47] M.H. Sherman., M.P. Modera , " Signal attenuation due to cavity leakage,," *Journal of Acoustical Society of America,* vol. 84, no. 6, 1988.

[48] P. Murvay and L. Loan Silea, "“ A Survey on Gas Leak Prevention and Localization Techniques," *Journal of Loss Prevention in the Process Industries,* vol. 25, no. 6, pp. 966-973, 2012.

[49] H. V. Fuchs” , "“ One Year of Experience Leak Detection by Acoustic Signal Analysis” ," *Applied Acoustics,* pp. 1-19, 1991.

[50] S. Blesito, P. Lombardi, P. Andreussi and S. Banerjee, "Leak Detection in Lique..ed Gas Pipelines by Arti..cial Neural Networks," *AICHE Journal,* pp. 2675- 2688, 1998.

[51] I. N. Ferraz and A. C. B. Garcia, "Arti..cial Neural Networks Ensemble Used for Pipeline Leak Detection Systems," *” Ipc2008,* vol. 1, pp. 739-747, 2009.

[52] A. Shibata, M. Konichi, Y. Abe, R. Hasegawa, M. Watanable and H. Kamijo, " Neuro Based Classi..cation Of Gas Leakage Sounds In Pipeline," *Proceedings of International Conference on Networking, Sensing and Control,* pp. 298-302, 2009.

[53] J. Zhao, D. Li, H. Qi, F. Sun and R. An, "The Fault Diagnosis Method Of Pipeline Leakage Based On Neural Network," *Proceedings of International Conference on Computer, Mechatronics, Control and Electronic Engineering,* pp. 322-325, 2010.

[54] A. Avelino, J. d. Paiva, R. D. Silva and G.J.M. Araujo, "Real Time Leak Detection System Applied To Oil Pipelines Using Sonic Technology And Neural Networks," *35th Annual Conference of IEEE,* pp. 2109-2114, 2009.

[55] A. Mishra and A. Son, "Leakage Detection Using Fibre Optics Distributed Temperature Sensing," *6th Pipeline Technology Conference,* 2011.

[56] G. Geiger, D. Vogt and R.Tetzner, "State-of-the-Art Leak Detection and Localization," *presented at the ADIPECC,* 2008.

[57] G. Geiger, D. Vogt and R.Tetzner, "State-of-the-Art Leak Detection and Localization," *presented at the ADIPECC,* 2008.

[58] W. Lowry, S. Dunn, R. Walsh, D. Merewether and D. Rao, "Method And System To Locate Leaks In Subsurface Containment Structures Using Tracer Gases," *US Patent 6035701,* 2000.

[59] G. Geiger., T .Werner., P. Matko, Leak Detection and Locating-A survey,, Bern, Switzerland: 35th Annual PSIG Meeting, 2003.

[60] L. Billmann and R. Isermann, "Leak Detection Methods For Pipelines," *Automatica,* pp. 381-385, 1987.

[61] A. Sieber and S. Klaibe, "Testing a Method for Leakage Monitoring of a Gasoline Pipeline," *Process Automation,* pp. 91-96, 1980.

[62] C. Verde, "Minimal order nonlinear observer for leak detection," *Journal of Dynamic Systems, Measurement and Control,* vol. 126, pp. 467-472, 2004.

[63] M. T. Angulo and C. Verde, "Second-Order Sliding Mode Algorithms For Reconstruction Of Leaks," *Conference on Control and Fault-Tolerant Systems, France,* 2013.

[64] O. M. Aamo, A. Smyshlyaev, M. Krstic and B. A. Foss, "“ Output Feedback Boundary Control Of A Ginzburg-Landau Model Of Vortex Shedding," *IEEE Trans. Autom. Control,* vol. 52, no. 4, pp. 742-748, 2007.

[65] E. Hauge, O. Aamo and J. Godhavn, "Model Based Pipeline Monitoring With Leak Detection," *7th IFAC Symp. on Nonlinear Control Systems,* 2007.

[66] J. Mashford, D. D. Silva, D. Marney and S. Burn, "An Approach To Leak Detection In Pipe Networks Using Analysis Of Monitored Pressure Values By Support Vector Machine,," *J. Mashford, et al., "An Approach To Leak Detection In Pipe Networks Using Analysis Of Monitored Pressure Values By Support Vector Nss: 2009 3rd International Conference on Network and System Security,* pp. 534-539, 2009.

[67] M. Ferrante, B. Brunone and S. Meniconi, "Wavelets For The Analysis Of Transient Pressure Signals For Leak Detection," *Journal of Hydraulic Engineering ASCE ,* vol. 133, no. 11, pp. 1274-1282, 2007.

[68] d. Silva, V. H. Morooka, K. Celso, Guilherme, R. Ivan, d. Fonseca, M. C. Tiago and R. Jose, "Leak Detection in Petroleum Pipelines Using a Fuzzy System," *Journal of Petroleum and Science and Engineering,* vol. 49, pp. 223-228, 2005.

[69] A. Kadir , Transmission Gas Pipeline Lecture Note, Gas Engineering and Management, School of Computing, Science and Engineering,, Manchester: University of Salford, 2005.

[70] A. John., A. Beavers., G. Neil, "Thompson CC Technologies, External Corrosion of Oil and Natural Gas Pipelines, ASM Handbook, Corrosion: Environments and Industries," *ASM International,* vol. 13C, 2006.

[71] C. Verde, "Multi-Leak Detection And Isolation In Fluid Pipelines," *Control Engineering Practice,* pp. 673-682, 2001.

[72] M. Hou and P. Müller, "Fault detection and isolation observers," *International Journal of Control,* vol. 60, no. 5, pp. 827-846, 1994.

[73] J. Salvesen, Leak Detection by Estimation in an Oil Pipeline, MSc Thesis,: NTNU, 2005.

[74] G. Batchelor, An introduction to fluid dynamics,, Cambridge University Press, 1973.

[75] L. Landau and E. Lifshitz, Fluid Mechanics, 2nd Edition (Course of Theoretical Physics, Butterworth-Heinemann, 1987.

[76] G. Falkovich, Fluid Mechanics (A short course for physicists), Cambridge University Press, 2011.

[77] A. Bedford and W. L. Fowler, Engineering Mechanics: Statics (5th ed.), Prentice Hall. , 2008.

[78] M. H. Chaudry, Applied Hydraulic Transients, van, 1979.

[79] E. B. Wylie and V. L. Streeter, Fluid Transient, McGr, 1978.

[80] H. K. Khalil, Nonlinear systems,, New Jersey: Prentice-Hall, 1997.

[81] C. Chen, Linear System Theory and Design, New York: 2ndn.Holt, Rinehart and Winston,, 1984.

[82] A. L. Vickers, "The future of water conservation: Challenges ahead," *Water Resources Update Universities Council on Water Resources,,* vol. 114, pp. 49-51, 1999.

[83] "National Water Research Institute - Meteorological Service of Canada, "Threats to water availability in Canada," Environment Canada," *NWRI Scientific Assessment Report Series* , vol. 1, no. 3, 2004.

[84] K.H. Al-Dhowalia, N.Kh. Shammas, A.A. Quraishi, and F.F. Al-Muttair, "Assessment of leakage in the Riyadh water distribution network," *First Progress Report, King Abdulaziz City for Science and Technology,* 1989.

[85] L. Billman, R. Isermann, " (1984). Leak detectionmethods for pipelines. 9th IFACWorld Congress".

[86] A. Benkherouf, A. Allidina, "Leak detection and location in gas pipielines.," *IEEE .Proceedings.Part D. Control Theory Applications,* vol. 135, no. 2, p. 142–148, 1988.

[87] C. Verde, " Accommodation of multi-leak location in a pipeline.," *Control Engineering Practice,* vol. 13, no. 8, p. 1071–1078, 2005.

[88] G. Besançon, D. Georges., O.Begovich, C. Verde, C. Aldana, " Direct observer design for leak detection and estimation in pipelines," *European Control Conference.Greece: Kos.,* p. 5666–5670, 2007.

[89] A. Weimann, " Modellierung und Simulation der Dynamik yon Gasverteilnetzen im Hinblick auf Gasnetzfiihrung und Gasnetziiberwachung," *Dissertation an der TU Manchen, Fachbereich ET.* , 1978.

[90] L. Billmann , " Studies on improved leak detection methods for gas pipelines. Internal Report.," *Institut f'ur Regelungstechnil TH-Darmstadt (in German).,* 1982.

[91] W. Krass, A. Kittel and A. Uhde, " Pipelinetechnik.," *TUEV,* 1979.

[92] Y. Çengel and J. Cimbala, Fluid Mechanics, New York: McGraw-Hill, 2006.

[93] J. Roberson, J.J.Cassidy and M.Caudhry, "Hydraulic Emgineering," *Houghton Mifflin Co Ibternational Inc,* 1989.

[94] G. Besancon, D.Georges, B. O, C. Verde and C. Aldana, "Direct observer design for leak detection and estimation in pipeline," *proceesing of the European control conference2007,* pp. 5666-5670, 2007.

[95] M. Thoma and M. Morari, Nonlinear Observers and Applications, New York: Springer-Verlag Berlin Heidelberg , 2007.

[96] "wikipedia," 21 march 2018. [Online]. Available: https://en.wikipedia.org/wiki/State_observer.

[97] D. Luenberger, "Observing the state of a linear system.," *IEEE Transactions on Military Electronics*, vol. 8, pp. 74-80, 1964.

[98] M. Guillén, J. Dulhoste, G. Besançon, I. Rubio-Scola, R. Santos and D. Georges, "Leak detection and location based on improved pipe model and nonlinear observer.," in *In Proceedings of 13th European Control Conference,*, Strasbourg, France., 2014.

[99] J. P. Gauthier, H. Hammouri and S. Othman, "A simple observer for nonlinear systems:Applications to bioreactors," *IEEE Transactions on Automatic Control*, vol. 37, no. 6, pp. 875-880, 1992.

[100] J. Gauthier and G. Bornard, "Observability for any u(t) of a class of nonlinear systems," *IEEE Transaction on Automatic Control*, vol. 26, no. 5, p. 922–926, 1981.

[101] H. Nijmeijer and A.J. van der Schaf, Nonlinear Dynamical Control Systems., New York:: Springer, 1990.

[102] A. Isidori, Nonlinear Control system, 3rd ed . springer, 1995.

[103] C. Verde, "Multi – leak detection in fluid pipe lines," *Control Eng. Practice*, vol. 2001, pp. 673-682.

[104] C. Verde, N. Visairo, "Multi- leak isolation in a pipeline by unsteady state test, ,," , 2005.," *in in joint CDC-ECC Conf, Sevilla, Spain*, 2005.

[105] Z. Kowalczuk, K. Gunawickrama, , "Leak detection and isolation for transmission pipelines via state estimation," *in proc 4th safe process*, pp. 943-948, 2000.

[106] J.F. Garc- Tirado, B. Leon, O. Begovich,, "Validation of a semi physical pipeline model for multi leak diagnosis purposes," Banff, Alberta, Canada,, 2009.

[107] L. Billman., R. Isermann, "Leak detection methods for pipelines," *Proceeding of the 8th IFAC Congresse*, vol. 1, pp. 1813-1818, 1984.

[108] M. F. Ghazali., S. B. M. Beck., J. D. Shucksmith., J. B. Boxall, W. J. Staszewski, "Comparative study of instantaneous frequency based methods for leak detection in pipeline networks," *Mechanical Systems and Signal Processing*, vol. 29, pp. 187-200, 2012.

[109] W. Mpesha, M. N. Chaudry and S. Gassman, "Leak detection in pipes by frequency responcy response method," *Journal of Hydraulic Engineering*, vol. 127, no. 1, pp. 137-147, 2001.

[110] D. Covas., H. Ramos, "Standing wave difference method for leak detection in pipeline systems," *Journal of Hydraulic Engineering*, vol. 131, no. 12, pp. 1106-1116, 2005.

[111] C. Verde., L. Torres., O. Gonzalez, "Decentralized scheme for leaks location in branched pipeline," *Journal of loss prevention in the process industries*, vol. 43, pp. 18-28, 2016.

[112] C. Verde., N. Visairo.,, "Identificability of multi- leak in pipeline," in *in proc. American Control Conf*, Boston , MA , USA, 4378-4383, 2004.

[113] C. Verde., N. Visairro., S. Gentil, "Two leak isolation in a pipeline by transient response," *advances in water resources*, vol. 30, no. 8, pp. 1711-1721, 2007.

[114] H. F. Duan, P. J. Lee, M. S. Ghidaoui , Y. K. Tung,, "Extended Blockage Detection in Pipelines by Using the System Frequency Response Analysis," *J. Water Resour. Plann. Manage*, Vols. 138,, no. 1, pp. 55-62, 2012.

[115] M. A. Adewumi, E. S. Eltohami and W. H. Ahmed, "Pressure Transients Across Constrictions," *J. Energy Resour. Technol*, vol. 122, no. 1, pp. 34-41, 2000.

[116] M. A. Adewumi, E. S. Eltohami and A. Solaja, "Possible Detection of Multiple Blockages Using Transients," *J. Energy Resour. Technol.*, vol. 125, no. 2, pp. 154-159, 2003.

[117] J. P. Vitkovsky, P. J. Lee, M. L. Stephens, M. F. Lambert, A. R. Simpson and J. A. Liggett, "Leak and Blockage Detection in Pipelines Via an Impulse Response Method," in *5th International Conference Pumps, Electromechanical Devices and Systems Applied to*, Valencia, Spain, 2003.

[118] X. J. Wang, M. F. Lambert , a. A. R. Simpson., "Detection and Location of a Partial Blockage in a Pipeline Using Damping of Fluid Transients," *J. Water Resour. Plann. Manage*, vol. 131, no. 3, pp. 244- 249, 2005.

[119] A. M. Sattar, M. H. Chaudhry, A. A. Kassem, "Partial Blockage Detection in Pipelines by Frequecy Response Method," *J. Hydraul. Eng*, vol. 134, no. 1, pp. 76-89, 2008.

[120] P.S. Murvay., I. Silea, "A survey on gas leak detection and localization techniques," *Journal of Loss Prevention in the Process Industries*, vol. 25, pp. 966-973, 2012.

[121] G. Brown, The Darcy–Weisbach Equation, Oklahoma State University–Stillwate, 2002.

[122] P.K. Swamee, A.K. ain, "Explicit equations for pipe-flow problems," *Journal of the Hydraulics Division*, vol. 102, no. 5, pp. 657-664, 1976.

[123] E. B. Wylie., V. L. Streeter, Fluid Transient, New York City, New York, United States: McGraw-Hill Education, 1978.

[124] L. Beilina, "Domain decomposition finite element/finite difference method for the conductivity reconstruction in a hyperbolic equation," *Communications in Nonlinear Science and Numerical Simulation*, vol. 37, pp. 222-237, 2016.

[125] G. Besancon, Nonlinear Observers and Applications, E. LNCIS-363, Springer, 2007.

[126] G. H. Golub and J. M. Ortega,, Scientific Computing and Differential Equation: An introduction to numerical methods, Academic Press, 1992.

[127] D. Simon, Optimal State Estimation, 1st. edition,, Ed. John Wiley and Sons, 2006.

[128] K. J. Astrom and B. Wittenmark, Computer-controlled Systems: Theory and Design, Englewood Cliffs, USA, : Prentice-Hall, , 2nd edition, 1990..

[129] J. G. Ziegler and N. B. Nichols, "Optimal settings for automatic controllers," *Transactions of the ASME*, vol. 64, no. , vol. 64, pp. 759–768, 1942., pp. 759-768, 1942.

[130] J. C. Basilio and S. R. Matos, "Design of PI and PID controllers with transient performance specification," *IEEE Transactions on Education*, vol. 45, no. 4, pp. 364-370, 2002.

[131] D. E. Rivera, M. Morari, and S. Skogestad, "Internal model control PID controller design," *Ind. Eng. Chem. Process Design Development,*, vol. 25, no. 4, pp. 252-265, 1986.

[132] J. C. Basilio, J. A. Silva Jr., L. G. B. Rolim, and M. V. Moreira, "H∞, "H∞ design of rotor flux-oriented current-controlled induction motor drives:speed control, noise attenuation and stability robustness," *IET Control Theory and Applications* , vol. 4, p. 2491–2505, 2010.

[133] Ffowcs Williams, J. E. & Zhao, B. C. , " The active control of vortex shedding," *Journal of Fluids and Structures*, vol. 3, p. 115–122, 1989.

[134] Roussopoulos, K, " Feedback control of vortex shedding at low Reynolds numbers," *J. Fluid Mech.*, vol. 248, p. 267–296, 1993.

[135] Baz, A. & Ro, J., "Active control of flow-induced vibrations of a flexible cylinder using direct velocity feedback.," *Journal of Sound and Vibration*, vol. 146, pp. 33-45, 1991.

[136] E. Berger, " Suppression of vortex shedding and turbulence behind oscillating cylinders," *Physics of Fluids*, vol. 10, p. S191–S193, 1967.

[137] Ffowcs Williams, J. E. & Zhao, B. C., " The active control of vortex shedding. J. Fluids," *Journal of Fluids and Structures*, vol. 3, no. 2, pp. 115-122, 1989.

[138] K. Roussopoulos, "Feedback control of vortex shedding at low Reynolds numbers," *Journal of Fluid Mechanics*, vol. 248, pp. 267-296, 1993 .

[139] Hiejima, S., Kumao, T. & Taniguchi, T., " Feedback control of vortex shedding around a bluff body by velocity excitation.," *Int. J. Comput. Fluid Dynam.*, vol. 19, pp. 87-92, 2005.

[140] Sung SW, Lee J, Lee I-B. , Process identification and PID control., IEEE Press; , 2009.

[141] Kusters A, Ditzhuijzen GAJM., "MIMO system identifica-tion of a slab reheating furnace," in *Proceedings of the Third IEEE Conference on Control Applications. : IEEE Conference Publications*, USA, 1994.

[142] O. A, Handbook of PI and PID controller tuning rules, London:: Imperial College Press, 2009.

[143] H. Choi, W. P. Jeon, J. Kim,, "Control of flow over a bluff body," in *Annual Review of Fluid Mechanics*, 2008.

[144] Collis, S. S., Joslin, R. D., Seifert, A. & Theofilis, V., " Issues in active flow control: theory,Issues in active flow control: theory, control, simulation, and experiment," *Progress in Aerospace Sciences*, p. 237–289, 2004.

[145] Gad-el-Hak, M., Pollard, A. & Bonnet, J. P., Flow control: fundamentals and practices, Berlin, Germany: Springer, 1998.

[146] E. A. Fadlun, R. Verzicco, P. Orlandi, and J. Mohd-Yusof,, " Combined immersed-boundary finite-difference methods for three-dimensional complex flow simulations," *J. Comput. Phys.*, vol. 161, pp. 35-60, 2000.

[147] J. Mohd-Yusof, "Combined Immersed-Boundary/B-Spline Methods for Simulations of Flow in Complex Geometries,," *Annual Research Briefs (Center for Turbulence Research, NASA Ames and Stanford University*, pp. 317-327, 1997.

[148] Nandy A., Mondal S., Chakraborty P., Nandi G.C., "Development of a Robust Microcontroller Based Intelligent Prosthetic Limb," *International Conference on Contemporary Computing*, pp. 452-462, 2012.

[149] Park, D. S., Ladd, D. M. & Hendricks, E. W. 1994 Feedback control of von Kármán vortex, " Feedback control of von Kármán vortex shedding behind a circular cylinder at low Reynolds numbers," *Phys. Fluids*, vol. 6, p. 2390–2405, 1994.

[150] K. Roussopoulos, "Feedback control of vortex shedding at low Reynolds numbers," *J. Fluid Mech.*, vol. 248, p. 267–296, 1993.

[151] E. Berger, "Suppression of vortex shedding and turbulence behind oscillating cylinders.," *Phys. Fluids*, vol. 10, pp. 191-193, 1967.

[152] F. Gene, J. Franklin,P. Davied Powell, A. Emami-Naeini, , Feedback Control of Dynamic Systems, 6th edition, 2010, pp 19 – 27..

[153] K. J. Åström,T. Hägglund, PID Controllers: Theory, Design and Tuning, 1995, pp 59..

[154] A. O. Dwyer, Handbook of a PI and PID Controller Tuning Rules, 3rd edition, 2009.

[155] A.Herrán-González ., J.M.De La Cruz ., B.De Andrés-Toro., J.L.Risco-Martín, "Modeling and simulation of a gas distribution pipeline network," *Applied Mathematical Modelling*, vol. 33, no. 3, pp. 1584-1600, 2009.

[156] Whitaker, Robert D, "An historical note on the conservation of mass," *Journal of Chemical Education*, vol. 52, no. 10, p. 658, 1975.

[157] L. F. Moody, "Friction factors for pipe flow," *Transactions of the ASME*, vol. 66, no. 8, p. 671–684, 1944.

[158] G. Brown, "The History of the Darcy-Weisbach Equation for Pipe Flow Resistance," in *Environmental and Water Resources History. American Society of Civil Engineers*, 2003.

[159] Rolda´n C, Campa FJ, Altuzarra O, et al., "Automatic identification of the inertia and friction of an electromechanical actuator.," *Mechanisms and Machine Science*, vol. 17, p. 409–416..

[160] L. wozniak, "A graphocal approach to hydrogenetor governer tuning," *transaction on energy conversion* , vol. 5, no. 3, pp. 417-421, 1990.

[161] D.S. Bernstein ., L. Bushnell, "The history of control: From idea to technology," *IEEE Control Systems Magazine*, vol. 22, no. 2, pp. 21-23, 2002.

[162] C. Michael Hackl, "Brief Historical Overview of Control Systems, Mechatronics and Motion Control," in Non-identifier Based Adaptive Control in Mechatronics," *Springer International Publishing AG 2*, pp. 9-18, 2017.

[163] M. A, Johnson., M. H. Moradi , J. Crowe,, PID control: new identification and design methods, London, UK:: Springer,, 2005.

[164] J. R. Rowland, Linear control systems: modeling, analysis, and design, New York, NY:: : John Wiley & Sons, Inc , 1986.

[165] FL, Lewis., D.M. Dawson., C.T. Abdallah, Robot Manipulator Control: Theory and Practice. 2nd edn., Marcel Dekker Inc, 2004.

[166] A. v. d. Bos, "Parameter Estimation for Scientists and Engineers , Appendix C: Positive Semidefinite and Positive Definite Matrices," p. 259–263, 2007.

[167] E.D. sontag, Y. Wang, "On characterizations of the input-to-state stability property.," *Systems and Control Letters*, vol. 24, no. 5, p. 351–359., 1995.

[168] De Cock K, De Moor B, Minten W, et al., A tutorial on PID control. Report ESAT-SISTA/TR., Leuven, Belgium: Katholieke Universiteit Leuven, 1997.

[169] G. Strang, Linear Algebra and Its Applications, San Diego: 3rd ed. Harcourt Brace Jovanovich, 1988.

[170] R. Kalman and R. S. Bucy, "New results in linear filtering and prediction theory," *Journal of Basic Engineering*, vol. 82, no. D, pp. 35-40, 1960.

[171] H. K. Khalil, Nonlinear systems, New Jersey: Prentice-Hall, 1996.

[172] C. Chen, Linear System Theory and Design, Holt, New York: Rinehart and Winston, 1984.

[173] J.F. Grcar, "Mathematicians of Gaussian elimination," *Notices of the American Mathematical Society*, vol. 58, no. 6, p. 782–792, 2011.

[174] H. K. Khalil, "Nonlinear systems," *New Jersey,: Prentice-Hall*, 1996.